University of Alberta

Performance Assessment and Systematic Design of Industrial Alarm Systems

by

Naseeb Ahmed Adnan

A thesis submitted to the Faculty of Graduate Studies and Research in partial fulfillment of the requirements for the degree of

Doctor of Philosophy

in

Controls

Department of Electrical & Computer Engineering

To my parents
Nazim Uddin Ahmed and Suraiya Zaman,
and my wife
Farhana Akther.

Abstract

In process plants, alarms are configured to notify operators of any abnormalities or faults. However, in practice a majority of raised alarms are false or nuisance and create problems for operators as they face an increasing number of alarms to handle. In the past, many catastrophic incidents happened only because of poor performance of alarm systems. Therefore, a dependable and efficient alarm system is needed to ensure plant safety and uninterrupted operation. To assess performance of a plant's alarm system, it is necessary to evaluate various performances indices. Motivated by this, this thesis develops quantitative relationships among commonly used alarm attributes and performance indices.

Alarm design techniques, like, deadbands and delay-timers can significantly reduce false and nuisance alarms. However, these techniques introduce some delay in raising the alarm (detection delay). In this thesis, detection delays are calculated using Markov processes for deadbands and delay-timers. A design procedure is then proposed that compromises between detection delay, false alarm rate (Type I error) and missed alarm rate (Type II error) for an optimal configuration. Inclusion of these indices in alarm design makes the system more reliable and effective in nature.

Filtering is another widely used alarm design technique in industries. Two most commonly used filter types in industry are the moving average filter and the exponentially weighted moving average filter. However, the effect of filter

parameters on the alarm detection delay is not well known. We investigated this relationship for the moving average filter and proposed a method to design filter order.

We proposed a generalized delay-timer framework where instead of consecutive n samples in the conventional case, n_1 out of n consecutive samples ($n_1 \leq n$) are considered to raise an alarm. For the generalized delay-timer, three important performance indices, namely, the false alarm rate (FAR), the missed alarm rate (MAR) and the detection delay (EDD) are calculated using Markov processes. Also the performance and sensitivity of generalized delay-timers are compared with conventional delay-timers. All theoretical development and alarm design technique proposed in this thesis are validated through simulations and several case studies are conducted to illustrate industrial applications.

Acknowledgements

I would like to express my sincere gratitude to my supervisor, Prof. Tongwen Chen. With his visionary guidance and encouragement, Dr. Chen steered me to the right direction throughout my PhD studies. It was an honor working with such a knowledgeable and experienced person, which I see as a lifelong learning experience.

Another person that I am grateful to is Dr. Iman Izadi. I spent significant time discussing various research concepts with Dr. Iman that helped me develop some of the key research outcomes. I am indebted to Prof. Byron Schmuland for extending exceptional help to me in discussions from time to time. I also thank my PhD committee members, Prof. Sirish L. Shah and Prof. Qing Zhao, for their constructive feedback on some of my works. Special thanks to Colin Lunty for taking time to support and guide on industrial case studies. I would also like to thank Gordon Meyer, Eric Lau, Kevin Brown and Dr. Ramesh Kadali for their support to the study.

It has been a great experience to work with team members of Advanced Control Systems lab, Advances in Alarm Management and Design group and many other members of university community. My sincere thanks to all friends and well-wishers, particularly, Salman, Mustafa, Razib, Kabir, Amin, Sandeep, Anuj, Fan, Yue, Ping, Sridhar, Dawei, Jiadong, Feng, Elham and Rumi. I would also like to thank Pinder Bains, Kathleen Forbes and Erin Lee for various administrative help. I am thankful to NSERC, Alberta Innovates-Technology Futures, FGSR and ISA for financial support. My colleagues in the Graduate Students' Association were very helpful and supportive during my office term. Whenever I needed some extra time for research, they always stepped forward to share the workload. My thanks to Ashlyn, Brent, Huimin, Nathan, Ellen, Heather, Courtney, Dyan and other GSA colleagues for their help throughout the term.

I am grateful to my parents, brother and sister for all their support and encouragement. Finally, my wife, Farhana Akther, for all her help without which the thesis would not have been possible.

Contents

List of Tables

List of Figures

Chapter 1

Introduction

1.1 Motivation

In any industrial setup, the most desired feature is smooth and uninterrupted operation of the plant. Modern industries are therefore monitored by hundreds and thousands of sensors. These sensors are installed in different areas and they communicate through a medium to monitor physical or environmental conditions of the plant. Under fault-free operating condition of the plant, the operator carries out routine actions. Whenever a process variable exceeds certain threshold, an alarm is raised to indicate abnormality. Operators are informed of any problem by alarms indicating abnormal behavior of the plant.

To ensure cost efficiency, safety of the work force and plant, and quality of products, faults must be identified promptly and appropriate actions should be taken as soon as possible. Failure in such actions may result in serious consequences, even human injuries and casualties. With virtually every aspect and location of the systems being monitored, the probability of an event going undetected is very low. Furthermore, the consequences of any nontrivial event are likely to be picked up independently by several sensors and reported in many separate alarm messages causing nuisance alarms. It gives a false impression about the nature of fault to the operator. Working under such a stressful environment, the performance level of operators can go down causing serious consequences in responding to a true alarm.

Too many configured alarms make the alarm system complex and operators often face difficulties during abnormal events. The effectiveness of alarm systems can be measured in terms of two functional requirements [1]. First, a well designed alarm system must be able to warn operators about any abnormal situation in the plant so that operators can take immediate actions. Second, the warning should be a true one, and must not mislead or overload operators while taking appropriate measures. Inefficient design and poor performance of alarm systems caused serious accidents in the past.

1.1.1 Importance of Alarm Management

Process safety management is an important requirement to assure health and safety of workplaces. Also environmental issues are getting more and more attention since any major incident in process plants significantly affects surrounding environment. With growing concerns for water, air and earth contaminations caused by incidents in the past, effective process monitoring and alarm management have become important issues these days. According to the Abnormal Situation Management Consortium, the US petrochemical industry alone loses 10-20 billion dollars annually because of issues including equipment failure, environmental damage, human casualties and injuries, and so on [2]. Although achieving the state of absolutely no risks in plant operations is the ultimate target, because of many practical limitations it is hardly possible in practice. However, protection layers can be designed in such a way to prevent incidents and improve lines of defense. An effective monitoring and alarm system can significantly improve overall safety measures. Whereas, poor alarm performance may cause catastrophic accidents. In the following section we discuss a few of such incidents in the past.

1.1.2 Major Industrial Incidents

Petrochemical plants on average suffer a major incident once every three years [2]. Surprisingly many of these incidents are not caused by major equipment failure, but rather inefficient monitoring. The following incidents are often cited in the literature that motivate for effective alarm system design:

The Deepwater Horizon oil spill in 2010 in the Gulf of Mexico on the BP operated Macondo Prospect is considered as the largest marine oil spill accident in the history of petroleum industry. The explosion killed 11 workers and many were injured. The drilling rig burned and ultimately sank in two days later. BP reported $32 billion loss including compensation related to this oil spill [3]. The incident was a result of poor risk management and failure to observe and respond to critical indicators. A national commission investigated the incident and one of the key recommendations in the report is to build more sophisticated and automated alarms to alert the driller and the mudlogger when anomalies arise as a future practice [4].

The Buncefield fire is known as a major conflagration caused by a series of explosions in 2005 at the Hertfordshire Oil Storage Terminal [5]. The automatic tank gauging system that measured the level of Tank 912 stopped registering the tank fuel level and all configured alarms were non-operational as the indicated level never crossed the limit. Therefore, the control room supervisors were not notified of a tank overfilling. The tank was also equipped with an independent high level switch to close the control valve in case of the tank reaching an unintended high level, as well as a sounding alarm to report such incidents. However, this critical safety alarm did not work as well. As a result large quantities of petrol overflowed eventually causing a massive explosion. A total of 43 people were injured with surprisingly no death. The overall cost of the incident was estimated to be $1.5 billion.

The BP Texas City refinery explosion in 2005 occurred at the ISOM process unit killing 15 workers and another 180 were injured. The incident happened because of false indications by critical alarms that failed to alert operators of high level in the isomerization unit. The tower level indicator showed a declining level when the tower was actually overfilling. As a result of the accident, BP paid more than $1.6 billion as compensation to victims and was charged with another $87 million fine by Occupational Safety and Health Administration (OSHA) [6].

The explosion at *Texaco refinery at Milford Haven* in 1994 injured 26 workers and plant damage, costing $100 million to repair. The incident investigation revealed that operators received one alarm every two to three seconds during the incident making it almost impossible for them to react. It was also found that in the last 10 minutes prior to the incident, two operators had to recognize, acknowledge and take actions on 275 alarms. In the DCS alarm configuration, there was no clearly defined alarm philosophy as 87% of configured alarms had high priority making it difficult for operators to recognize critical alarms. As a result operators failed to recognize a stuck outlet valve that lead to release of flammable hydrocarbon which subsequently exploded [7].

In October 23, 1989, *the Phillips 66 Company disaster* at the Texas, USA, killed 23 employees and injured 314. The accident was caused by release of extremely flammable process gas through an open valve. The valve was connected the wrong way only because both close and open ends of the valve had similar outlook. As a result, the valve was open although the switch in the control room was at the valve close position. No alarms were configured to detect such anomalies that could prevent the deadly incident [8].

The Three-Mile Island (TMI) nuclear power plant accident is considered as the worst one in US commercial nuclear power plant history. Although there was no human casualty and very little radiation was reported in the environment, the incident had serious economic and social impacts. It took more than a decade to clean up the facility with a cost of $1 billion and $2.4 billion in property damage. The TMI plant was designed with ability to provide alarms for every small problem; but during the accident, operators were flooded with information, much of it irrelevant and misleading [9].

All these major incidents had different causes, but it is important to remember that most could have been prevented with better monitoring and alarm systems. Therefore an efficient alarm system is of paramount importance.

Table 1.1: Independent protection layers [10, 11]

Layers	Definitions	Functions
IPL8	Community emergency response	Minimize damage from an incident
IPL7	Plant emergency response	
IPL6	Physical protection (containment dikes)	
IPL5	Physical protection (relief device)	
IPL4	Automatic action SIS or ESD	Prevent an incident from happening
IPL3	Critical alarms, operators supervision and manual intervention	
IPL2	Basic control, process alarm and operator supervision	
IPL1	Process design	

1.2 Alarm Systems in Process Safety Design

To provide protection from hazardous incidents, eight independent protection layers (IPLs) as shown in Table 1.1 are largely followed in process design and safety considerations [10, 11]. The IPL1 layer is the most important one as it is possible to reduce overall risks significantly at the process design level. The IPL2 layer is primarily involved with supervision of an operating plant in the normal operating mode. At this level, operators are notified of any abnormalities in the plant raising alarms when a monitored process variable deviates from its normal operating range. In this layer of protection, operators are expected to take corrective measures mitigating the problem at the early stage of abnormality. The IPL3 layer represents critical alarms and manual operator's intervention may be required at this stage. Higher levels of protection layers involve safety instrumentation systems, emergency shutdown, plant emergency response and so on. Table 1.1 also illustrates the importance of alarm systems in process safety indicating how an effective alarm protection layer could prevent incidents from happening and therefore saving associated costs. Alarms indicating faults should be unmistakable and for each cause there should be no more than one alarm [12, 13].

Fault detection and isolation (FDI) form a very active area of research, mainly on the basis of mathematical or knowledge based models. Several model-based FDI methods were developed in the last decades [14, 15, 16, 17].

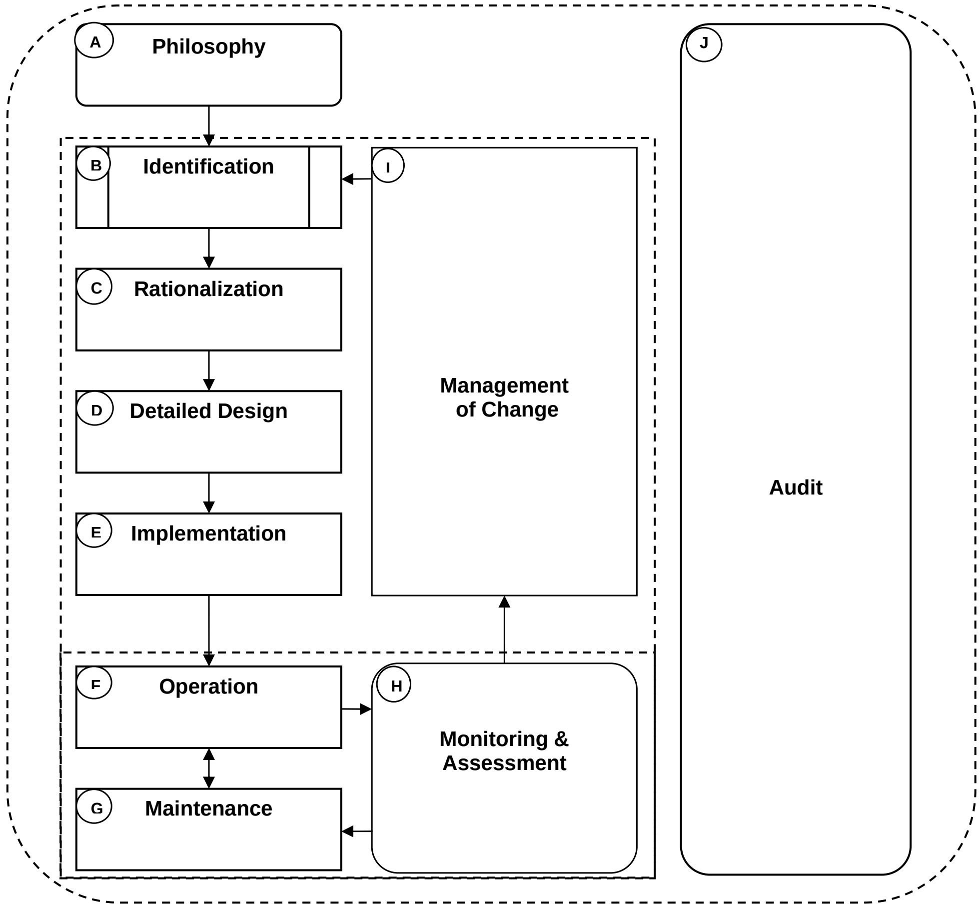

Figure 1.1: Alarm management lifecycle [18]

The main focus in the model-based approach is to obtain a proper mathematical model which is relatively difficult to do for complex plants. An alternative to model-based methods of fault detection is the signal-based methods. In signal-based fault detection, process variables are directly monitored and compared with some thresholds (or alarm limits) [16, 17]. Signal-based methods of process monitoring are the most commonly used techniques in industry and are readily implementable on almost all modern distributed computer systems (DCS).

Once a fault is detected, an alarm should be raised to notify the concerned operator about the fault. A detailed description of an alarm system is discussed in [18, 19]. According to the alarm management lifecycle (Fig. 1.1), the philosophy part is defined at the very beginning to document objectives. After that potential alarm problems are identified. The need to change alarm setpoint, design, prioritization, etc., are documented in the rationalization stage. Based on requirements of the documentation, alarm attributes are designed in the detailed design part. Blocks of implementation, operation, maintenance, and monitoring phases are quite self-explanatory. The total process is reviewed periodically from time to time in the audit section.

Generally, alarm systems can be designed in two frameworks: univariate and multivariate. In univariate design, which is the most commonly practiced method of alarming, the alarm thresholds and processing technique (deadband, delay-timer, filter, etc.) are individually designed for each process variable. In multivariate design, alarms are designed for some latent variables which are typically linear combinations of multiple process variables. Several multivariate design methods are available to group correlated alarms, identify statistical similarities and rationalize accordingly [2, 11, 20, 21, 22]. In this work, we concentrate on univariate alarm design for commonly used techniques balancing false alarm rate, missed alarm rate and detection delay not addressed elsewhere earlier.

The signal based methods based on simple limit checking have the advantage of simplicity and ease of implementation. However, incorrect settings of the alarm limits or thresholds may result in problems of false, missed and nuisance alarms [2, 12, 13]. An alarm that is raised in the fault-free operation of a plant is known as a *false alarm*. An alarm that is true but redundant as operator has already been notified of the fault by another alarm is a *nuisance alarm*. On the other hand the situation where an alarm is not raised in the presence of a fault is known as a *missed alarm*.

Another associated problem in the alarm system is delay in raising the alarm. In case of a fault occurrence, alarms may not be raised instantly due to different delays in the system. Also the alarm configuration (deadband, delay-timer, etc) can cause delay in raising the alarm. The difference in time between the actual moment of fault occurrence and the moment an alarm is activated is defined as the *detection delay*.

Table 1.2: The Engineering Equipment and Materials Users Association (EEMUA) benchmark

	EEMUA	Oil and Gas	Petrochemical	Power
average alarms per hour	≤ 6	36	54	48
average standing alarms	9	50	100	65
peak alarms per hour	60	1320	1080	2100
distribution % (low/med/high)	80/15/5	25/40/35	25/40/35	25/40/35

The performance measurement of alarm systems is an important concern in industries. For the univariate alarm systems, the performance can be assessed in terms of accuracy of the design and swiftness or latency to raise an alarm. The *false alarm rate (FAR)* and the *missed alarm rate (MAR)* provide a measure of alarm systems accuracy and the *expected detection delay (EDD)*, which is the averaged time required to activate an alarm provides a measure of alarm system latency. There are a number of methods for alarm configuration. It is widely accepted that proper implementation of these methods can improve the performance of alarm systems. Table 1.2 presents a typical survey of alarm counts and priority distribution from oil and gas, petrochemical and power industries [2]. When compared with industry standards, it is clear that the reality is far from what is recommended by standards. However, very limited research is conducted so far on how to obtain optimal settings for commonly used alarm configuration techniques. The exact quantitative relationship between performance specifications and design methods is not well known yet. This thesis aims at obtaining quantitative expressions that relate each configuration technique to the performance measure. Later this relationship is used to design the alarm system.

1.3 Thesis Contributions

The research on performance specifications of alarm systems is very limited in literature. Many problems are unresolved to comply with available standards - the ISA 18.2 and the EEMUA 191. The main objective of this thesis is "*developing quantitative relationship between commonly used alarm design techniques and performance specifications of alarm systems*". In order to meet the objective, we set the following goals to achieve for this thesis:

1. Deadbands, delay-timers and filtering techniques are widely used in industries. However, it is not well known the average time it may take to notify operators of an abnormal event for different alarm configuration settings and process types. Therefore, the first goal is to calculate detection delays caused by these common design techniques that can be used for optimal alarm configuration.

2. The next goal is to use the average delay information in alarm systems design. The design should be such that it provides sufficient time to an operator to respond to an alert of abnormality. Also the design should balance false alarm rate and missed alarm rate depending on the process type and other requirements.

3. As the next goal, extension of the commonly used delay-timer concept to a more generalized setup with analysis of associated sensitivity and accuracy indices is considered. In a conventional delay-timer setup, consecutive few samples are required to cross alarm limit to activate or deactivate an alarm. Here instead of consecutive samples, n_1 out of n consecutive samples are considered, where $n \geq n_1$.

4. Finally, with industrial case studies we want to demonstrate application of developed design methods and derived equations.

1.4 Organization of the Thesis

Chapter 2 includes preliminaries of alarm systems and literature review. A short description of problem definition and Markov processes, which are used as a tool for some of the main derivations, are also discussed in this chapter.

Chapter 3 discusses on calculation of detection delay for delay-timers, deadbands and simple limit checking. Later an alarm design method is also given considering detection delay, false alarm and missed alarm rates.

Chapter 4 focuses on detection delay calculation for filtering. Filtering is a widely practiced method to suppress noise in signals and it is shown that the downside of this advantage is delay caused by variable signal processing time.

Chapter 5 introduces a new concept of generalized delay-timers. In a conventional delay-timer, a consecutive few samples are considered to raise or clear an alarm. The concept is extended to a generalized framework, where instead of consecutive n samples, n_1 out of n samples ($n_1 \leq n$) are considered. For the generalized setup, impacts on accuracy and sensitivity are also discussed.

Chapter 6 includes application of derived equations and design methods to industrial problems. Historical process and alarm data obtained from industry are analyzed and based on that possible rationalization and effective alarm configuration techniques are discussed.

Chapter 7 discusses on conclusion and future work. A summary of work presented in the thesis is given, and directions for possible future extension are also discussed.

Chapter 2

Preliminaries

In this chapter the background material necessary to understand the contents of this thesis is discussed. In the following section, a literature review of the existing research related to alarm management and design is given. An introduction to the performance specifications of alarm systems, which is focus of this thesis is introduced. In Chapter 3 and 5, the detection delay caused by delay-timers and deadbands is calculated using Markov processes. Therefore, concepts of the Markov process used in later chapters are reviewed.

2.1 Literature Survey

The complexity and degree of automation of technical processes are continuously increasing with growing demands for plant reliability, higher efficiency, better performance and product quality. In the early days, a limited number of selected variables were monitored and sensors were hardwired to the control room. Due to significant advancement in communications and computer technologies nowadays a large number of process variables are monitored during plant operations. A downside of this advancement, however, is a large increase in the number of configured alarms. An alarm is an announcement to the operator (in visual or auditory form) to inform about any abnormality in the plant; and an alarm system is the system to generate and process alarms and presenting them to the operator. In this section, we review the existing literature that covers different aspects of alarm systems design and management.

Model-based vs Signal-based Design

There are several methods for fault detection as discussed in [14, 15, 16, 17]. These detection techniques can be broadly classified into two categories: model-based, and signal processing based. Compared to signal processing based, model-based fault detection is a more active area in the field of control theory and engineering [16]. However, for most practical systems it is difficult to obtain precisely known mathematical models or they are highly nonlinear and not feasible for implementation from economic point of view [17]. Therefore the application of the model-based scheme is limited. Furthermore, model creation is a time-consuming task and it is not always certain that the model will be valid; a created model is also required to be revised if changes are made in the process [12]. The most common and frequently used fault detection method in industry is simple limit checking of a directly measured variable (signal processing based fault detection) [12, 17]. This method has the advantages of simplicity and ease of implementation. However, incorrect settings of alarm limits or thresholds may result in problems of false, missed and nuisance alarms as well as cause detection delays [2, 12, 13, 23, 24]. The knowledge of FAR, MAR and EDD is therefore important to include preventive measures in the system design. To reduce the number of unnecessary redundant alarms, a conventional approach is to review top ten worst alarms. In this method, from a list generated, alarms are reviewed one by one starting from the most frequent one and the root cause is identified [25]. Many of these generated alarms can simply be removed by properly adjusting alarm thresholds [12]. Alarm thresholds are normally set considering certain confidence range, e.g. $\mu \pm 3\sigma$ (where μ is mean and σ is standard deviation of the process variable) [2]. In [26], a method of alarm threshold design is described; adding a margin to the upper and lower boundaries of the normal process fluctuation range is proposed in this method. But it does not discuss how to justify the optimality of selected margins. If a margin is set too high, it poses the risk of high missed alarms; and a too tight margin may lead to higher false alarms. In [27], considering the regulatory standard of EEMUA 191 [19], alarm system management and optimization are discussed. But very little is written about the trade-offs among false alarm rates, missed alarm rates and detection delays except [2, 13, 24, 20]. In [2], trade-offs between the detection delay and the false alarm, and between the false alarm rate and the missed alarm rate are discussed. An ROC curve is a technique to visualize and select classifiers based on their performance. In [13], a threshold design process is discussed based on ROC curves balancing the false alarm rate and the missed alarm rate for the filter, time delay and deadband.

Delay in Alarm Activation

An FDI method is judged satisfactory if it detects failure quickly [28]. To quantitatively measure the effect of variable processing, it is necessary to estimate the detection delay. The designer must have a clear idea about how long it will take to activate the alarm if a particular design scheme is used. This knowledge is important to include preventive measures in system design to compensate for activation delay. The detection delay has been discussed to some extent in [29, 30] for some change detection algorithms, e.g., the CUSUM-type algorithm. In [30], both analytical results and Monte-Carlo simulation results for the probability distribution of the detection delay and the time between false alarms are presented. The probability distribution of the fault detection delay and the time between false alarms are investigated in [31]. The authors derived analytical probability distribution expressions for sequential fault-detection schemes: CUSUM and GLR-based methods. In [24, 23], detection delays caused by the simple limit checking, deadbands and delay-timers are calculated; also a design method is proposed to balance the FAR, MAR and EDD. The common alarm attributes (e.g. alarm limit, deadbands, delay-timers) described in the ISA 18.2 standard [18] and EEMUA 191 [19] for basic alarm design are important for effective monitoring; these were not addressed elsewhere earlier. There are some popular methods such as the sequential hypothesis analysis or Wald's test [29, 32] for change detection. However, for offline analysis fault information and change point are mostly identifiable from data historian using expert knowledge [33, 34].

Correlation of Alarms

A large increase in the number of monitored variables in recent days has subsequently increased the number of alarms to be processed by an operator. These monitored variables are not all independent. There have been some studies on alarm systems based on correlation analysis [11, 25, 20, 35]. In [20], a method of suggesting alarm limits is discussed considering correlations between the process data and the alarm data. The idea is to study the similarity of correlation maps of physical process variables and their alarm history through causal maps. Then alarm limits should be set to reduce discrepancy of correlations. This method requires the process connectivity information, and in the presence of time lag, it cannot provide any solution. References [25, 35] discussed an alarm reduction method based on finding the event correlations from statistical similarities of alarms. In this method, alarms were divided into a limited number of groups considering several factors, e.g., sequentiality in alarm generation. From these groups unnecessary alarms were identified. The idea of event correlation analysis was first proposed in [11] to improve the performance of independent protection layers (IPL) 2 and 3 and evaluated the effectiveness in a chemical plant. Another important aspect of alarm systems is the human factors or operators actions due to their direct and indirect participation in handling of abnormal situations. Under a set of assumed malfunctions an operator model to be used as virtual subject for evaluating an alarm systems is discussed in [36]. Correlation of alarms and virtual subject modeling is out of scope of this work.

Chattering and Nuisance Alarms

Another problem related to alarm systems is several alarms raised in a short period of time for a single variable known as alarm chattering [37]. The chattering index is calculated based on the statistical properties of process variable in [38]. It has been discussed in some literature how filtering, delay-timers and deadbands can reduce the problem of nuisance and false alarms on a single process variable [13, 19, 18, 39]. The relationship of deadband, chattering and alarm limit is discussed in [40], where the authors also show that a fixed threshold with increasing deadband is less effective in reducing chattering impact. There are certain trade-offs in application of these techniques [2, 13]. For example, noise in signals may cause chattering for a fixed threshold and by filtering the noise can be reduced. Subsequently the noise reduction may result in reduced number of alarms. But to what extent filtering can be done is a major concern as it causes delay in triggering the alarm [13]. The trade-off between *accuracy and latency* is very important and must be taken into account before processing data. In [41], authors discussed about detection delay for other techniques including filtering and provided a formula to compute expected detection delay for moving average framework. But for moving average filter the correlation among contiguous samples of filtered data is ignored in their work. If the process data is independent and identically distributed (IID), after filtering the data no longer remains independent. Considering this fact relationship between the alarm limit, filter order and the detection delay is also derived later in [42].

Alarm Flood and Causality Analysis

The alarm flood is a very crucial problem in process industries which is defined as the period when operators receive more than 10 alarms per 10 minutes. Such incidents often lead to emergency shutdown or major plant upsets. In [21], the authors discussed about grouping of alarm floods according to patterns of occurrence using a nonlinear time alignment method of time dependent sequences called dynamic time warping (DTP). It is discussed that the root cause identification of historical alarm floods can be used as a signature and may benefit operators in future to react at early stage of a plant upset in similar cases. A similar work using a modified Smith Waterman algorithm is discussed in [43]. Since alarm flood is represented by a time-stamped sequence, the algorithm is modified to include time-stamp information and then calculate the similarity index. An automatic alarm data analyzer (AADA) algorithm is proposed taking into account causal dependencies in [44]. However, the method has limitations in terms of detecting variation in sequence as well as significant alarm dependencies. Graphical tools to analyze alarms could be very effective in overall plant alarm assessments. But it is a real challenge to present them graphically for longer time period analysis. For example, ISA 18.2 recommends considering at least 30 days of data to calculate the metrics. However, it is quite difficult task to condense data from such large time frame and usefully present them for information extraction. A high density alarm plot to chart top alarms over a given time period and alarm similarity color map to highlight redundant and similar alarms are presented in [45, 22]. Authors also illustrated usefulness of the tool by industrial case studies involving half a million observations for fifty alarm tags.

Rationalization of alarm systems is a key concern in process industries. Nowadays use of DCS has made it possible to store large amount of data in historian which can be used as a great resource for effective alarm rationalization [46]. Normally process engineers are well aware of normal behavior of the plant and are expected to be able to differentiate between fault-free and faulty process data. The calculated equations in this work can be applied to historical process data to get an accurate measure of performance specifications, namely, FAR, MAR and EDD. Later, changing different tuning parameters (delay-timer settings, alarm limits etc.) desired alarm settings can be obtained with the help of these equations.

2.2 Performance Specifications of Alarm Systems

The performance of alarm systems can be seen from two perspectives. When the overall macro scenario is considered, the performance can be measured by average annunciated alarm rate per operators, peak alarm rates, alarm floods, chattering or fleeting alarms, and priority distribution [18]. However, at the micro level it is not the overall system performance, rather how well alarms are performing individually is more important. A systematic approach of well-tuned individual alarm tags can improve overall performance significantly. Whereas, a few bad actors can cause the overall performance metric to degrade below the expectation level. The performance of alarm systems in this work is considered at the individual alarm tag level. It is a reasonable bottom-up approach where individual effectiveness adds to overall performance at the macro level.

For univariate alarm systems, raising of an alarm can be discussed from the perspective of two-class classification problem, where each instance is mapped to a class. If P and N are number of positive and negative instances with outcomes p (positive) and n (negative) respectively, then there are four possible outcomes from the given classifier problem. In such case, the outcomes can be described by a 2×2 confusion matrix (also known as contingency table) (Fig. 2.1).

If both prediction and actual outcomes are true (p), then it is called a true positive. But if the actual one is false (n), then it is a false positive. In the literature of alarm systems, the false positive is termed as the false alarm rate (FAR). On the other hand, a prediction outcome, n and an actual value, p is known as a false negative, which is the missed alarm rate (MAR) in alarm systems [12, 13, 24].

The performance measurement of alarm systems is an important concern in industries. For univariate alarm systems, one way to assess the performance is to compute accuracy of the design. The *false alarm rate (FAR)* and the *missed alarm rate (MAR)* provide a measure of alarm systems accuracy. A good design of higher accuracy indicates lower false and missed alarm rates. For the process data shown in Fig. 2.2, for a high alarm limit some part of the fault-free data falls above the limit causing false alarms and some part of the faulty data falls below the limit causing missed alarms.

		Actual Value		**Total**
		p	***n***	
Predicted Outcome	***p′***	**True Positive**	**False Positive**	**P′**
	n′	**False Negative**	**True Negative**	**N′**
	Total	**P**	**N**	

Figure 2.1: Confusion matrix of two-class classification problem

The accuracy of an alarm system can be presented by the receiver operating characteristics (ROC) curve [13]. In the signal detection theory, ROC curves are used to describe trade-offs between hit rates (also known as true positive rate) and false alarm rates [49]. However, in alarm systems ROC curves were first introduced in [13], where instead of the hit rate the missed alarm rate (1-hit rate or false negative) was used for convenience. If the objective of the alarm system design is to minimize both the false alarm rate and missed alarm rate, then the optimum point in the ROC curve is the point closest to the origin (Fig. 2.3). The ROC curve and the optimum point also depend on types of alarm design method used and weight given on FAR and MAR.

Another important performance index in alarm systems is the swiftness

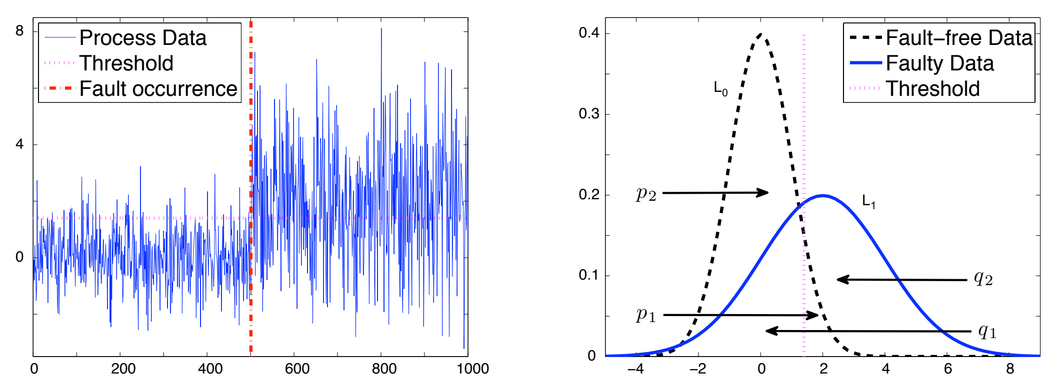

Figure 2.2: Process data and corresponding PDFs; p_1, p_2, q_1, q_2 denotes probabilities and L_0, L_1 denotes likelihoods for fault-free and faulty classes.

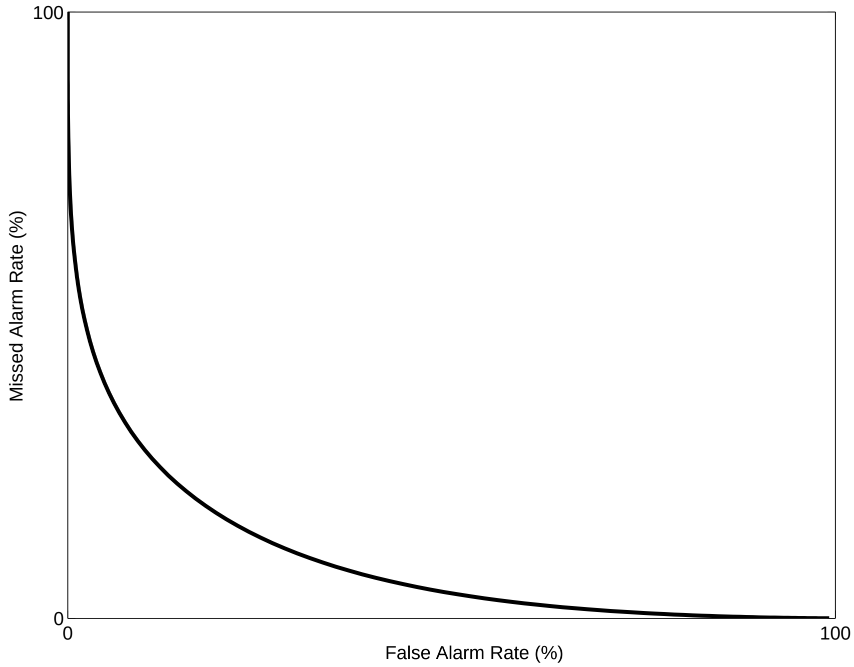

Figure 2.3: The receiver operating characteristic (ROC) curve

or latency to raise an alarm. Once an abnormality occurs, estimation of the average time required to raise an alarm is a critical concern for safety reasons. The average required time to activate a true positive outcome is known as the *expected detection delay (EDD)*, which provides a measure of alarm systems latency.

In Fig. 2.2, the fault-free data is Gaussian distributed with mean 0, variance 1, and faulty data is also Gaussian distributed with mean 2, variance 2. If the high alarm limit is set at 2, alarm is activated instantly when fault occurred. However, setting the limit at 4 in this example delays alarm activation by 7 seconds (assuming 1 sec sampling). It is therefore important to know how alarm settings cause delay in raising alarms.

A quantitative relationship among alarm configuration and performance indices is necessary for efficient alarm systems design. In the following section, calculation of these three indices (FAR, MAR, and EDD) are discussed. Calculation is mainly based on modeling the alarm systems by Markov chains.

2.3 Markov Processes

A Markov process is an independent process where outcome at any time instance depends only on the outcome that precedes it and none before that [47]. The stochastic process $(X_n)_{n=0}^{\infty}$ is called a Markov chain if, for any n and any collection of states $i_0, i_1, \cdots, i_{n+1}$

$$\mathbb{P}(X_{n+1} = i_{n+1} | X_n = i_n, \cdots, X_1 = i_1, X_0 = i_0) = \mathbb{P}(X_{n+1} = i_{n+1} | X_n = i_n) \tag{2.1}$$

In this thesis Markov processes are used to estimate the detection delay for deadbands and delay-timers. Consider a Markov process with a limited number of states. Assume that the transitional probability, p_{ij}, is the probability of going from state i at time t to state j at time $t+1$ and define

$$\mathbf{P} = \begin{pmatrix} p_{11} & p_{12} & \cdots & p_{1j} & \cdots \\ p_{21} & p_{22} & \cdots & p_{2j} & \cdots \\ \vdots & \vdots & \vdots & \vdots & \vdots \\ p_{i1} & p_{i2} & \cdots & p_{ij} & \cdots \\ \cdots & \cdots & \cdots & \cdots & \cdots \end{pmatrix},$$

The matrix $\mathbf{P}$ is known as transition probability matrix. A probability vector π is called invariant for the Markov process if $\pi = \pi\mathbf{P}$. In other words, π is a left eigenvector of $\mathbf{P}$ with eigenvalue 1 [48]. It is a known fact that an invariant vector π exists if the Markov process satisfies the following two conditions:

1. The sum of all entries in each row of $\mathbf{P}$ is 1 ($\sum_j p_{ij} = 1$).

2. All the entries of $\mathbf{P}$ are non-negative ($p_{ij} \geq 0$).

To satisfy these conditions and the definition of Markov processes, we make the following assumptions on the process data:

1. Process data is independent and identically distributed (I.I.D.), i.e., at each sampling instant, the process data (random variable) has the same probability distribution as the other instants and all are mutually independent.

2. Probability density functions of the fault free and faulty data are known. These distributions can be estimated from historical data.

Therefore enough relevant data points must be available to estimate these distributions that can be obtained from historical process data. Although these two assumptions are restrictive to some extent, they are not impractical [13, 23, 71]. Other cases of non-stationary distributions will be addressed in the future.

Chapter 3

Detection Delays for Deadbands and Delay-timers

Deadbands and delay-timers are two widely exercised techniques in process industries to mitigate problems of false and nuisance alarms. Unlike simple limit checking, in deadbands alarms are raised and cleared according to two different limits; and in delay-timers consecutive few samples are required to cross alarm limits to raise or clear an alarm. Although these techniques may significantly reduce false alarms, detection-delay is the unwanted consequence in alarm activation. The detection delay is not often considered in the design of alarm systems because of the common misconception that delay-timers equally delay all alarms [12], which is not true in practice [23, 24]. In this chapter[1,2], detection delays for deadbands and delay-timers are calculated using Markov processes. A design procedure is also proposed considering detection delay, false alarm rate (Type I error) and missed alarm rate (Type II error) for an optimal configuration. Inclusion of the detection delay in the alarm design enhances reliability and provides better insight to the consequences.

In Section 3.1, detection delays are discussed in the simplest case of threshold limit comparison. Sections 3.2 and 3.3 discuss detection delays due to

[1] A shorter version of this chapter has been published as: N. A. Adnan, I. Izadi, and T. Chen, *Computing Detection Delays in Industrial Alarm Systems*, in proceedings of the American Control Conference (ACC 2011), pp. 786-791, June 29 - July 1, 2011, San Francisco, CA, USA.

[2] Sections of this chapter have been published as: N. A. Adnan, I. Izadi, and T. Chen, *On expected detection delays for alarm systems with deadbands and delay-timers*, Journal of Process Control, vol. 21, no. 9, pp. 1318-1331, 2011.

deadbands and delay-timers, respectively. Section 3.4 presents an analysis for finding the optimum set level of threshold and a design procedure. In Section 5.6, concluding remarks and future work are discussed.

3.1 Detection Delay

In case of a fault occurrence, alarms may not be raised instantly due to different delays in the system. The delay can be caused by various reasons including network delays, bad implementation, hardware problems, sensor failure, data loss. Also the alarm configuration (deadband, delay-timer, etc) can cause delay in raising the alarm. Detection delay is the difference of samples between the actual instance of fault occurrence and the instance of alarm raised. If a process variable moves from fault-free region of operation into faulty region of operation at time t_f and alarm is raised at time t_a, then detection delay (DD) is given by,

DD = number of samples between t_a and t_f

In the ideal case fault should be detected instantly at the moment of occurrence, which is hardly seen due to different delays. In practical condition, the problem is to detect the occurrence of the change as soon as possible [29]. Techniques like delay-timers, deadbands, and filters are widely used in alarm systems to enhance the effectiveness of the limit checking method, but they increase the detection delay. However, even if no delay-timer, deadband and filter is configured, there may still be some detection delays as it is directly related to the position of the alarm threshold limit. In this section, we discuss detection delay for the simple threshold comparison alarm configuration.

In the fault free operating region assume the probability of one sample exceeding alarm limit (y_{tp}) is p_1 and the probability of one sample falling within the alarm limit is p_2. Similarly under the faulty region of operation, q_1 is the probability of one sample falling within the alarm limit and q_2 is the probability of one sample exceeding limit. Therefore $p_2 = 1 - p_1$ and $q_2 = 1 - q_1$ as shown in Fig. 3.1.

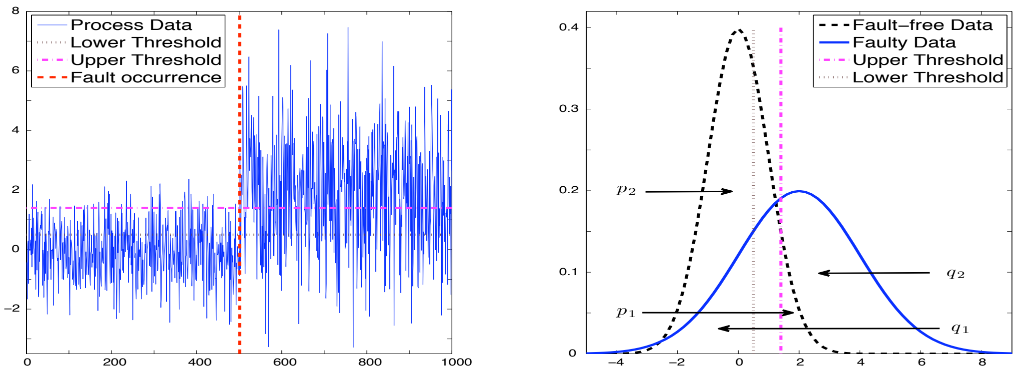

Figure 3.1: Process data with deadbands and fault occurrence instance (left); corresponding probability density functions of fault-free and faulty data (right). Only the upper threshold is considered for simple limit checking with no deadband

Probability of zero detection delay is given by the probability of an alarm being raised instantly at the time of fault; probability of detection delay one means alarm activation is delayed by one sample from the fault instance. Similarly detection delay of z samples denotes alarm is raised z samples later from the actual instance of fault. Assume that, abnormality occurred at time $t = t_f$, A denotes an *alarm* state and NA denotes a *no alarm* state. Probability of detection delays are

$$\begin{aligned}
\mathbb{P}(\mathrm{DD} = 0) =& \mathbb{P}(\mathrm{A \ at\ } t = t_f) = q_2 \\
\mathbb{P}(\mathrm{DD} = 1) =& \mathbb{P}(\mathrm{A \ at\ } t = t_f + 1 \ \& \ \mathrm{NA \ at\ } t = t_f) = q_2 q_1 \\
&\vdots \\
\mathbb{P}(\mathrm{DD} = z) =& \mathbb{P}(\mathrm{A \ at\ } t = t_f + z \ \& \ \mathrm{NA \ at\ } t = t_f + z - 1 \ \& \\
& \ \ldots \ \& \ \mathrm{NA \ at\ } t = t_f + 1 \ \& \ \mathrm{NA \ at\ } t = t_f) \\
=& q_2 q_1^z
\end{aligned} \tag{3.1}$$

Here the detection delays are in terms of samples, though the detection delay is normally known as a measure of time. But it will not affect the real

Threshold, y_{tp}	0	0.75	1.5	2.25	3	4	5
Expected detection delay	0.19	0.36	0.67	1.22	2.24	5.30	13.97

Table 3.1: Effect of threshold change on expected detection delays

scenario as in practice the sampling time is constant and these values can be converted to actual time measurements.

From the above equations it can be seen that in the simple case the probabilities of detection delay only depend on the probabilistic distribution of the faulty data. Fault-free region of operation does not have any effect on raising or clearing of alarm. The expected value of detection delay is

$$\mathrm{EDD} = \mathbb{E}(\mathrm{DD}) = \sum_{z=0}^{\infty} z\mathbb{P}(\mathrm{DD} = z) = \sum_{z=0}^{\infty} z q_2 q_1^z = q_1/q_2 \tag{3.2}$$

Since the expected detection delay is directly related to the threshold limit, changing the limit will greatly affect the detection delay. A comparative picture on change of threshold position can be found in Table. 3.1 for the process data in Fig. 3.1. Here fault-free data has a Gaussian distribution with mean 0, variance 1 and faulty data is also Gaussian distributed with mean 2, variance 2. It can be seen from Table 3.1, setting the threshold limit up to 3 results in detection delay of 2.241 *samples* or lower. But after 3, the detection delay increases rapidly as the number of samples able to cross the threshold decrease significantly.

Expected value of detection delay (or average detection delay) is an important parameter in alarm design as it indicates the average time it take to raise an alarm once there is an abnormality in the system. Therefore, it is always desired to reduce average detection delay to ensure more reliable operation of the plant. A method of threshold limit design will be discussed in details in Section 3.4.

3.2 Detection Delay for Deadbands

Deadbands are widely used in industry to eliminate repeating oscillations or chattering alarms. With deadband configured, alarms are raised and cleared according to two different limits, instead of the same limit in regular cases. For example, for high alarms a limit is set, as usual, for raising the alarm. However, once an alarm is activated it will not be cleared even if the variable falls below the limit. To clear the alarm, the variable must go below a lower threshold.

When a variable transits from the fault-free state to the faulty state, due to presence of noise, it crosses the alarm limit a few times before settling in the abnormal state. This oscillation results in subsequent raising and clearing of the alarm causing the chattering effect. Using deadband (i.e., separating raising and clearing limits) is, then, helpful here in preventing alarm chattering [37].

Deadbands should typically be configured based on the normal operating range of the process variables, measurement noise, and type of the process variables [18, 37]. There are certain standards for setting deadbands, e.g. in ISA 18.2 [18] or EEMUA [19]. The correct configuration of a deadband (setting limits appropriately) is essential in maximizing the benefits of the deadband.

When deadband is configured, as it can be seen in Fig. 3.1, the probabilities of one sample going over the raising limit and below the clearing limit do not add up to one, i.e., $p_1 + p_2 \neq 1$, $q_1 + q_2 \neq 1$; where p_1, p_2, q_1, q_2 are defined as before in Section 3.1.

To calculate the probabilities of false alarm and missed alarm, notice that a process operating in either the fault-free or faulty region, can be in two states from alarm point of view: alarm state (A) and no alarm state (NA). These states can be modeled with a Markov chain [13]. A Markov process for deadband is shown in Fig. 3.2 for fault-free operating region. The Markov

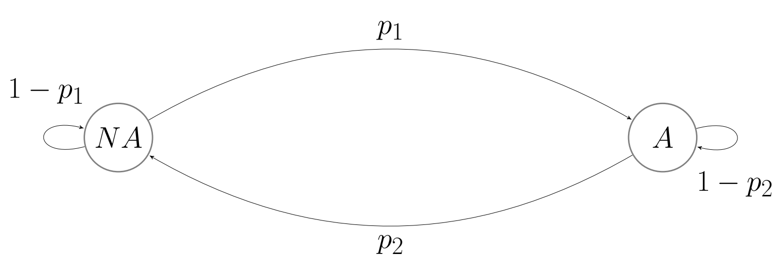

Figure 3.2: Markov diagram of a system with deadband in the normal region of operation

model in faulty region is similar. Transitional probabilities from one state to other are represented by transition probability matrix $\mathbf{P}_n$, in the fault-free region of operation and by $\mathbf{P}_f$ in the faulty region of operation:

$$\mathbf{P}_n = \begin{bmatrix} 1-p_1 & p_1 \\ p_2 & 1-p_2 \end{bmatrix}, \mathbf{P}_f = \begin{bmatrix} 1-q_2 & q_2 \\ q_1 & 1-q_1 \end{bmatrix} \tag{3.3}$$

If the process remains in the fault-free operating region, after a transient time the Markov process reaches its steady state and the vector of state probabilities converges to the invariant vector. The steady state vector of probabilities (invariant vector) for $\mathbf{P}_n$ is [13]

$$\pi_n = \left[\begin{array}{cc} \dfrac{p_2}{p_1+p_2} & \dfrac{p_1}{p_1+p_2} \end{array} \right] \tag{3.4}$$

When a fault occurs, the Markov process changes from fault-free model (represented by $\mathbf{P}_n$) to the faulty model (represented by $\mathbf{P}_f$). Therefore, the steady-state probabilities for the fault-free operation (i.e., π_n) should be used as the initial state probabilities for the faulty operation. The Markov process considered here is an ergodic Markov process; aperiodic and positive recurrent. For an ergodic process, the steady-state invariant vector is unique [48]. Therefore the Markov process in the faulty operation always has this unique steady-state invariant vector as initial condition.

If the system transfers from fault-free to faulty state at time t_f, using the forward Chapman-Kolmogorv equations [48], probabilities of alarm and no-alarm states can be calculated as

$$\begin{aligned} [P_{NA}(t_f) \;\; P_A(t_f)] &= [P_{NA}(t_f-1) \;\; P_A(t_f-1)]\, \mathbf{P}_f \\ &= \pi_n \mathbf{P}_f = \begin{bmatrix} \dfrac{p_1q_1+p_2(1-q_2)}{p_1+p_2} & \dfrac{p_2q_2+p_1(1-q_1)}{p_1+p_2} \end{bmatrix} \end{aligned} \tag{3.5}$$

Therefore the probability of detection delay zero (probability of alarm being raised immediately after transition from normal to abnormal) is

$$\begin{aligned} \mathbb{P}(\mathrm{DD}=0) &= \mathbb{P}(\mathrm{A \ at \ } t=t_f) \\ &= P_A(t_f) = \frac{p_2q_2+p_1(1-q_1)}{p_1+p_2} \end{aligned} \tag{3.6}$$

Threshold, y_{tp}	0	0.5	1	1.5	2.01	3.01
EDD for						
x=1	0.1	0.22	0.40	0.65	1.00	2.27
x=2	0.03	0.10	0.03	0.59	0.98	2.26
x=3	0.01	0.02	0.09	0.38	0.91	2.26
x=4	0.01	0.004	0.01	0.08	0.54	2.25

Table 3.2: Effect of threshold change on expected detection delays for different deadbands (x)

The probability of detection delay 1 is

$$\begin{aligned}\mathbb{P}(\mathrm{DD}=1) &= \mathbb{P}(\mathrm{A\ at\ } t=t_f+1 \ \&\ \mathrm{NA\ at\ } t=t_f) \\ &= \mathbb{P}(\mathrm{NA\ at\ } t=t_f)\ \ \mathbb{P}(\mathrm{A\ at\ } t=t_f+1\ |\mathrm{NA\ at\ } t=t_f) \\ &= \frac{p_1q_1+p_2(1-q_2)}{p_1+p_2}\times q_2\end{aligned} \tag{3.7}$$

where the first term is calculated from Chapman Kolmogorov equation discussed earlier in this section and second term from the transitional probability matrix $\mathbf{P}_f$.

Probabilities of higher detection delays can be similarly expressed in terms

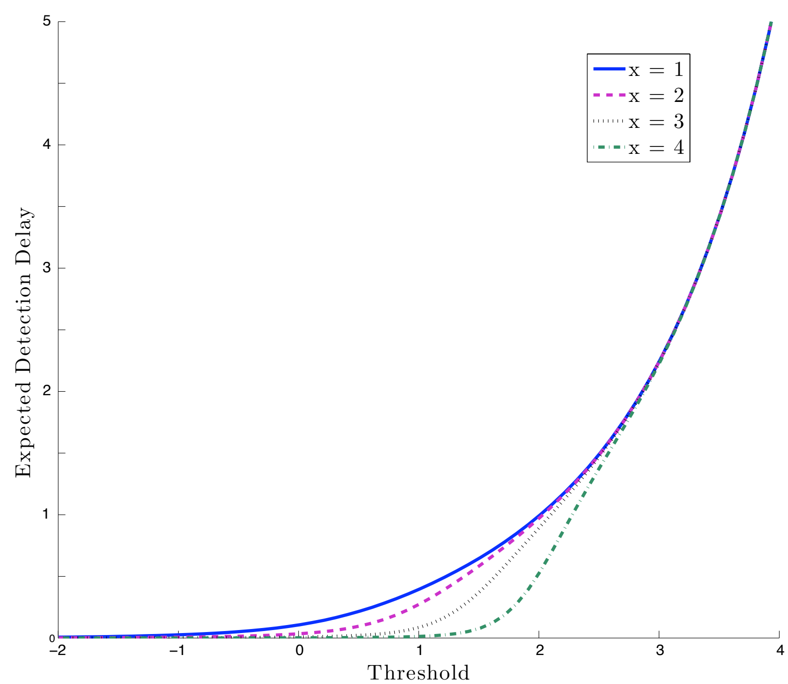

Figure 3.3: Changes in expected detection delays for different deadbands

of conditional probabilities as

$$
\begin{aligned}
\mathbb{P}(\mathrm{DD}=2) =& \mathbb{P}(\text{A at } t=t_f+2 \ \& \ \text{NA at } t=t_f+1, \text{ NA at } t=t_f) \\
=& \frac{p_1q_1+p_2(1-q_2)}{p_1+p_2} q_2(1-q_2) \\
& \vdots \\
\mathbb{P}(\mathrm{DD}=z) =& \mathbb{P}(\text{A at } t=t_f+z \ \& \ \text{NA at } t=t_f+z-1, \ \dots \ , \\
& \qquad \text{NA at } t=t_f) \\
=& \frac{p_1q_1+p_2(1-q_2)}{p_1+p_2} q_2(1-q_2)^{z-1}, \qquad z \geq 1
\end{aligned} \tag{3.8}
$$

The average detection delay (i.e., the expected value of the detection delay) is then given by

$$
\begin{aligned}
\mathrm{EDD} = \mathbb{E}(\mathrm{DD}) =& \sum_{z=0}^{\infty} z \ \mathbb{P}(\mathrm{DD}=z) \\
=& \sum_{z=1}^{\infty} z \ q_2(1-q_2)^{z-1} \frac{p_1q_1+p_2(1-q_2)}{p_1+p_2} = \frac{p_1q_1+p_2(1-q_2)}{q_2(p_1+p_2)}
\end{aligned} \tag{3.9}
$$

In Fig. 3.3, changes in detection delays due to different deadbands configured on the process data of Fig. 3.1 are presented. In industry, the normal operating range of a process variable is known and the deadband is defined as a certain percentage (%) of that range. However, since the normal operating range is unknown here, we define the deadband as the absolute number (in terms of units of measurement of the process variable). So, for example for a high alarm limit y_{tp}, x unit of deadband means the alarm will be cleared at $y_{tp} - x$. The threshold limit (y_{tp}) is moved from minimum of the process data to its maximum value with x unit $[x = 1, 2, 3, 4]$. It can be seen from Table 3.2, for the considered process data, when deadband is changed from $x = 1$ to $x = 4$, expected detection delay varies. For higher deadbands [*e.g.* $x = 4$] detection-delay remains low compared to lower ones till about $y_{tp} = 2.5$. After this point, changes in detection delay are almost the same for all x. This is quite expected as very few samples will be able to cross that high threshold of y_{tp}. Beyond that limit, only threshold (y_{tp}) is dominant in expected detection delay and deadband (x) has hardly any role for the considered process data.

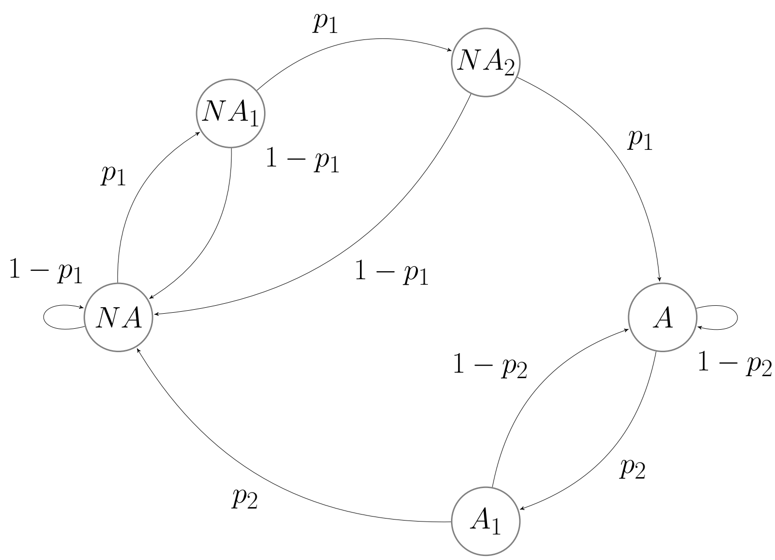

Figure 3.4: Markov diagram of a system with delay-timer $n = 3$ and $m = 2$ in the fault-free region of operation

3.3 Detection Delay for Delay-timers

A delay-timer is a simple yet effective technique that can reduce the number of false and nuisance alarms significantly. By their intuitive nature, human beings prefer to wait for a while before reacting to an abnormality to avoid any temporary overreaction or underreaction. Delay-timers use the same concept in alarm generation. If a delay-timer is configured on a variable, the alarm is raised if n consecutive samples cross the alarm limit (y_{tp}). This case is known as on-delay. Similarly, once the alarm is raised, it will only be cleared if m consecutive samples go below the limit, known as off-delay. For on-delay, if the system goes back to normal operating state during the intermediate states, alarm is not activated and vice-versa for the off-delay case. Alarm standards (EEMUA [19] and ISA [18]) recommend some values for delay-timers based on the nature of the process variable. Similar to the deadband case, we can model the alarm/no-alarm states of a process variable with delay-timers by Markov chains [13]. Fig. 3.4 shows the Markov model of a system in its fault-free operation with $n = 3$ samples on-delay and $m = 2$ samples off-delay. A similar Markov model with probabilities q_1 and q_2 can be constructed for the faulty region of operation.

In Fig. 3.4, assuming NA or no alarm state is the initial state for the process, $1-p_1$ denotes the probability that it will remain in the same state. If the next sample exceeds alarm threshold with probability p_1 then it moves to state NA_1, which is the first intermediate state for $3-$samples delay case before going to alarm state. Exceeding threshold by consecutive $3-$samples with probability p_1 will take the system to the alarm state. If in between the states NA and NA_2, any sample falls below threshold with probability $1-p_1$, then system will go back to no alarm state. Only consecutive 3-sample crossing over threshold can raise the alarm, taking the system to the alarm state. Once the system goes to alarm state, to clear the alarm same principal is followed as raising. Consecutive 2 samples falling below threshold with probability p_2 (where $p_2 = 1-p_1$) can only clear the alarm. In intermediate states as output, the system will always provide either alarm or no alarm, depending on from where these intermediate states started. Transitional probability matrices for $n-$samples on-delay and $m-$samples off-delay for both the fault-free ($\mathbf{P}_n$) and faulty ($\mathbf{P}_f$) region of operations are given by

$$\mathbf{P}_n = \left[\begin{array}{cc} \mathbf{P}_{n11} & 0_{n\times(m-1)} \\ \hline \mathbf{P}_{n21} & \mathbf{P}_{n22} \end{array}\right],\ \mathbf{P}_f = \left[\begin{array}{cc} \mathbf{P}_{f11} & 0_{n\times(m-1)} \\ \hline \mathbf{P}_{f21} & \mathbf{P}_{f22} \end{array}\right] \tag{3.10}$$

where,

$$\mathbf{P}_{n11} = \begin{pmatrix} 1-p_1 & p_1 & 0 & \cdots & 0 \\ 1-p_1 & 0 & p_1 & \cdots & 0 \\ \vdots & \vdots & \vdots & \ddots & \vdots \\ 1-p_1 & 0 & 0 & \cdots & p_1 \end{pmatrix},$$

$$\mathbf{P}_{n21} = \begin{pmatrix} 0 & 0 & \cdots & 0 \\ \vdots & \vdots & \vdots & \vdots \\ 0 & 0 & \cdots & 0 \\ p_2 & 0 & \cdots & 0 \end{pmatrix}, \mathbf{P}_{n22} = \begin{pmatrix} 1-p_2 & p_2 & 0 & \cdots & 0 \\ 1-p_2 & 0 & p_2 & \cdots & 0 \\ \vdots & \vdots & \vdots & \ddots & \vdots \\ 1-p_2 & 0 & 0 & \cdots & p_2 \\ 1-p_2 & 0 & 0 & \cdots & 0 \end{pmatrix},$$

here, horizontal line in $\mathbf{P}_n$ is used to indicate, number of columns in $\mathbf{P}_{n11}$ and $\mathbf{P}_{n21}$ or in $0_{n\times(m-1)}$ and $\mathbf{P}_{n22}$ are not equal; similarly for $\mathbf{P}_f$. Furthermore $\mathbf{P}_{f11}, P_{f21}$ and $\mathbf{P}_{f22}$ have the same structures as $\mathbf{P}_{n11}, \mathbf{P}_{n21}$ and $\mathbf{P}_{n22}$ respectively, only p_1 and p_2 are replaced by q_2 and q_1. $\mathbf{P}_{n11}$ and $\mathbf{P}_{f11}$ are $n\times(n+1)$;

$\mathbf{P}_{n21}$ and $\mathbf{P}_{f21}$ are $m \times n$; and $\mathbf{P}_{n22}$ and $\mathbf{P}_{f22}$ are $m \times m$. Hence, $\mathbf{P}_n$ and $\mathbf{P}_f$ are of dimensions $(n+m) \times (n+m)$.

Similar to the deadband case, at the moment of fault occurrence, the Markov model of the system switches from the fault-free model (represented by $\mathbf{P}_n$) to the faulty model (represented by $\mathbf{P}_f$). Therefore, to calculate the probabilities of the state after fault occurrence, $\mathbf{P}_n$ is assumed to reach its steady state; and the steady state probabilities of the fault-free model, should be used as initial states for the faulty model. The steady state vector of probabilities for the fault-free state of operation (e.g., the invariant vector for $\mathbf{P}_n$) is [13]

$$\pi_n = \frac{1}{p_2^m \sum_{i=0}^{n-1} p_1^i + p_1^n \sum_{j=0}^{m-1} p_2^j} \times \begin{bmatrix} p_2^m & p_1 p_2^m & \cdots & p_1^{n-1} p_2^m & p_1^n & p_2 p_1^n & \cdots & p_2^{m-1} p_1^n \end{bmatrix} \tag{3.11}$$

To calculate the detection delay for delay-timers, we use the concept of *hitting time* [48]. In our context, hitting time is the minimum number of samples required for system currently in the no-alarm state to switch to the alarm state for the first time.

We divide the whole state space into two subspaces. The first subspace, denoted by $\mathcal{D}$, contains all the no-alarm state(s) $(NA, ..., NA_{n-1})$. The second subspace contains all the alarm state(s) $(A, ..., A_{m-1})$ and is denoted by $\mathcal{E}$. With these definitions, the detection delay is the same as the hitting time: the time required to switch to states $\mathcal{E}$, assuming the system is initially started in states $\mathcal{D}$.

Let $\mathbf{Q}$ be the matrix of transitional probabilities from $\mathcal{D}$ to itself in the faulty region. $\mathbf{Q}$ is obtained from $\mathbf{P}_f$ by keeping all the probabilities corresponding to no-alarm states and replacing all other probabilities with zero. For the Markov process in Fig. 3.4, $\mathbf{Q}$ is

$$\mathbf{Q} = \left[\begin{array}{cc} \mathbf{P}_{f11} & 0_{n\times(m-1)} \\ \hline 0_{m\times n} & 0_{m\times m} \end{array}\right] \tag{3.12}$$

It can be shown that probability of $z-$sample detection delay for delay-timer (e.g., hitting time for switching from no-alarm states $\mathcal{D}$, to alarm states $\mathcal{E}$) is given by

$$\mathbb{P}(\mathrm{DD} = z) = \pi_n \mathbf{P}_f \mathbf{Q}^z \left[0 \cdots 0 \; 1 \cdots 1\right]^T \tag{3.13}$$

Here in the column vector there are n zeros and m ones. Similar to Section 3.2, if the system transfers from fault-free to faulty state at time t_f, using the forward Chapman-Kolmogorv equations [48], probabilities of alarm and no-alarm states can be calculated as

$$\begin{aligned}
&[P_{NA}(t_f) \;\; P_{NA_1}(t_f) \;\; \cdots P_{NA_{n-1}}(t_f) \;\; P_A(t_f) \\
&\qquad P_{A_1}(t_f) \;\; \cdots \;\; P_{A_{m-1}}(t_f)] \\
&= [P_{NA}(t_f-1) \;\; P_{NA_1}(t_f-1) \;\; \cdots P_{NA_{n-1}}(t_f-1) \;\; P_A(t_f-1) \\
&\qquad P_{A_1}(t_f-1) \cdots \;\; P_{A_{m-1}}(t_f-1)] \, \mathbf{P}_f \\
&= \pi_n \mathbf{P}_f
\end{aligned} \tag{3.14}$$

Let $\phi_0 = \pi_n \mathbf{P}_f$. Then the distribution at time z, ϕ_z, is given by $\phi_z = \phi_0 \mathbf{P}_f^z$ [48]. Now, the interest is to calculate the detection delay - time required to move from *no alarm* states to *alarm* states in the Markov chain. Therefore in the transitional probability matrix $\mathbf{P}_f$, rows representing *no alarm* states are required only and in the equation of the probability of detection delay, $\mathbf{P}_f$ is replaced by the substochastic matrix $\mathbf{Q}$, where all probabilities in *alarm* state rows are zeros :

$$\mathbf{Q} = \left[\begin{array}{cc} \mathbf{P}_{f11} & \mathbf{P}_{12} \\ \hline 0_{m\times n} & 0_{m\times m} \end{array}\right] \tag{3.15}$$

Finally, the structure of the column vector with n zeros and m ones is quite self explanatory. At time z, the sum of all *alarm* state probabilities will provide the probability of detection delay at that moment.

The expected detection delay for delay-timer can then be expressed as (proof in Appendix A)

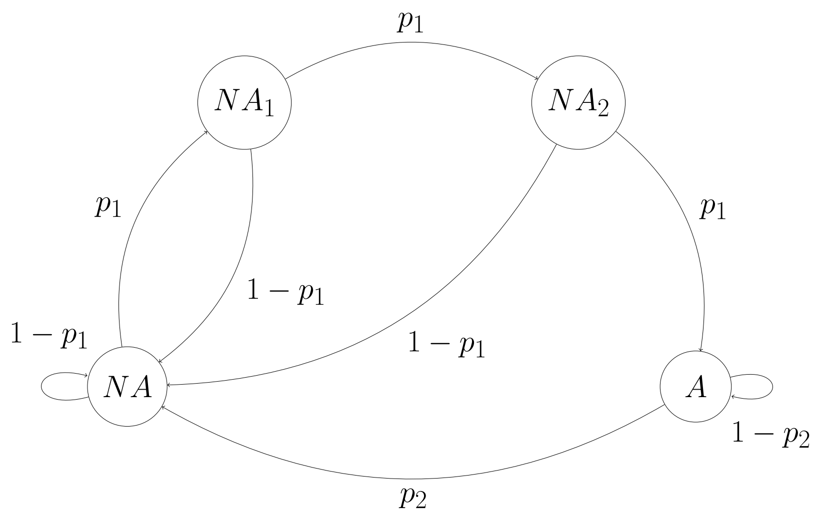

Figure 3.5: Markov diagram of a system with 3-sample on-delay-timer only in the normal region of operation

$$
\begin{aligned}
\text{EDD} = \mathbb{E}(\text{DD}) &= \sum_{z=0}^{\infty} z\ \mathbb{P}(\text{DD} = z) = \pi_n \mathbf{P}_f \mathbf{Q}(I-\mathbf{Q})^{-2}\left[0\cdots 0\ 1\cdots 1\right]^T \\
&= \frac{p_2^{m-1}\left(p_1^n q_1 \sum_{i=0}^{n-1} q_2^i + p_2\left(\sum_{j=0}^{n-1} p_1^j \sum_{k=0}^{n-j-1} q_2^k - q_2^n \sum_{i=0}^{n-1} p_1^i\right)\right)}{q_2^n\left(p_2^m \sum_{i=0}^{n-1} p_1^i + p_1^n \sum_{i=0}^{m-1} p_2^i\right)}
\end{aligned} \tag{3.16}
$$

Since $\mathbf{Q}$ is a *substochastic matrix*, i.e. a matrix with nonnegative entries whose row sums are less than or equal to 1 and $\mathbf{Q}^n \to 0$ as $n \to \infty$; therefore, all eigenvalues of $\mathbf{Q}$ have absolute values strictly less than 1; and the series in the summation converges [48].

Special cases

Detection delays for delay-timers are calculated so far for $n-$samples on-delay and $m-$samples off-delay. Some special cases based on these n and m will be discussed now.

3.3.1 No Delay-timer

In this case $n = 1$ and $m = 1$. The expected detection delay is then simplified to

$$\mathbb{E}(\mathrm{DD}) = \frac{p_1 q_1 + p_2(1 - q_2)}{q_2(p_1 + p_2)} \tag{3.17}$$

which is consistent with the result we obtained in Section 3.2 for deadbands. Furthermore if we assume there is no deadband, then $p_2 = 1-p_1$ and $q_2 = 1-q_1$ and the result is further simplified to

$$\mathbb{E}(\mathrm{DD}) = q_1(1 - q_1)^{-1} \tag{3.18}$$

which is again consistent with the result obtained in Section 3.1 for the simple case (no deadband, no delay-timer).

3.3.2 Pure On-delay

In this case, only on-delay timer is configured, i.e., $m = 1$. To raise an alarm, n consecutive samples should cross the threshold limit. But once the alarm is raised, it will be cleared right away if one sample goes below the threshold (Fig. 3.5). In this case the expected detection delay can be simplified to

$$\mathbb{E}(\mathrm{DD}) = \frac{p_1^n q_1 \sum_{i=0}^{n-1} q_2^i + p_2 \left(\sum_{j=0}^{n-1} p_1^j \sum_{k=0}^{n-j-1} q_2^k - q_2^n \sum_{i=0}^{n-1} p_1^i \right)}{q_2^n \left(p_1^n + p_2 \sum_{i=0}^{n-1} p_1^i \right)} \tag{3.19}$$

3.3.3 Pure Off-delay

In this case only off-delay is configured and on-delay is one sample, e.g., $n = 1$. After an alarm is raised by one sample crossing the alarm limit, m consecutive samples should fall within the acceptable limits before the alarm is cleared. The expected detection delay for $m-$sample off-delay case is expressed by

$$\mathbb{E}(\mathrm{DD}) = \frac{p_2^{m-1} \left(p_2 - p_2 q_2 + p_1 q_1\right)}{q_2 \left(p_2^m + p_1 \sum_{i=0}^{m-1} p_2^i \right)} \tag{3.20}$$

In Fig. 3.7, Monte Carlo simulations [50] to verify the expected detection delay (EDD) expression is presented. The expected detection delay is plotted for different delay-timers (assuming $m = n$) as a function of the threshold. Monte Carlo simulation is shown for two different distributions, *Gaussian* and *Gamma*. Fault-free data has mean 0 and variance 1; faulty data has mean 2 and variance 2. The threshold was changed from 0 to 1.4 with an increment of 0.1. The data was simulated for 2000 iterations and the mean EDD was estimated for each value of the threshold. The proposed EDD equation is also plotted with Monte Carlo simulation. It can be seen that, there is very negligible differences between the Monte Carlo simulations and the calculated EDD by our formula.

3.4 Design of Alarm Systems

Generally, alarm systems can be designed in two frameworks: univariate and multivariate. In univariate design, which is the most commonly practiced method of alarming, the alarm limits and processing technique (deadband, delay-timer, filter, etc.) are individually designed for each process variable.

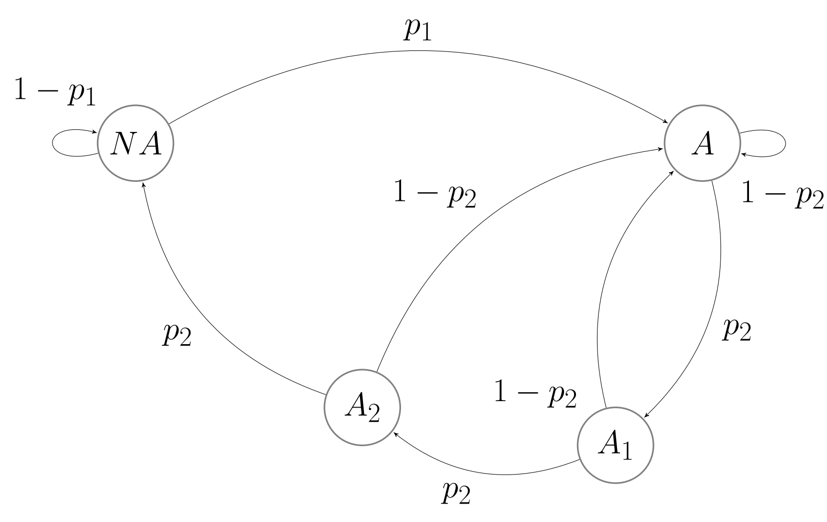

Figure 3.6: Markov diagram of a system with 3-sample off-delay-timer only in the normal region of operation

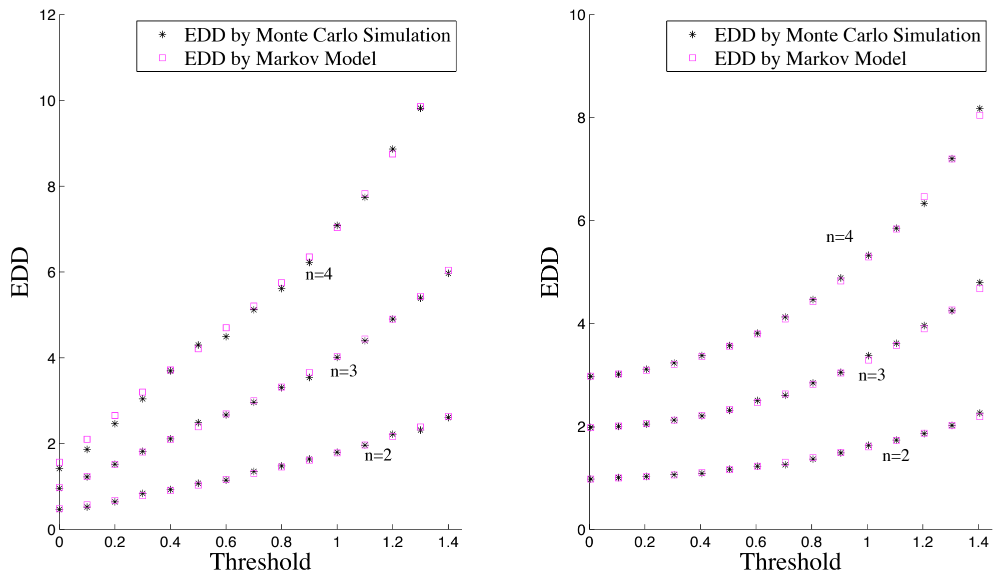

Figure 3.7: Verification of the EDD formula by Monte-Carlo simulation: (left) assuming Gaussian data distribution; (right) assuming Gamma data distribution

In multivariate design, alarms are designed for some latent variables which are typically linear combinations of multiple process variables. In this section, we propose a technique for univariate alarm design. For multivariate design, several data-mining methods are available to detect statistical similarities, group correlated alarms and apply multivariate analysis for rationalization [25, 11].

An alarm design procedure is described in [13] based on the receiver operating characteristic (ROC) curve. The ROC curve is the plot of the probability of missed alarms versus the probability of false alarms when the alarm limit or threshold changes from $-\infty$ to $+\infty$. As it can be seen in Fig. 3.8, lowering the trip point decreases the probability of false alarms, but the probability of missed alarms will increase. The ROC curve shows this trade-off between false alarm and missed alarm rates when the trip point changes. A typical ROC curve is shown in Fig. 3.8 [right] for the corresponding fault-free and faulty data. However, setting the threshold merely based on these two facts may not be desirable as it does not consider detection delay.

In the rest of this section, we focus our design on delay-timers only. For

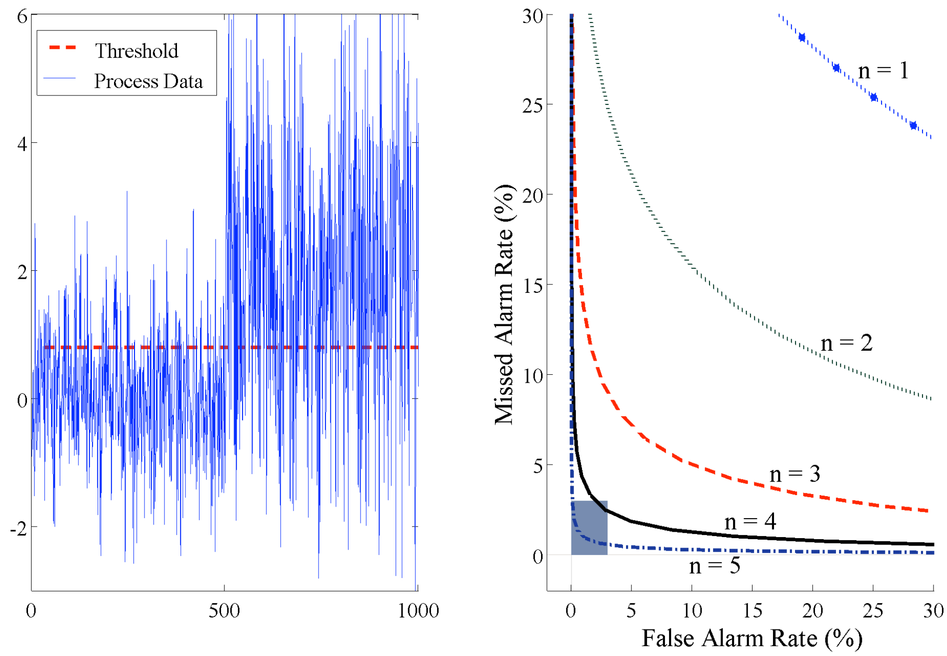

Figure 3.8: Process data (left); ROC curve for different delay-timers (right)

a given set of normal and abnormal data, the design parameters are then the threshold (y_{tp}), the number of on-delay samples (n) and number of off-delay samples (m). For simplicity we assume $m = n$. An acceptable design should not only minimize false and missed alarm rates, but also guarantee a small detection delay. Therefore, for design of an alarm system, three performance specifications are to be considered: false alarm rate (FAR), missed alarm rate (MAR) and expected detection delay (EDD). For practical design, however, the false and missed alarm rates are usually combined in a function that measures how far a point on the ROC curve is from the ideal point (zero false alarm and zero missed alarm). In most cases the ROC curve is symmetrical, and it can be assumed that at the optimal point FAR and MAR are approximately equal. Therefore for simplicity we assume the optimal point is approximately the point where FAR = MAR in design. For simulations, assume the fault-free part of the data has a Gaussian distribution with average of 0 and variance 1. The faulty part of the data has also a Gaussian distribution with average 2 and variance 2. The data is sampled at 1 *sec* rate. To design a system with requirements FAR $\leq 4\%$, MAR $\leq 3\%$ and EDD ≤ 6 samples, a four-step procedure is followed.

In Fig. 3.8, the delay timer is changed to different values and the corresponding ROC curves are plotted; it can be seen that as the delay timer is increasing, the ROC curve is moving closer to the origin [13]. On the other hand this increase of delay timer increases the expected detection delay as well. Fig. 3.10 shows the expected detection delay for different delay timers for the threshold where FAR = MAR; these equal thresholds were estimated from Fig. 3.9, where FAR and MAR are plotted with corresponding threshold limits and the intersecting points provide the required estimations. It can be seen that as the threshold is increased the FAR decreases but the MAR increases. The intersecting points of these two lines are the points of equal FAR and MAR for different delay-timers.

Step 1

In this step, alarm thresholds that satisfy the optimality condition FAR = MAR are estimated. These thresholds can be estimated from Fig. 3.9. For the given process data, thresholds corresponding to the point of equal FAR and

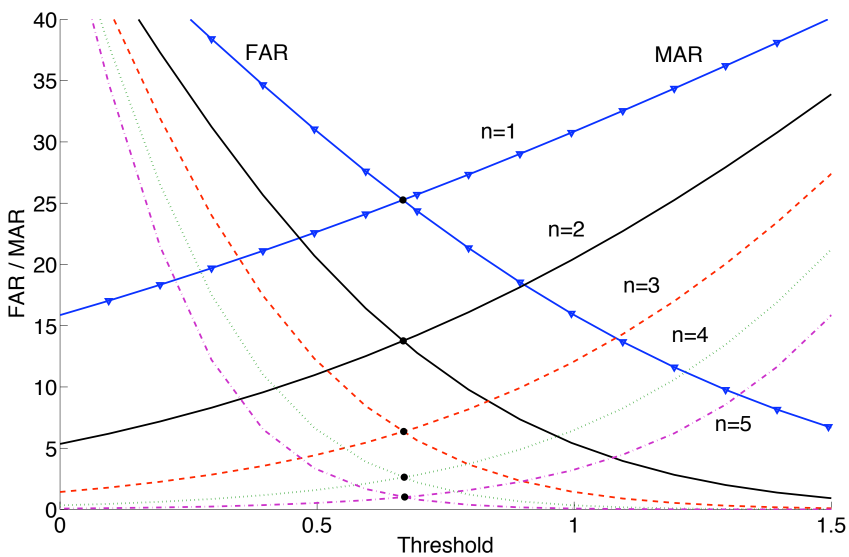

Figure 3.9: Estimation of the threshold when FAR = MAR

MAR are shown by dots, for different values of delay timers. The estimated thresholds are given in Table 3.3.

Step 2

In step 2, the smallest delay-timer n_1 is selected from Fig. 3.9 or Table 3.3 such that FAR = MAR $\leq 3\%$; where $n \geq n_1$. The corresponding area for FAR and MAR (for $\leq 3\%$) is shown by the shaded area in Fig. 3.8. The smallest delay-timer that satisfies the condition is $n_1 = 4$. Though the design requirement was for FAR $\leq 4\%$, n_1 is selected for the one with lower percentage ($\leq 3\%$) requirements among FAR and MAR. Since n_1 is selected for a more conservative range, the selected delay-timer does not violate the original requirements and is expected to provide better performance.

Step 3

The EDD is taken into account in step 3 for the design of delay-timer. The largest value of delay-timer n_2 is selected such that EDD ≤ 6; where $n \leq n_2$. From Fig. 3.10, $n_2 = 4$.

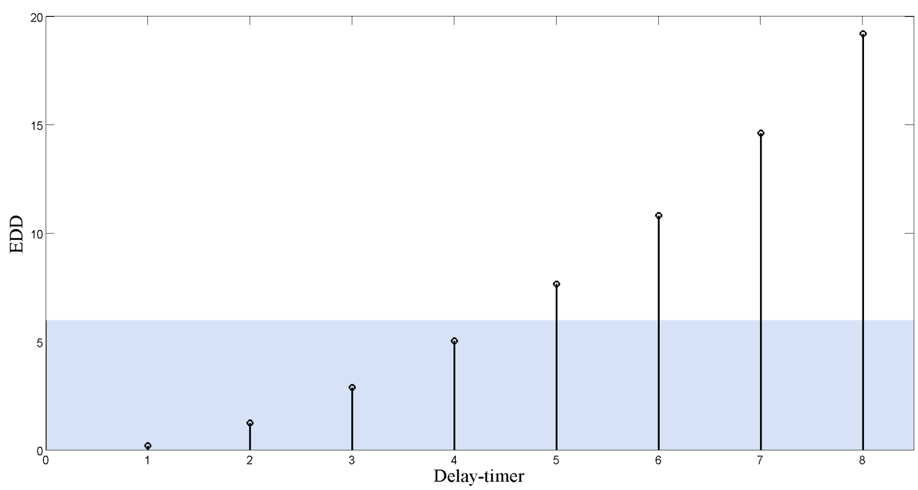

Figure 3.10: Effect on EDD for different delay-timers

Table 3.3: Design parameter selection chart for delay-timers

Delay-timer (n)	Threshold (y_{tp})	FAR = MAR (%)	EDD
1	0.67	25.26	0.21
2	0.67	13.76	1.26
3	0.67	6.37	2.89
4	0.67	2.63	5.04
5	0.67	1.01	7.66

Step 4

Once n_1 and n_2 are estimated, the next step is to select the range of delay timers to finalize the design process. If $n_2 \geq n_1$, any n satisfying $n_1 \leq n \leq n_2$ is a solution of the delay-timer. Here the only delay-timer that satisfies the condition is, $n = 4$; from Table 3.3 the shaded row is the solution of given design problem. $n = 3$ satisfies the condition of EDD but does not satisfy the requirement of FAR / MAR; other delay-timers also do not satisfy requirements. The optimum threshold of operation is 0.67 and delay-timer is 4 samples, and it is expected to take 5.04 samples to raise the alarm.

If such a range of delay-timer cannot be found; or in other words, if no such n exists to satisfy $n_1 \leq n \leq n_2$, design requirements need adjustments. Less demanding design requirements are recommended for such cases. For example, if the requirement of EDD is changed to no more than 3 *samples*, this particular process data cannot satisfy the requirement and no solution exists. Therefore this technique can also be applied to check whether the design requirement of FAR, MAR, and EDD are achievable or not.

A Monte Carlo simulation was performed to check consistency of the calculated values. Setting the threshold to 0.67, associated false alarm rates, missed alarm rates and detection delays were calculated. From a Monte Carlo simulation of 5000 iterations (for Gaussian distributed fault-free data with mean 0, variance 1 and faulty data with mean 2 and variance 2), the calculated FAR is 2.58%, MAR is 2.84 %, and detection delay is 4.92 samples. Which are consistent with the theoretical values.

3.5 Conclusion and Future Work

The expected detection delay, as a measure of the time it takes for the alarm system to respond to a fault, is an important parameter in the design of alarm systems. In this chapter, the expected detection delay is calculated for two common techniques in alarm systems, namely, deadbands and delay-timers. We also presented a simple design procedure, based on three important performance measures of an alarm system: false alarm rate, missed alarm rate and the expected detection delay. To show the utility of the proposed method two case studies are discussed later in application chapter. The proposed method can also be applied to identify inconsistencies among design requirements and investigate whether desired performance is achievable or not. As a future extension, a more systematic approach to the design of parameters of the alarm system (on-delay timer, off-delay timer and the trip-point) can be considered.

Chapter 4

Detection Delays for Filters

In modern DCS based systems, measured process signals are often filtered in various ways. Primarily, filtering is applied to reduce noise in signals that may affect control performance [39]. However there has been very limited study on performance specifications of various alarm filtering methods, and the quantitative relations between filter properties and alarm performance indices are not well known. In this chapter[1], we investigate the effect of filtering on detection delay which is an important alarm performance index.

The rest of the chapter is organized as follows: in Section 4.1, the role of filtering in alarm design is discussed. Section 4.2 discusses relevant works in literature and the problem formulation. The detection delay for moving average filter is calculated in Section 4.3. Selection of the trip point and filter order are presented in Section 4.4. In Section 4.5, concluding remarks and future work are discussed.

4.1 Filters in Alarm Management

The effectiveness of filtering in reducing false and nuisance alarms is mentioned in [12, 13]. One of the main reasons of false and nuisance alarms is the presence of noise in signals. This noise may cause chattering effect for a fixed threshold, and by filtering, chattering can be reduced. The down side, however, is that

[1] Sections of this chapter has been published as: N. A. Adnan, and I. Izadi, *On detection delays of filtering in industrial alarm systems*, in proceedings of the 21st Mediterranean Conference on Control and Automation, pp. 113-118, June 25-28, 2013, Crete, Greece.

filtering introduces delay in detection of the fault and activation of alarms. For example, a 10-sample moving average filter may reduce the effect of noise in the signal significantly; but it may delay activation of alarm due to the averaging.

Detailed calculation of detection delays for deadbands and delay-timers are discussed in [24, 33]. Some preliminary discussions of this performance index is discussed for the filtering technique in [13]. However, discussion on filtering is mainly based on simulation and no exact quantitative relation is given. In [41], the detection delay is discussed for some techniques including filters and an expression is given to compute expected detection delay for moving average filters. However, in this study for moving average filter the correlation among contiguous samples of filtered data is ignored. If the process data, $X_i, i \in Z^+$, is independent and identically distributed (IID), once filtered the data no longer remains independent.

In this chapter, we address the issue of detection delay for moving average filters. The detection delay for other filter types of filters may be addressed as an extension of this work. In the following sections, while computing the detection delay, the correlation factor among contiguous samples is taken into consideration.

In the study of alarm systems, generally a discrete time random variable is monitored to raise or clear an alarm. Suppose an independent random observation $\{X_i\}_{i\geq 1}$ is collected, such that $X_1, X_2, X_3 \cdots, X_{t_f}$ are each distributed according to a probability distribution function (PDF) p_n known a priori and $X_{t_f+1}, X_{t_f+2}, X_{t_f+3} \cdots$ each belongs to a PDF p_{ab}, also known. Here, p_n and p_{ab} are PDFs of X_i in normal and abnormal conditions of the process operation respectively. Generally, to raise an alarm X_i is monitored, processed, and compared with a limit or trip point y_{tp}.

In Fig 4.1, the normal data is Gaussian distributed with mean 0 and variance 1, and abnormal data is also Gaussian distributed with mean 3 and variance 4. When the high alarm limit y_{tp} is set at 1.7, it causes 39 false alarms and 263 missed alarms but alarms are activated almost instantly. However,

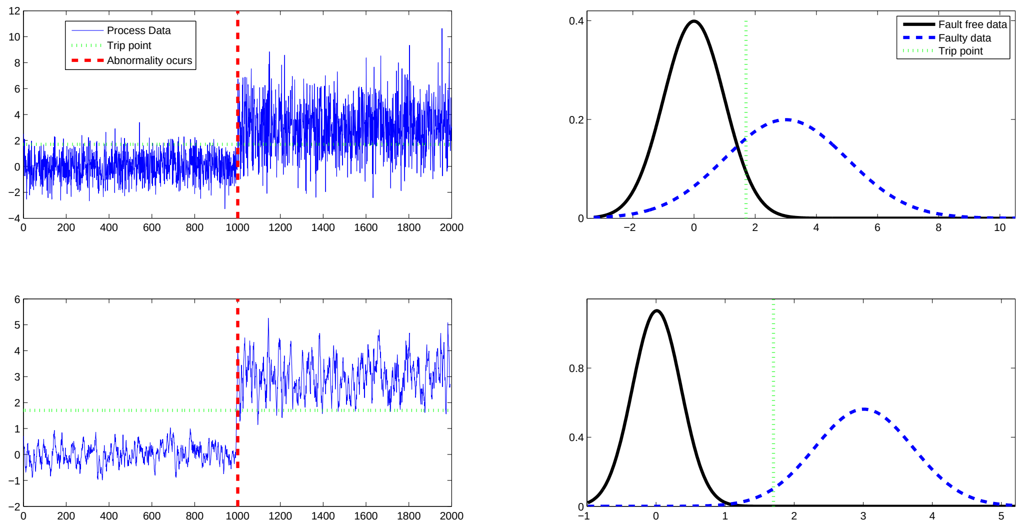

Figure 4.1: Raw process data and corresponding PDFs (top); filtered process data (moving average filter of window size 8) and corresponding PDFs (bottom)

when a moving average filter of order 8 is applied on the process data, accuracy increases significantly by reducing false alarms to 0 and missed alarm to 31 [Fig 4.1 (bottom)]. On the other hand it introduces 6 seconds delay in alarm activation. It is therefore important to know how alarm settings affect these performance indices. Knowing the quantitative relationship is an essential requirement for efficient alarm systems design. In the following sections, calculation of the detection delay is discussed for moving average filters.

4.2 Problem Formulation

In practice, when the process moves from "normal" to "abnormal", one of the aims of alarm design is to detect the change as quickly as possible. However, this is not always achievable as swiftness of alarm activation is greatly dependent on the design technique (e.g., delay-timers, deadbands, and filtering) and parameter selection. For example, there is a common conception that a 10-second delay-timer will delay the alarm activation by about 10 seconds [12]. This is hardly true in practice. In [24], it is shown that actual activation delay of a 10-second delay-timer varies based on types of data distribution, trip point y_{tp} and a number of other factors. Let t_a be the time that alarm is activated. If fault occurs at time t_f, then the detection delay is defined as

$$\mathrm{DD} = t_a - t_f \tag{4.1}$$

For an independent random observation X_i, a causal filter of length m is an operator defined as

$$Z_k = f(X_k, X_{k-1}, \cdots, X_{k-m}) \tag{4.2}$$

It can be shown that, if normal and abnormal data follows Gaussian distributions and only change in mean is considered because of abnormality, the optimal linear filter in terms of accuracy of design is a moving average filter [51, 52]. Since most often an abnormality in the process moves the operating point, changes in mean of the variable is the most common type of problem [13]. Therefore, this work focuses on moving average filter and associated detection delay calculation. The goal of the work is to establish quantitative relationship between the trip point, filter order and the detection delay. For simplicity, Gaussian distribution is considered; however, the method works for any other distributions. No particular assumption on distribution is necessary in practice as the PDF can be estimated empirically from historical data.

4.3 Moving Average Filters

The two most commonly used filters in industry are the moving average and the exponentially weighted moving average filters. A moving average filter is easy to implement and particularly useful in removing noise from process data. It is also widely used to separate frequency components, extract features and remove periodic effects when computed with the length of known periodicity. From Fig 4.1, it can be seen that the application of a moving average filter significantly reduced noise in process data making the trip point more effective in generating an alarm with higher accuracy. However, at the same time the filtering introduced higher detection delay. A filter is particularly effective when it increases accuracy by reducing FAR and MAR with a minimum detection delay.

A moving average filter is defined as

$$Z_i = \frac{1}{m}(X_{i-m+1} + \cdots + X_{i-1} + X_i), \tag{4.3}$$

where m is the order of the filter to be designed and X is the pre-filtered process data.

Filter of order 2

If pre-filtered data is assumed to be independent and identically distributed (IID) with a Gaussian distribution, filtered data is also Gaussian distributed. Let the normal and abnormal data follow Gaussian distributions with $\mathcal{N}(\mu_n, \sigma_n^2)$ and $\mathcal{N}(\mu_{ab}, \sigma_{ab}^2)$ respectively.

We first calculate the detection delay for a moving average filter of size 2 and then discuss the general case. Assume that the fault occurs at time t_f. For the moving average filter of order 2, the probability of the alarm being raised at time t_f (i.e., detection delay (DD) equals zero) is given by

$$\begin{aligned} \mathbb{P}(\mathrm{DD} = 0) =& \mathbb{P}\{X_{t_f-1} + X_{t_f} > 2y_{tp}\} = \mathbb{P}\{Z_{t_f} > 2y_{tp}\} \\ =& \int_{2y_{tp}}^{\infty} f(Z_{t_f})\, dZ_{t_f} \end{aligned} \tag{4.4}$$

where, $Z_{t_f} (= X_{t_f-1} + X_{t_f}) \sim \mathcal{N}(\mu_n + \mu_{ab}, \sigma_n^2 + \sigma_{ab}^2)$ and the distribution function is given by [47]

$$f(Z_{t_f}) = \frac{1}{\sqrt{2\pi(\sigma_n^2 + \sigma_{ab}^2)}} \exp\left\{ -\frac{[Z_{t_f} - (\mu_n + \mu_{ab})]^2}{2(\sigma_n^2 + \sigma_{ab}^2)} \right\} \tag{4.5}$$

The probability of detection delay being 1 (i.e., there is no alarm at time t_f and alarm is raised at time $t_f + 1$) is calculated as

$$\begin{aligned} &\mathbb{P}(\mathrm{DD} = 1) \\ &= \mathbb{P}\{[X_{t_f-1} + X_{t_f} \leq 2y_{tp}] \;\&\; [X_{t_f} + X_{t_f+1} > 2y_{tp}]\} \\ &= \mathbb{P}\{[Z_{t_f} \leq 2y_{tp}] \;\&\; [Z_{t_f+1} > 2y_{tp}]\} \\ &= \int_{-\infty}^{2y_{tp}} \int_{2y_{tp}}^{\infty} f(Z_{t_f}, Z_{t_f+1})\, dZ_{t_f} dZ_{t_f+1} \end{aligned} \tag{4.6}$$

Here filtered data Z_{t_f} and $Z_{t_{f+1}}$ are no longer independent as they have X_{t_f} common in them; and only mean and variance are not sufficient to model the detection delay. Their covariance has to be considered with joint probability distribution. The computation of the joint probability requires the calculation of associated mean and covariance matrix.

The joint distribution function in equation (4.6) is given by

$$
\begin{aligned}
f(Z_{t_f}, Z_{t_f+1}) = & \frac{1}{2\pi\sqrt{\sigma_1\sigma_2(1-\rho^2)}} \exp\left\{-\frac{1}{2(1-\rho^2)}\left[\frac{(Z_{t_f}-\mu_1)^2}{\sigma_1}\right.\right. \\
& \left.\left. + \ \frac{(Z_{t_f+1}-\mu_2)^2}{\sigma_2} - 2\rho\frac{(Z_{t_f}-\mu_1)(Z_{t_f+1}-\mu_2)}{\sqrt{\sigma_1\sigma_2}}\right]\right\}
\end{aligned} \tag{4.7}
$$

where, $\mu_1 = \mu_n + \mu_{ab}$, $\mu_2 = 2\mu_{ab}$, $\sigma_1 = \sigma_n^2 + \sigma_{ab}^2$, $\sigma_2 = 2\sigma_{ab}^2$ and ρ is correlation coefficient, $\rho = \mathrm{Corr}(Z_{t_f}, Z_{t_f+1}) = \sigma_{12}/\sqrt{\sigma_1\sigma_2}$ [47].

For the higher n-sample detection delay, the first $n-1$ filtered samples should be below the trip point and the n-th one above it. So, the probability will be

$$
\begin{aligned}
& \mathbb{P}(\mathrm{DD} = n) \\
& = \mathbb{P}\{[X_{t_f-1} + X_{t_f} \leq 2y_{tp}] \ \& \ [X_{t_f} + X_{t_f+1} \leq 2y_{tp}] \ \& \\
& \qquad \ldots \& \ [X_{t_f+n-1} + X_{t_f+n} > 2y_{tp}]\} \\
& = \mathbb{P}\{[Z_{t_f} \leq 2y_{tp}] \ \& \ [Z_{t_f+1} \leq 2y_{tp}] \ \& \ \ldots \& \ [Z_{t_f+n} > 2y_{tp}]\} \\
& = \int_{-\infty}^{2y_{tp}} \int_{-\infty}^{2y_{tp}} \cdots \int_{2y_{tp}}^{\infty} f(Z_{t_f}, Z_{t_f+1}, \cdots, Z_n)\, dZ_{t_f} dZ_{t_f+1} \cdots dZ_{t_f+n}
\end{aligned} \tag{4.8}
$$

The joint multivariate distribution function in Eq. (4.8) can be computed similar to Eq. (4.7).

Filter of order m

For a general case of moving average filter of order m, the filtered signal will be a multivariate normal one. To compute the probability of detection delay, calculation of joint distribution function is required. The n-sample detection delay for a filter of order m is given by

$$\begin{aligned}
&\mathbb{P}(\mathrm{DD}=n)\\
&=\mathbb{P}\{[X_{t_f-m+1}+\cdots+X_{t_f-1}+X_{t_f}\le my_{tp}]\ \&\\
&\quad[X_{t_f-m+2}+\cdots+X_{t_f}+X_{t_f+1}\le my_{tp}]\ \&\ \ldots\\
&\quad\&\ [X_{t_f+n-m+1}+\cdots+X_{t_f+n-1}+X_{t_f+n}>my_{tp}]\}\\
&=\mathbb{P}\{[Z_{t_f}\le my_{tp}]\ \&\ [Z_{t_f+1}\le my_{tp}]\ \&\ \ldots\&\ [Z_{t_f+n}>my_{tp}]\}\\
&=\int_{-\infty}^{my_{tp}}\int_{-\infty}^{my_{tp}}\cdots\int_{my_{tp}}^{\infty}f(Z_{t_f},Z_{t_f+1},\cdots,Z_{t_f+n})\,dZ_{t_f}dZ_{t_f+1}\cdots dZ_{t_f+n}
\end{aligned}\tag{4.9}$$

The mean vector and covariance matrix for the probability of detection delay n for joint distribution function is given by

$$\bar{Z}_{(n+1)\times 1}=\begin{pmatrix}(m-1)\mu_n+\mu_{ab}\\(m-2)\mu_n+2\mu_{ab}\\\vdots\\\mu_n+(m-1)\mu_{ab}\\m\mu_{ab}\\m\mu_{ab}\\\vdots\\m\mu_{ab}\end{pmatrix}$$

$$\Sigma=\begin{bmatrix}A_{11}&A_{12}\\A_{21}&A_{22}\end{bmatrix},\tag{4.10}$$

where

$$A_{11}=\begin{pmatrix}(m-1)\sigma_n^2+\sigma_{ab}^2&(m-2)\sigma_n^2+\sigma_{ab}^2&\cdots&\cdots&\sigma_n^2+\sigma_{ab}^2\\(m-2)\sigma_n^2+\sigma_{ab}^2&(m-2)\sigma_n^2+2\sigma_{ab}^2&\cdots&\cdots&\sigma_n^2+2\sigma_{ab}^2\\\vdots&\vdots&\ddots&&\vdots\\\vdots&\vdots&&\ddots&\vdots\\\sigma_n^2+\sigma_{ab}^2&\sigma_n^2+2\sigma_{ab}^2&\cdots&&\sigma_n^2+(m-1)\sigma_{ab}^2\end{pmatrix}$$

$$A_{12}=\begin{pmatrix}\sigma_{ab}^2&0&0&\cdots&0\\2\sigma_{ab}^2&\sigma_{ab}^2&0&\cdots&0\\\vdots&\vdots&&\vdots&\\\vdots&\vdots&&\vdots&\\(m-1)\sigma_{ab}^2&(m-2)\sigma_{ab}^2&\cdots&\cdots&0\end{pmatrix}$$

$$A_{21} = \begin{pmatrix} \sigma_{ab}^2 & 2\sigma_{ab}^2 & \cdots & \cdots & (m-1)\sigma_{ab}^2 \\ 0 & \sigma_{ab}^2 & \cdots & \cdots & (m-2)\sigma_{ab}^2 \\ \vdots & & \ddots & & \vdots \\ \vdots & & & \ddots & \vdots \\ 0 & 0 & \cdots & \cdots & \sigma_{ab}^2 \\ 0 & 0 & \cdots & \cdots & 0 \end{pmatrix}$$

and

$$A_{22} = \begin{pmatrix} m\sigma_{ab}^2 & (m-1)\sigma_{ab}^2 & \cdots & \cdots & 0 \\ (m-1)\sigma_{ab}^2 & m\sigma_{ab}^2 & \cdots & \cdots & 0 \\ \vdots & & \ddots & & \\ \vdots & & & \ddots & \\ & & & & m\sigma_{ab}^2 \end{pmatrix}$$

Example

This example is to validate the general equation of probability of detection delay given in (4.9). The normal and abnormal data follow Gaussian distributions $\mathcal{N}(0,1)$ and $\mathcal{N}(3,4)$ respectively. The sampling period is at 1 sec. In Fig 4.2, a Monte Carlo simulation is shown to verify the theoretical results. 5000 Monte Carlo simulations are performed for different filter orders from $m = 2$ to 4. The trip point is kept constant at $y_{tp} = 1.7$ and the average $\mathbb{P}(\mathrm{DD})$ is computed from Monte-Carlo simulation to get a single estimate. The frequency of outcome for each $\mathbb{P}(\mathrm{DD})$ is plotted against the theoretical value (theoretical value is multiplied by number of Monte-Carlo simulations performed for consistency). To compute the joint distribution function of the derived equations, the MATLAB function *mvncdf* is used. It can be seen that the theoretical and simulation results are consistent.

The expected detection delay is given by

$$\mathrm{EDD} = \mathbb{E}(\mathrm{DD}) = \sum_{n=0}^{\infty} n \; \mathbb{P}(\mathrm{DD}) \tag{4.11}$$

There is no closed form solution to compute the $\mathbb{E}(\mathrm{DD})$, but it can be calculated numerically.

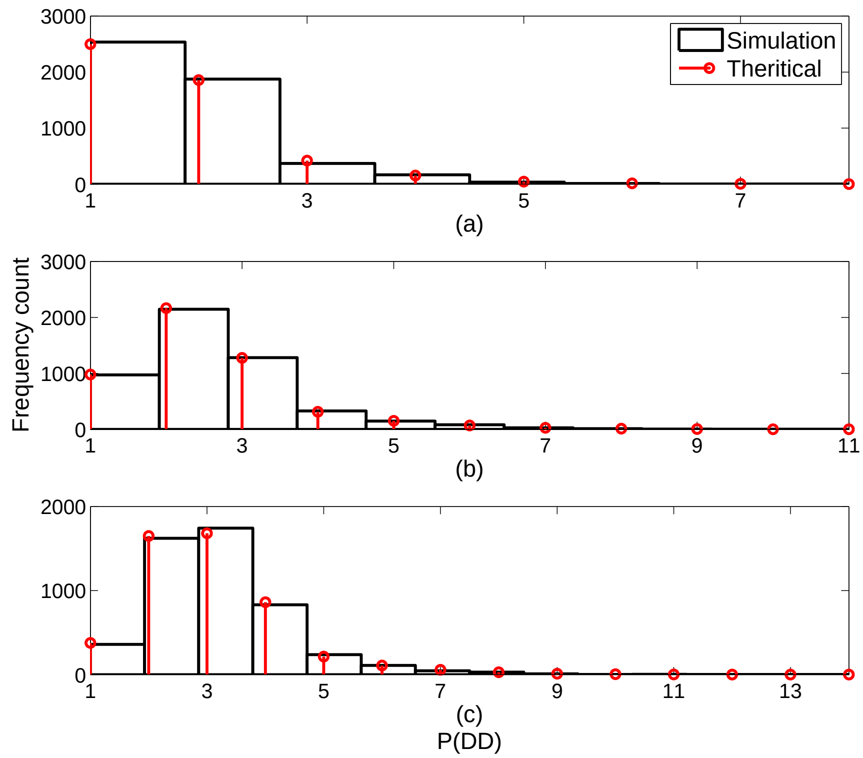

Figure 4.2: Verification of the $\mathbb{P}$(DD) formula by Monte-Carlo simulations for different filter orders (a) $m = 2$, (b) $m = 3$, (c) $m = 4$.

Detection delay for non-Gaussian distributions

The computation of detection delay requires numerical computation of multivariate distribution functions, which is much more complex than computation of univariate distributions due to higher dimensional issue [53]. In this work, Gaussian distributions of data are considered. However, if the data is non-Gaussian, detection delay can be still computed similarly. For non-Gaussian distributions, several integral approximating approaches by Monte-Carlo and deterministic methods are discussed in [54]. This work is limited to Gaussian distributions only and other types of distribution will be addressed in the future.

4.4 Alarm System Design

In the design of alarm systems three performance indices should be balanced for optimal configuration, namely, the false alarm rate, the missed alarm rate and the expected detection delay [13, 24]. In this section, the design of alarm systems is considered to find the optimum settings of trip point and filter order satisfying requirements of FAR, MAR and EDD. An optimal configuration is expected to increase accuracy of the design, i.e., reduce FAR and MAR, and also increase the swiftness of alarm activation, i.e., reduce EDD. The proposed objective function including these constraints can be described by [51]

$$\begin{aligned} &J(f) = k_1 \int_{y_{tp}}^{\infty} f_n(.)dZ + k_2 \int_{-\infty}^{y_{tp}} f_{ab}(.)dZ \\ &\text{subject to} \qquad \text{EDD} \leq \eta \end{aligned} \tag{4.12}$$

Here, $f_n(.)$ and $f_{ab}(.)$ are the PDFs of filtered signal for the normal and abnormal operations respectively; η is the maximum allowable delay; and the two integrals represent FAR and MAR respectively.

The objective function is a weighted sum of FAR and MAR, which can be represented by the receiver operating characteristic (ROC) curve. The ROC curve is the plot of FAR vs MAR curve as the trip point y_{tp} is moved from minimum to the maximum of the process data (Fig 3.8). For a high alarm limit, when the limit is kept at the minimum of normal process data the FAR is the highest. As the limit goes up it decreases the FAR, but increases the MAR. If equal weight (k_1, k_2) is given on both the FAR and MAR, then the optimum point is the one closest to the origin. However, since filtering introduces delay in alarm activation, the objective function is to be computed subject to allowable expected detection delay. In this work, a four step alarm design method is considered for filtering similar to the method introduced earlier to design settings of delay-timers in alarm systems [24]. With a little modification to that method a four step trip point and filter order design process for alarm systems is described here. For a given set of normal and abnormal data, the design parameters are the trip point y_{tp} and filter order m. The same set of data is considered here for design as given in the example

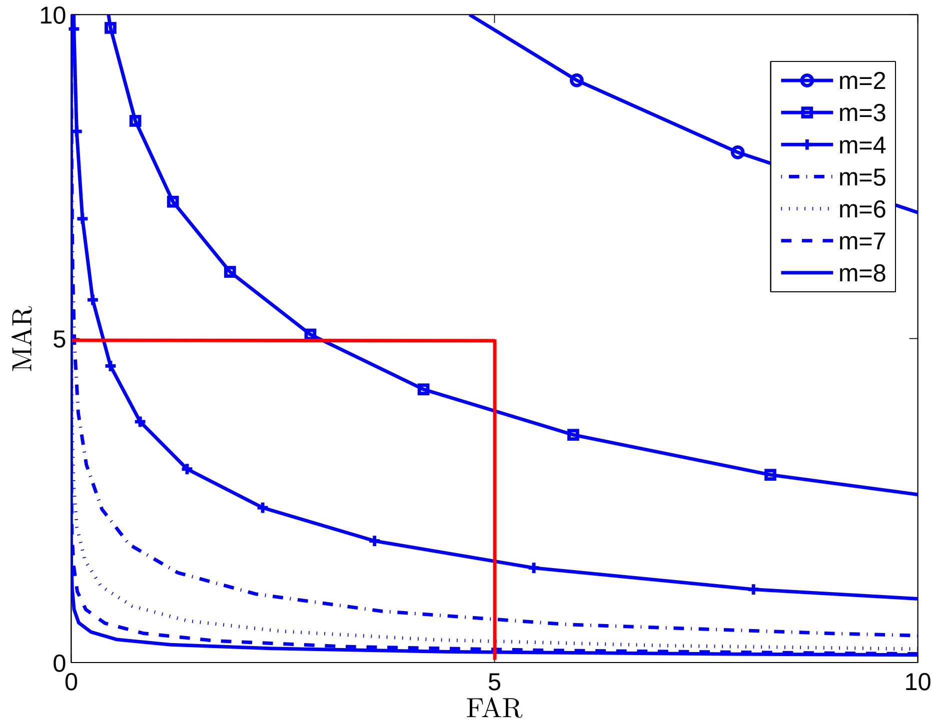

Figure 4.3: ROC curves when changing filter order

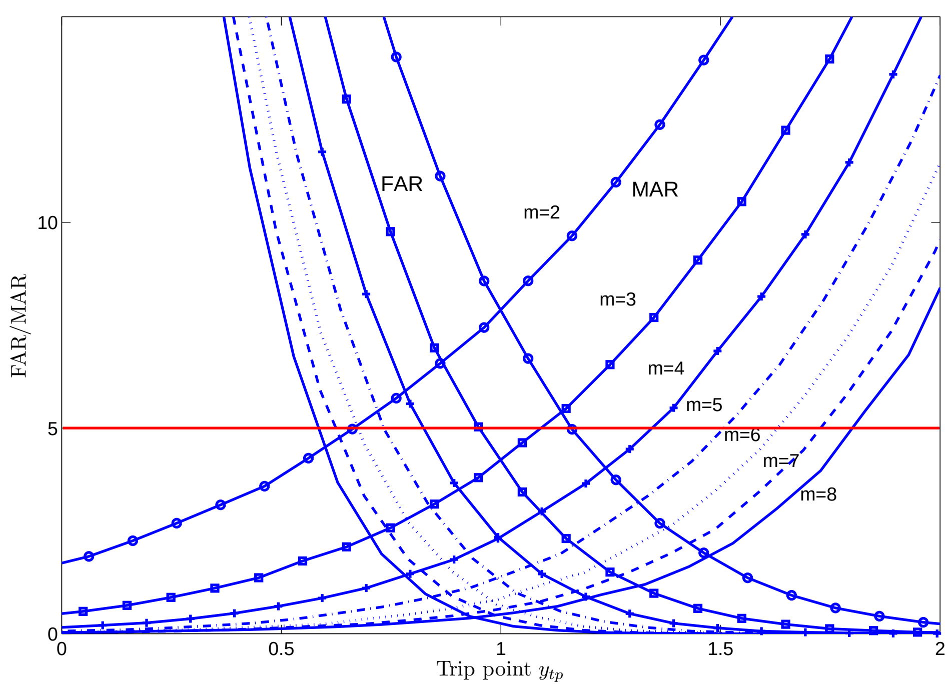

Figure 4.4: Estimation of the threshold when FAR = MAR

of Section 4.3.

To design a system with FAR $\leq 5\%$, MAR $\leq 5\%$ and EDD ≤ 2 seconds, the procedure given below is followed. In Fig 4.3, filter orders are changed from $m = 2$ to 8 and corresponding ROC curves are plotted; it can be seen that as the order of filter is increased the accuracy is improved, moving the curve closer to the origin. On the other hand the increased accuracy resulted in higher detection delay. Fig 4.5 shows that higher filter order causes higher delay in detection (EDD) for the same trip point. The trip point where FAR and MAR are equal can be estimated from Fig 4.4.

Step 1

The first step is regarding accuracy of design. The ROC curve is plotted as the performance curve for the filter order selection step satisfying accuracy criteria. The smallest filter order, m_1, that satisfy the FAR $\leq 5\%$ and MAR $\leq 5\%$ is selected from Fig 4.3; where $m \geq m_1$. It can be seen that moving average filters of order 3 and higher in this case satisfy the requirements of FAR and MAR.

Step 2

Once filter orders that satisfy the requirement of accuracy is found, in the second step the corresponding operating limit or trip point y_{tp} is estimated from Fig 4.4. Here, the plots from upper left are FAR and from upper right are MAR curves obtained by changing trip points. Intersection of these two curves are the points where FAR and MAR are equal and given in Table 4.1.

Step 3

In step 3, the expected detection delay is estimated for corresponding recorded trip points in step 2. The largest value of filter order m_2 is estimated from Fig 4.5 for EDD$\leq$ 2 seconds and given in Table 4.1; here $m_2 = 4$.

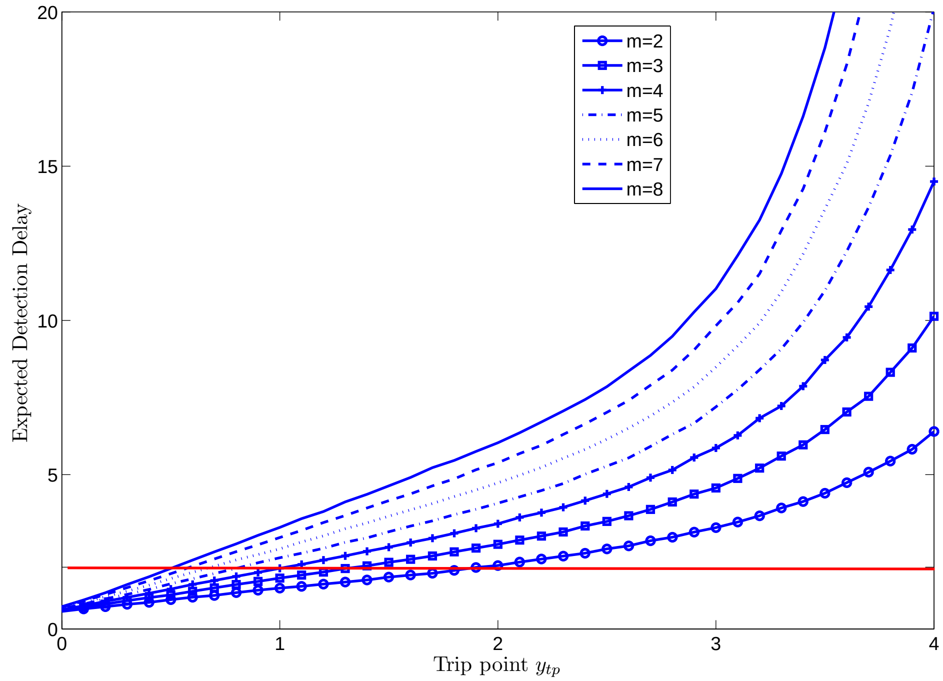

Figure 4.5: Effect on EDD changing filter orders

Step 4

Once m_1 and m_2 are estimated, the final step is to select the order of the moving average filter to complete the design process. If $m_2 \geq m_1$, any m satisfying $m_1 \leq m \leq m_2$ is a solution for filter order satisfying the requirements. From Table 4.1, both moving average filters of order 3 and 4 satisfy given requirements resulting in FAR/MAR between 4.2% to 2.3% and EDD between 1.65 to 1.95 seconds respectively.

If a range of filter order is not available, or in other words no m satisfies $m_1 \leq m \leq m_2$, then the requirements need adjustments. In that case it can be concluded that the requirements are too stringent to achieve for the given process type. Therefore this method not only provides a way to select filter parameters, but also can be applied to check whether for the current design the desired performance is achievable or not.

Table 4.1: Design parameter selection chart for moving average filters

Filter order (m)	Trip point (y_{tp})	FAR = MAR (%)	EDD
2	1	7.9	1.33
3	1	4.2	1.65
4	0.99	2.3	1.95
5	0.99	1.4	2.3
6	0.97	0.9	2.6
7	0.96	0.5	2.9
8	0.94	0.3	3.1

4.5 Conclusion and Future Work

The detection delay is an important parameter that measures the time it takes to activate an alarm. The designer must have a clear idea of how long it will take to raise an alarm once an abnormality occurs in the system for the practiced design method. In this chapter, the detection delay is computed for one of the widely applied methods in alarm systems, moving average filters assuming Gaussian distribution of data. A design method to select trip point and filter order is also discussed. As a future extension, calculation of performance indices for other filtering techniques and non-Gaussian distributions may be considered.

Chapter 5

Generalized Delay-timers

In this chapter[1,2], a generalized delay-timer framework is discussed where instead of consecutive n samples in the conventional case, n_1 out of n consecutive samples ($n_1 \leq n$) are considered to raise an alarm. For the generalized delay-timer, three important performance indices, namely, the false alarm rate (FAR), the missed alarm rate (MAR) and the expected detection delay (EDD), are calculated using Markov processes. Moreover, the performance and sensitivity of generalized delay-timers are compared with conventional delay-timers.

The rest of the Chapter is organized as follows: section 5.1 discusses the conventional delay-timers in brief. Rules proposed by the Western Electric Company are discussed in section 5.2. The generalized delay-timer is described in section 5.3. Section 5.4 is devoted to the algorithm to formulate the Markov chain for the generalized case. Comparison of performance and sensitivity analysis are provided in section 5.5. Finally, some concluding remarks are given in section 5.6.

[1] A shorter version of this chapter has been published as: N. A. Adnan, Y. Cheng, I. Izadi, and T. Chen, *A generalized delay-timer for alarm triggering*, in proceedings of the American Control Conference (ACC 2012), pp. 6679-6684, June 27-29, 2012, Montreal, QC.

[2] Sections of this chapter have been published as: N. A. Adnan, Y. Cheng, I. Izadi, and T. Chen, *Study of generalized delay-timers in alarm configuration*, Journal of Process Control, vol. 23, no. 3, pp. 382-395, 2013.

5.1 Conventional Delay-timer

Generally alarms are raised and cleared based on a single sample comparing with the threshold. For high alarms, if the sample is above the threshold, an alarm is raised; and when it goes below the threshold the alarm is cleared. A similar idea is applied in the case of low alarms. However, often this simple limit or threshold checking is not considered as a good design due to the problem of nuisance and false alarms [13]. To reduce nuisance and false alarms delay-timer is a popular technique in industry. The idea of delay-timers is very simple yet effective. In alarm systems two types of delay-timers are used: on-delay and off-delay [13, 23]. For on-delay timers, an alarm is only raised if n consecutive samples cross the threshold. In other words, the process measurement remains in the alarm state for n units of time before activating the alarm [18]. With off-delay configured, a raised alarm will only be cleared if a number of consecutive samples fall below the threshold.

It is essential to conduct a careful safety analysis in tuning the delay-timer parameters (time and alarm limit). From safety point of view, compared to off-delay, on-delay timers are more sophisticated. Since on-delay is connected with alarm activation, the setting should allow operators sufficient time before the abnormal situation becomes an incident. Later in this section detailed equations are provided that can be used to calculate this activation time for any settings of delay-timers.

The Markov process for 3-sample on-delay and 3-sample off-delay is shown in Fig. 5.1. Here p_1 is the probability of one sample above the threshold in fault-free region of operation (we only consider the case of high alarm for simplicity). Therefore the probability of one sample falling below the threshold is, $1 - p_1$ (Fig. 2.2). In cases where deadbands are applied with or without delay-timers, $p_1 + p_2 \neq 1$ [23].

Assume initially the process is in fault-free region of operation and no alarm is raised, which is the state NA in the Markov process. It will require 3 consecutive samples with probability p_1 to move the Markov process to state

A and raise an alarm. Any intermediate sample with probability $1 - p_1$ will bring the chain back to the original no alarm (NA) state. In this case, the sample temporarily exceeding the threshold is treated as an outlier sample. A similar process is followed in off-delay for clearing a raised alarm. Similar to the fault-free region, there will be another Markov process in the faulty region with probability q_2 and q_1 (see Fig. 2.2 for definitions).

5.1.1 False Alarm Rate

The most common practice in process monitoring is to compare a variable with thresholds (also known as alarm limits or trip points) to detect out of range conditions. A general situation is presented in Fig. 2.2, where L_0 and L_1 are the likelihoods for fault-free and faulty classes. For the process data shown in Fig. 2.2, some part of the probability distributions of the fault-free data falls over the threshold and will cause false alarms (also known as Type I error or false positive). Probability of false alarms from likelihoods or distributions from Fig. 2.2 can be computed as

$$\mathbb{P}(\text{False Alarm}) = \int_{y_{tp}}^{\infty} L_0(x)\,\mathrm{d}x \tag{5.1}$$

where y_{tp} is the decision threshold or alarm limit. Equation (5.1) is the simplest case when a single sample is compared with a threshold to raise an

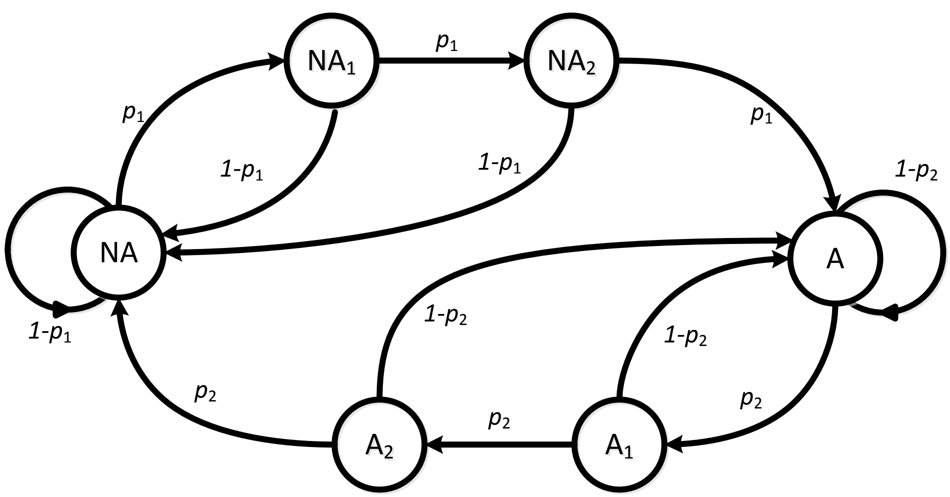

Figure 5.1: Combined on- and off-delays for $n = m = 3$

alarm. But in practical cases many other design constraints are added to the simplest threshold comparison. For example, delay-timers are widely exercised in industries where consecutive few samples are checked before raising or clearing an alarm. For different cases of delay-timers probability of false alarms calculations are discussed below:

For a conventional or regular delay-timer (Fig. 5.1), Markov processes are used to calculate the probability of false alarms. There are three possible cases: n-sample on-delay, m-sample off-delay and combined on- and off-delays. For combined n-sample on-delay and m-sample off-delay the transition probabilities in the fault-free region from one state to another is given as follows

$$\mathbf{P_n} = \left[\begin{array}{cc} P_{n11} & 0_{n\times(m-1)} \\ \hline P_{n21} & P_{n22} \end{array}\right], \tag{5.2}$$

where,

$$P_{n11} = \begin{pmatrix} 1-p_1 & p_1 & 0 & \cdots & 0 \\ 1-p_1 & 0 & p_1 & \cdots & 0 \\ \vdots & \vdots & \vdots & \ddots & \vdots \\ 1-p_1 & 0 & 0 & \cdots & p_1 \end{pmatrix},$$

$$P_{n21} = \begin{pmatrix} 0 & 0 & \cdots & 0 \\ \vdots & \vdots & \vdots & \vdots \\ 0 & 0 & \cdots & 0 \\ p_2 & 0 & \cdots & 0 \end{pmatrix}, P_{n22} = \begin{pmatrix} 1-p_2 & p_2 & 0 & \cdots & 0 \\ 1-p_2 & 0 & p_2 & \cdots & 0 \\ \vdots & \vdots & \vdots & \ddots & \vdots \\ 1-p_2 & 0 & 0 & \cdots & p_2 \\ 1-p_2 & 0 & 0 & \cdots & 0 \end{pmatrix},$$

here, horizontal line in $\mathbf{P_n}$ is used to indicate, the numbers of columns in P_{n11} and P_{n21} or in $0_{n\times(m-1)}$ and P_{n22} are not equal. $\mathbf{P_n}$ is of dimension $(n+m)\times(n+m)$. After a transient time in the fault-free region, the Markov chain reaches its steady state and converges to the invariant vector. For the system operating in the fault-free region, the probability of false alarm is the summation of all alarm state probabilities in the steady state and can be calculated according to the theory of Markov chains [48]. It can be shown that the probability of false alarm (the steady-state probability of all alarm states) is

$$\mathbb{P}(\text{False Alarm}) = \mathbb{P}(A + A_1 + \cdots + A_{m-1}) = \frac{p_1^n \displaystyle\sum_{i=0}^{m-1} p_2^i}{p_1^n \displaystyle\sum_{i=0}^{m-1} p_2^i + p_2^m \displaystyle\sum_{j=0}^{n-1} p_1^j} \tag{5.3}$$

5.1.2 Missed Alarm Rate

Missed alarms (also known as type II error or false negative) occur when the system is in faulty state of operation but an alarm is not raised. From the process data in Fig. 2.2, it can be seen that the missed alarm rate can be decreased by lowering the threshold. However, it will increase the false alarm rate. Therefore, it leads to the problem of balancing between the false alarm rate and the missed alarm rate [13, 23]. Calculation of missed alarm rates for different cases of delay-timers are similar to that of false alarm rates. To calculate the missed alarm rate the probability density function of the faulty data should be used (Fig. 2.2, likelihood function L_1). Here q_2 is the probability of one sample above the threshold and q_1 (or $1 - q_2$) is the probability of one sample below the threshold in the abnormal region. From Fig. 2.2, the probability of missed alarm is

$$\mathbb{P}(\text{Missed Alarm}) = \int_{-\infty}^{y_{tp}} L_1(x)\,\mathrm{d}x \tag{5.4}$$

When delay-timers are applied, the missed alarm rate is the sum of all probabilities of no alarm states in the Markov chain under the faulty region of operation. For calculation of MAR, the probability distribution of faulty data and the transition probability matrix, $\mathbf{P_f}$, should be used, where $\mathbf{P_f}$ can be obtained replacing probabilities $p_1,\ p_2$ by $q_2,\ q_1$, respectively, in equation (5.2). For the n-sample on-delay and m-sample off-delay, the probability of missed alarm is

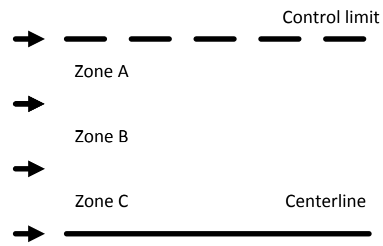

Figure 5.2: Divided zones for testing unnatural patterns

$$\mathbb{P}(\text{Missed Alarm}) = \mathbb{P}(NA + NA_1 + \cdots + NA_{n-1}) \tag{5.5}$$
$$= \frac{q_1^m \sum_{i=0}^{n-1} q_2^i}{q_1^m \sum_{i=0}^{n-1} q_2^i + q_2^n \sum_{j=0}^{m-1} q_1^j}$$

Besides the false alarm and missed alarm rates, detection delay is another important performance index in alarm systems which is discussed in details for conventional delay-timer in Chapter 3.

5.2 Western Electric Rule

Based on the Shewhart control limits the Western Electric Co. proposed the *tests for instability* in 1956. These tests are also known as the Western Electric Rules [55]. In the tests, the area between the centerline (mean) of the process data and one of the thresholds (either upper threshold or lower threshold which is 3σ away from the mean, where σ is the standard deviation) is divided into three zones; each zone has a width of σ (Fig. 5.2). According to the rules, a pattern is unnatural and needs attention if any of the following combinations are formed:

1. One sample falls outside of the three sigma threshold.

2. Two out of three successive samples fall in zone A or beyond.

3. Four out of five successive samples fall in zone B or beyond.

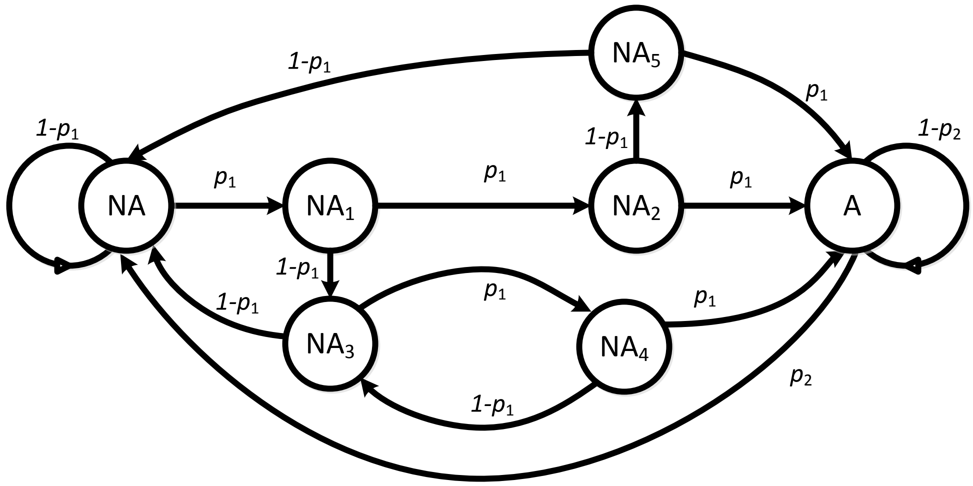

Figure 5.3: Generalized on-delay with $n_1 = 3,\ n = 4$

4. Eight successive samples fall in zone C or beyond.

The idea of test 1 is the same as a simple threshold checking. Here probability of false alarm is p_1 and probability of missed alarm is q_1 based on a single sample. Tests 2 and 3 are similar to the generalized delay-timer (to be discussed in section 5.3) for 2-out-of-3 and 4-out-of-5 on-delay timers. Test 4 is similar to the conventional delay-timer (as discussed in section 5.1) for an 8-sample delay-timer. Tests 2 and 3 suggest that from the industrial point of view, application of a generalized delay-timer is not impractical. Rather it has certain advantages over the conventional case, e.g., in section 5.5, it is discussed that the generalized delay-timer is less sensitive to changes in thresholds than the conventional one.

5.3 Generalized Delay-timers

Sometimes conditions to raise an alarm in the conventional delay-timer are difficult to satisfy. For example, consider a system with 10 samples on-delay. When the system enters from the normal state to the faulty state of operation, consecutive 10 samples must cross the threshold to raise the alarm. It is very likely to have some delay in raising the alarm during this transition as first 10 samples may not satisfy the strict requirement. However if the condition is relaxed to for instance 8 out of 10 samples crossing the threshold, intuitively the probability of early detection is higher. Accordingly we propose the following two definitions:

n_1 out of n samples generalized on-delay: an alarm will be raised if n_1 out of n consecutive samples are above the threshold.

m_1 out of m samples generalized off-delay: an alarm will be cleared if m_1 out of m consecutive samples fall below the threshold.

The Markov process for $n_1 = 3$ and $n = 4$ is shown in Fig. 5.3 where 3 out of 4 samples are required to raise an alarm and no off-delay is configured. It can be seen that in the generalized on-delay, the total number of intermediate no alarm states (NA_i) is 5. Compared to the conventional 3 samples on-delay case (NA_1, NA_2 in Fig. 5.1), this requires more intermediate states. The reason of this requirement can be explained by Table 5.1. Assume initially the alarm is cleared and the Markov process is in the state NA. To raise an alarm the Markov process has to reach state A with the condition that 3 samples out of 4 have probabilities p_1. Unlike conventional on-delay where there is a single path to reach state A from state NA (Fig. 5.1), the Markov process here can achieve this in three different paths. Each row of Table 5.1 represents a path. The first element of each row is p_1, which is required to move to the first intermediate state NA_1. From NA_1 depending on probability of next sample it can either move to state NA_2 (with probability p_1) or to state NA_3 (with probability $1 - p_1$). This process will carry on until the Markov chain reaches state A. Since the number of paths is increased in the generalized on-delay compared to the conventional on-delay, the number of intermediate states has also been increased.

Table 5.1: Possible paths to reach from state NA to A: (*) represents not applicable

Sample 1	Sample 2	Sample 3	Sample 4
p_1	p_1	p_1	*
p_1	$1-p_1$	p_1	p_1
p_1	p_1	$1-p_1$	p_1

Due to the possibility of several paths, generalized delay-timer calculation is more complex than the conventional case. Therefore with larger n, computational complexity increases significantly and it is difficult to provide a general representation of the Markov diagram for all combinations. Below some special cases of generalized delay-timers (2 out of n samples on-delay and 2 out of m samples off-delay cases) are discussed. In Section 5.4, a numerical algorithm to calculate the FAR, MAR and EDD in the general case is given.

5.3.1 False Alarm Rate

2 out of n samples on-delay

Consider a 2 out of n on-delay, where $n \geq 2$. To calculate the probabilities of false alarms, Markov chain is used. The general Markov chain for $n_1 = 2$ and any n is shown in Fig. 5.4(a). The corresponding transitional probability matrix is

$$\mathbf{P_n} = \begin{pmatrix} 1-p_1 & p_1 & 0 & \cdots & \cdots & 0 & 0 \\ 0 & 0 & 1-p_1 & \cdots & \cdots & 0 & p_1 \\ \vdots & \vdots & & \ddots & & & \vdots \\ \vdots & \vdots & & & \ddots & & \vdots \\ 0 & 0 & 0 & \cdots & \cdots & 1-p_1 & p_1 \\ 1-p_1 & 0 & 0 & \cdots & \cdots & 0 & p_1 \end{pmatrix}, \tag{5.6}$$

Here $\mathbf{P_n}$ is of dimension $(n+1) \times (n+1)$. The corresponding steady-state invariant vector is

$$\begin{aligned} \pi &= \left[\ \mathbb{P}(NA) \quad \mathbb{P}(NA_1) \quad \mathbb{P}(NA_2) \quad \cdots \quad \mathbb{P}(NA_{n-1}) \quad \mathbb{P}(A)\ \right] \\ &= \frac{1}{p_1(1-p_2^{n-1}) + p_2(2-p_2^{n-1})} \left[\ p_2 \quad p_1p_2 \quad p_1p_2^2 \quad \cdots \quad p_1p_2^{n-1} \quad p_1(1-p_2^{n-1})\ \right] \end{aligned} \tag{5.7}$$

It can be shown that the probability of false alarm in the steady state is

$$\mathbb{P}(\text{False Alarm}) = \mathbb{P}(A) = \frac{p_1(1-p_2^{n-1})}{p_1(1-p_2^{n-1}) + p_2(2-p_2^{n-1})} \tag{5.8}$$

2 out of m samples off-delay

Similar to the generalized on-delay, generalized off-delay will require m_1 out of m samples below the threshold to clear an alarm. As a special case, the

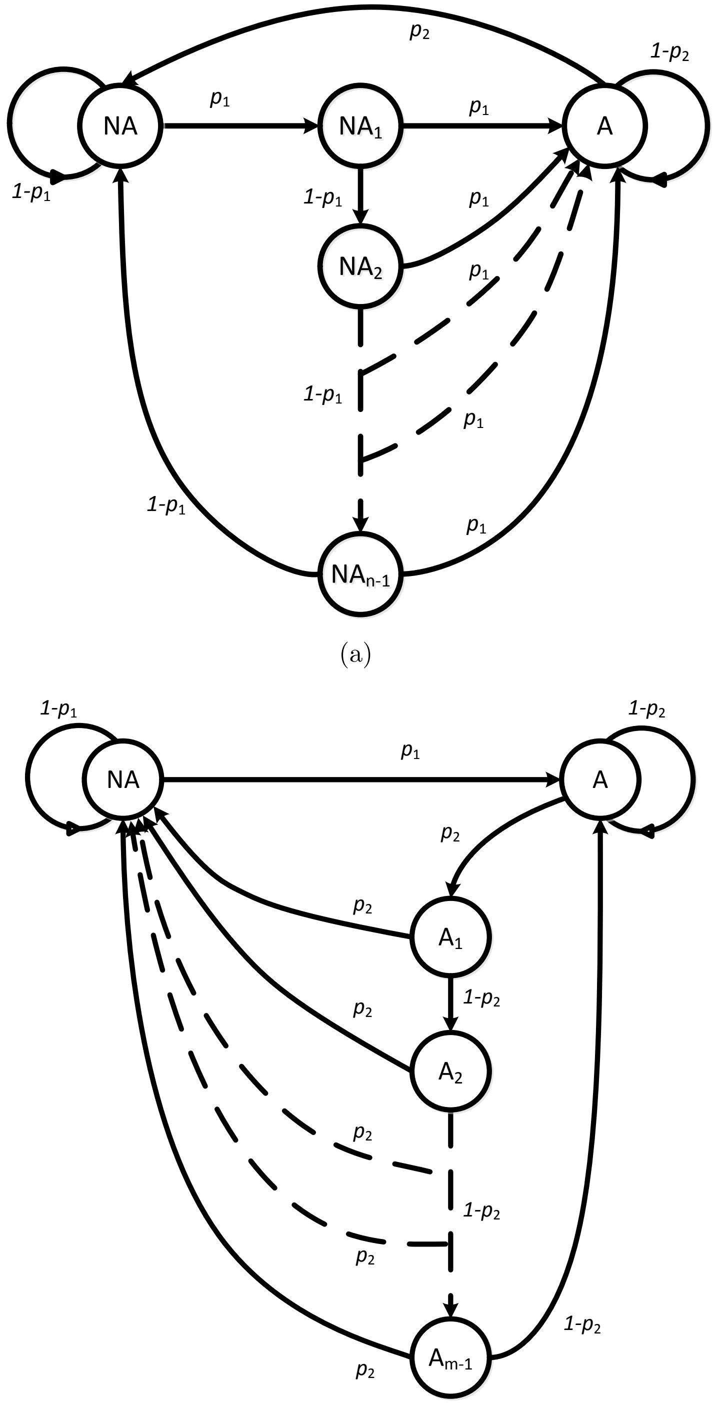

(a)

(b)

Figure 5.4: (a) 2 out of n generalized on-delay; (b) 2 out of m generalized off-delay

Markov process for 2 out of m samples is considered (Fig. 5.4(b)). In the fault-free region of operation, any 2 samples out of m will clear an already raised alarm. The transitional probability matrix is

$$\mathbf{P_n} = \begin{pmatrix} 1-p_1 & p_1 & 0 & 0 & \cdots & \cdots & 0 \\ 0 & 1-p_2 & p_2 & 0 & \cdots & \cdots & 0 \\ p_2 & 0 & 0 & 1-p_2 & \cdots & \cdots & 0 \\ \vdots & \vdots & \vdots & & \ddots & & \vdots \\ \vdots & \vdots & \vdots & & & \ddots & \vdots \\ p_2 & 0 & 0 & \cdots & \cdots & \cdots & 1-p_2 \\ p_2 & 1-p_2 & 0 & \cdots & \cdots & \cdots & 0 \end{pmatrix}, \tag{5.9}$$

The steady-state invariant vector is

$$\begin{aligned} \pi &= \begin{bmatrix} \mathbb{P}(NA) & \mathbb{P}(A) & \mathbb{P}(A_1) & \cdots & \mathbb{P}(A_{m-2}) & \mathbb{P}(A_{m-1}) \end{bmatrix} \\ &= \frac{1}{p_1(2-p_1^{m-1})+p_2(1-p_1^{m-1})} \begin{bmatrix} p_2(1-p_1^{m-1}) & p_1 & p_1p_2 & p_1^2p_2 & \cdots & p_1^{m-1}p_2 \end{bmatrix} \end{aligned} \tag{5.10}$$

The probability of false alarm in steady state can be calculated as

$$\begin{aligned} \mathbb{P}(\text{False Alarm}) &= \mathbb{P}(A + A_1 + \cdots + A_{m-1}) \\ &= \frac{p_1(2-p_1^{m-1})}{p_1(2-p_1^{m-1})+p_2(1-p_1^{m-1})} \end{aligned} \tag{5.11}$$

Combined on and off-delay

Similarly, if both 2 out of n samples on-delay and 2 out of m samples off-delay are applied together, the probability of false alarm is

$$\mathbb{P}(\text{False Alarm}) = \frac{p_1(2-p_1^{m-1})(1-p_2^{n-1})}{p_1(2-p_1^{m-1})(1-p_2^{n-1})+p_2(1-p_1^{m-1})(2-p_2^{n-1})} \tag{5.12}$$

Example 1

This example is to validate the expression of FAR derived in equations (5.8), (5.3.1), and (5.12). The process variable is Gaussian distributed. Fault-free data has mean 0, variance 1 and faulty data has mean 2, variance 1. The data length is 1000 for both fault-free and faulty data. 1 sec uniform sampling is

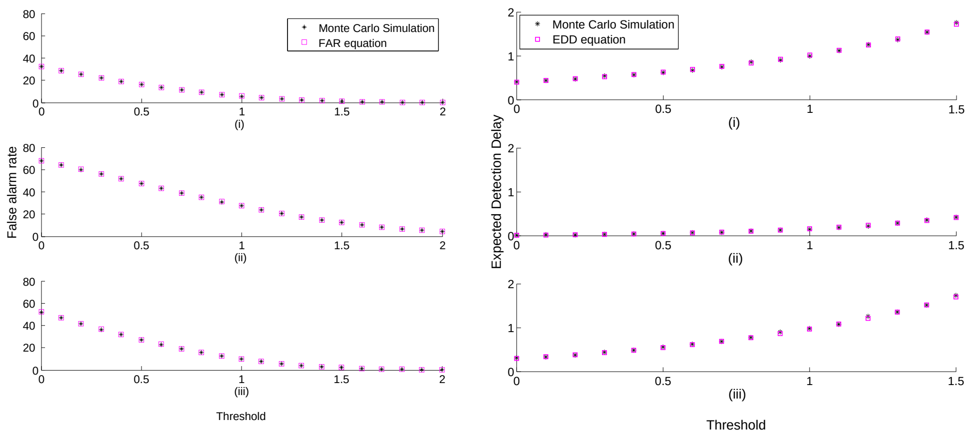

(a) (i) 2 out of 5 samples on-delay, (ii) 2 out of 4 samples off-delay, (iii) 2 out of 4 samples on-delay and 2 out of 3 samples off-delay

(b) (i) 2 out of 4 samples on-delay, (ii) 2 out of 3 samples off-delay, (iii) 2 out of 4 samples on-delay and 2 out of 5 samples off-delay

Figure 5.5: [a] Verification of the FAR formula by Monte-Carlo simulations; [b] Verification of the EDD formula by Monte-Carlo simulations

used. The threshold is varied from 0 to 2 with 0.1 increment. In Fig. 5.5(a), three different cases of only on-delay, only off-delay and both on- and off-delays applied together are shown. For each cases, 2000 Monte Carlo simulations are performed and averaged to get a single estimate. It can be seen that the theoretical and simulated results are consistent.

5.3.2 Missed Alarm Rate

Calculation of the missed alarm rate is similar to that of the false alarm rate. But the probability density function of the abnormal data should be used. The transition probability matrix ($\mathbf{P_n}$ in Subsection 5.3.1) of the fault-free operation would be replaced by the matrix for the faulty operation ($\mathbf{P_f}$); where probability entries p_1, p_2 would be replaced by q_2, q_1 respectively. The probability of missed alarm for 2 out of n-sample on-delay and 2 out of m-sample off-delay can be expressed as

$$\mathbb{P}(\text{Missed Alarm}) = \frac{q_1(2-q_1^{n-1})(1-q_2^{m-1})}{q_2(1-q_1^{n-1})(2-q_2^{m-1}) + q_1(2-q_1^{n-1})(1-q_2^{m-1})} \quad (5.13)$$

5.3.3 Detection Delay

2 out of n samples on-delay

The probability of z samples detection delay can be calculated using equation (3.10). Here the transition matrix is

$$\mathbf{P_f} = \begin{pmatrix} 1-q_2 & q_2 & 0 & \cdots & \cdots & 0 & 0 \\ 0 & 0 & 1-q_2 & \cdots & \cdots & 0 & q_2 \\ \vdots & \vdots & & \ddots & & & \vdots \\ \vdots & \vdots & & & \ddots & & \vdots \\ 0 & 0 & 0 & \cdots & \cdots & 1-q_2 & q_2 \\ q_1 & 0 & 0 & \cdots & \cdots & 0 & 1-q_1 \end{pmatrix}, \tag{5.14}$$

The $\mathbf{Q}$ matrix can be obtained from $\mathbf{P_f}$ replacing all the alarm state rows by zeros and the steady-state vector is given in equation (5.7). It can be shown that the expected detection delay for 2 out of n samples on-delay is

$$\text{EDD} = \frac{p_2(1-q_1^n+q_1)+p_1q_1(1-p_2^{n-1})(2-q_1^{n-1})+p_1p_2q_1\sum_{i=0}^{n-2}p_2^i(1-q_1^{n-1}+q_1^{n-2-i})}{\{p_1(1-p_2^{n-1})+p_2(2-p_2^{n-1})\}q_2(1-q_1^{n-1})} \tag{5.15}$$

2 out of m samples off-delay

Similar to the previous 2 out of n samples on-delay, the expected detection delay for 2 out of m samples off-delay is

$$\text{EDD} = \frac{(p_2+p_1q_1-p_2q_2)(1-p_1^{m-1})}{q_2[p_2(1-p_1^{m-1})+p_1(2-p_1^{m-1})]} \tag{5.16}$$

Combined on and off-delay

For the special case of combined 2 out of n on-delay and 2 out of m off-delay, the expected detection delay is

$$\text{EDD} = \frac{X_1 + X_2 + X_3}{Y_1 Y_2}$$

where

$$X_1 = p_2(1 - p_1^{m-1})(1 - q_1^n + q_1), \quad X_2 = p_1 p_2 q_1 (1 - p_2^{n-1})(2 - q_1^{n-1}) \sum_{j=0}^{m-2} p_1^j$$

$$X_3 = p_1 p_2 q_1 (1 - p_1^{m-1}) \sum_{i=0}^{n-2} p_2^i (1 - q_1^{n-1} + q_1^{n-2-i})$$

$$Y_1 = p_2(1 - p_1^{m-1})(2 - p_2^{n-1}) + p1(1 - p_2^{n-1})(2 - p_1^{m-1}), \quad Y_2 = q_2(1 - q_1^{n-1}) \tag{5.17}$$

Example 2

This example is to validate the expression of EDD derived in equation (5.15), (5.16), and (5.17). The same process variable as in Example 1 is used. The threshold is varied from 0 to 1.5 with 0.1 increment. In Fig. 5.5(b), three different cases of only on-delay, only off-delay and both on- and off-delays applied together are shown. For 2000 Monte Carlo simulations the averaged EDD is estimated to compare with theoretical values. It can be seen that the theoretical and simulated results are consistent.

5.3.4 Resetting Markov Processes

For the generalized delay-timer, in certain cases it may appear that there is a conflict of logic. Consider a 3 out of 4 samples on-delay timer and 1 off-delay timer for the series of samples shown in Fig. 5.6. The markov process for this example is shown in Fig. 5.3. Assume initially there is no alarm. Conditions to raise an alarm is satisfied at sample 4 and the Markov process moves to state A. Then the alarm is cleared at sample 5 since it has probability $1-p_1$ to fall back within the threshold and the Markov process moves back to the state NA. Once it goes back to state NA, the next window to check for conditions of alarm raising will start from sample 6; we call this window shifting resetting

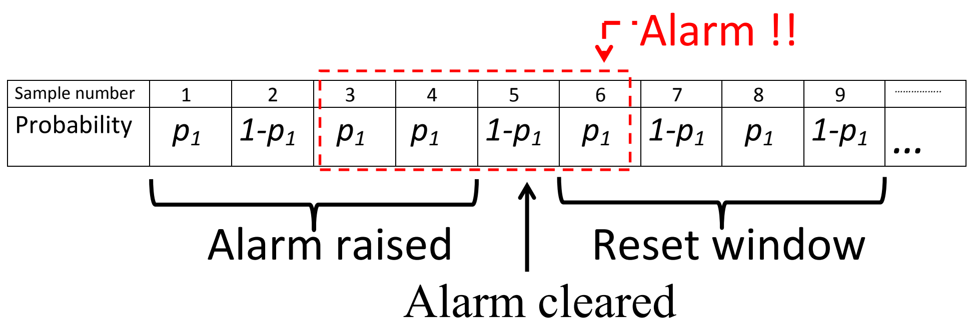

Figure 5.6: Resetting of the Markov process

of the Markov process. In this work resetting is important as otherwise it may seem that conditions to raise and clear alarms are conflicting. For example, if we consider the dotted rectangle in Fig. 5.6 it may appear that there should be an alarm at sample 6; however, it is not true as resetting is done.

5.4 Numerical Calculation of FAR, MAR and EDD

The calculations of FAR, MAR and EDD are based on the information of the transition matrix ($\mathbf{P}$). Except for some special cases discussed in earlier sections, there is no closed form solution so far for the general n_1 out of n samples on-delay and m_1 out of m samples off-delay. In this section we propose an algorithm that can numerically generate the transition matrix, which then can be used to calculate FAR, MAR and EDD. It can generate and reduce the transition matrix for an n_1 out of n on-delay and m_1 out of m off-delay timer whose one sample above threshold probability is p_1.

The algorithm comprises three phases: the generating phase, the discarding phase, and the lumping phase. In the generating phase, a full size transition matrix is generated, in the discarding phase, the transient states are discarded, while in the lumping phase, states are lumped to the coarsest partition and thus we obtain the reduced size transition matrix.

5.4.1 Generating Phase

To generate the full size transition matrix, we firstly define the description sequence of a state.

Definition: An $l = \max(n, m)$ bits binary sequence is called a description sequence for the n_1 out of n on-delay and m_1 out of m off-delay timer. The first bit of the sequence shows whether currently it is an alarm or no-alarm situation; while the rest bits provide the one sample above threshold information of the current and $l-2$ past samples.

Obviously, there are totally 2^l states. Thus, we can obtain a Markov chain with 2^l states. For each state, it is easy to determine the next state to move to in the cases that the next sample is greater and smaller than the threshold, respectively. In other words, each state has two successor states with probability p_1 and $1-p_1$, respectively. After this procedure, an $2^l \times 2^l$ full size transition matrix is established.

To make it clearer, we provide a simple example: A segment of the values of a process variable is $[1.3, 3.5, 5.7, 2.6, 10.2, 11.3]$. The threshold is 8, and the delay timer rule is 2 out of 3 on-delay. In this case, we need a total of $2^3 = 8$ states. At instant 4, the current and previous values, namely, 2.6 and 5.7, are both less than the threshold, and it is in the no-alarm situation. As a result, the description sequence is $'000'$. At instant 5, although the new value 10.2 exceeds the threshold, there is only 1 out of 3 values greater than the threshold. Hence it is still in the no-alarm situation. So the description sequence is $'001'$. When the last value 11.3 comes, 2 out of 3 values are greater than the threshold, which raises the alarm. Therefore, the description sequence changes to $'111'$.

The Markov chain represented by the full size transition matrix have one ergodic set, and all the transient sets include only one state. This is reasonable since the probability that the Markov chain moves to the ergodic set in finite steps is 1.

5.4.2 Discarding Phase

In this phase transient states are discussed. Based on the requirement we mentioned above, the discarding procedure is straight forward:

Step 1: Search for such columns i_k in the transition matrix that all the elements in the column are zero. Assume that $K \neq 0$ columns, $\{i_1, i_2, \cdots, i_K\}$, are found, initialize the discarding states list to $\{i_1, i_2, \cdots, i_K\}$.

Step 2: For an index i_k that appears in the discarding states list, set the two non-zero entries in the i_k-th row to zero, and check those two columns containing these two non-zero entries. If any of them is all-zero column, add its index into the discarding states list. Repeat step 2 for the new added indices in the list until no more such state can be found.

Step 3: Remove all the columns and rows in the discarding list from the transition matrix.

5.4.3 Lumping Phase

The goal of lumping is to group the states based on alarm or no-alarm as well as to refine groups based on successor states. The lumping phase can further decrease the size of the Markov chain.

The Markov chain applied in our work is in a special case: each state has only two possible successor states, and there is a unique probability p_1 for all states. Because of this, the Markov chain is equivalent to a deterministic finite automaton (DFA) with 2^l states and 2 inputs that correspond to p_1 and $1 - p_1$.

The DFA minimization problem is a classical one in the field of computer science that has been extensively studied. Since the goal of lumping the states in our special Markov chain is exactly the same as the purpose of DFA minimization, we can directly adopt the algorithm for the lumping phase.

The essence of the DFA algorithm is to first partition the states according to their outputs (in our case alarm or no-alarm). Then the groups are repeatedly refined based on the successor states on a given input for the states in the same group. If the successor states are in a single group, no further partition

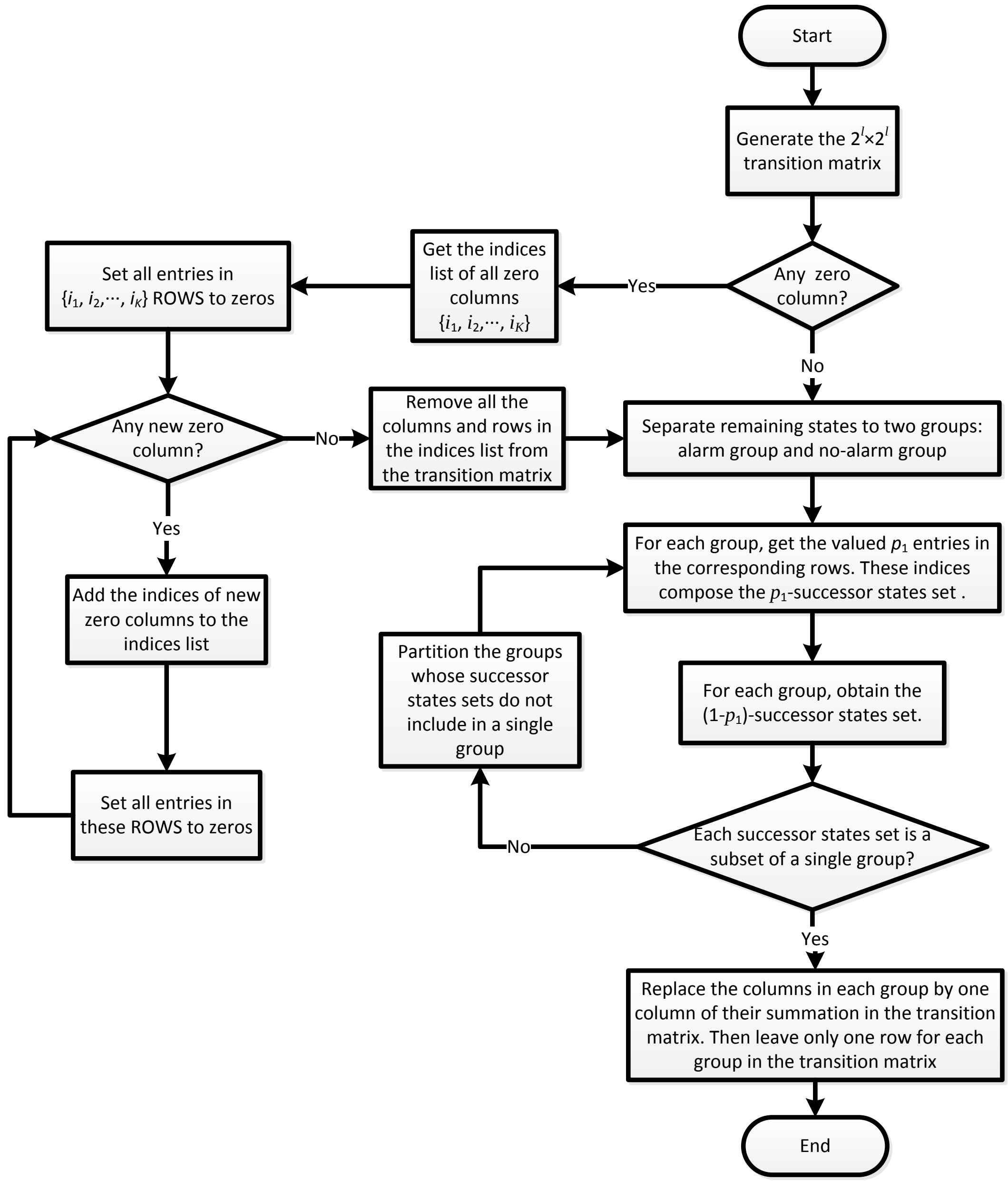

Figure 5.7: Flow chart for generation of transition probability matrices

is required; otherwise partition the group to subgroups whose successor states are in a single group. When no further partition is needed, all states in the same group can be lumped to one state. In reference [56], authors introduced a method that speeded up the algorithm to an $O(n \log(n))$ time bound, where n is the number of states of the automaton.

The reason why we need to reduce the size of the transition matrix is that as the length of the delay-timer increases the size of the transition matrix increases exponentially. Large transition matrices cause great computational burden for invariant vectors, necessary for FAR, MAR and EDD calculation. We conjecture from observation that the algorithm can reduce the size of the transition from 2^l to $C_{n_1-1}^{n} + C_{m_1-1}^{m}$; where C represents combination. A flow chart of the algorithm is given in Fig. 5.7.

Example: 3-out-of-4 on-delay timer, and 2-out-of-3 off-delay time

Generating Phase: Since $l = \max(4, 3) = 4$, the length of description sequence should be 4. So there will be $2^4 = 16$ states, which means that the size of the initial transition matrix should be 16×16. The non-zero entries in the matrix are designed as follows: The first state, state 0, has a description sequence '0000'. The first '0' means no-alarm situation, the following three '0' show that all the latest three samples are under the threshold. The probability that next sample exceeds the threshold is p_1. Then the latest four samples become '0001'. Because of the 3-out-of-4 on-delay timer, the no-alarm situation can be kept. So there is a probability of p_1 that state 0 moves to state 1, namely, '0001' (the first '0' means no-alarm, the following sequence '001' describe the latest three samples). Similarly, there is a probability of $1 - p_1$ that the state is kept. So in the first row, the two non-zero entries are the first and second entries. The values are of them are $1 - p_1$ and p_1, respectively.

Operate on the following 15 states in the same way, finally the initial transition matrix is obtained as follows:

$$
\begin{bmatrix}
1-p_1 & p_1 & 0 & 0 & 0 & 0 & 0 & 0 & 0 & 0 & 0 & 0 & 0 & 0 & 0 & 0 \\
0 & 0 & 1-p_1 & p_1 & 0 & 0 & 0 & 0 & 0 & 0 & 0 & 0 & 0 & 0 & 0 & 0 \\
0 & 0 & 0 & 0 & 1-p_1 & p_1 & 0 & 0 & 0 & 0 & 0 & 0 & 0 & 0 & 0 & 0 \\
0 & 0 & 0 & 0 & 0 & 0 & 1-p_1 & 0 & 0 & 0 & 0 & 0 & 0 & 0 & 0 & p_1 \\
1-p_1 & p_1 & 0 & 0 & 0 & 0 & 0 & 0 & 0 & 0 & 0 & 0 & 0 & 0 & 0 & 0 \\
0 & 0 & 1-p_1 & 0 & 0 & 0 & 0 & 0 & 0 & 0 & 0 & 0 & 0 & 0 & 0 & p_1 \\
0 & 0 & 0 & 0 & 1-p_1 & 0 & 0 & 0 & 0 & 0 & 0 & 0 & 0 & 0 & 0 & p_1 \\
0 & 0 & 0 & 0 & 0 & 0 & 1-p_1 & 0 & 0 & 0 & 0 & 0 & 0 & 0 & 0 & p_1 \\
1-p_1 & 0 & 0 & 0 & 0 & 0 & 0 & 0 & 0 & p_1 & 0 & 0 & 0 & 0 & 0 & 0 \\
1-p_1 & 0 & 0 & 0 & 0 & 0 & 0 & 0 & 0 & 0 & 0 & p_1 & 0 & 0 & 0 & 0 \\
1-p_1 & 0 & 0 & 0 & 0 & 0 & 0 & 0 & 0 & 0 & 0 & 0 & 0 & p_1 & 0 & 0 \\
0 & 0 & 0 & 0 & 0 & 0 & 0 & 0 & 0 & 0 & 0 & 0 & 0 & 0 & 1-p_1 & p_1 \\
1-p_1 & 0 & 0 & 0 & 0 & 0 & 0 & 0 & 0 & p_1 & 0 & 0 & 0 & 0 & 0 & 0 \\
1-p_1 & 0 & 0 & 0 & 0 & 0 & 0 & 0 & 0 & 0 & 0 & p_1 & 0 & 0 & 0 & 0 \\
1-p_1 & 0 & 0 & 0 & 0 & 0 & 0 & 0 & 0 & 0 & 0 & 0 & 0 & p_1 & 0 & 0 \\
0 & 0 & 0 & 0 & 0 & 0 & 0 & 0 & 0 & 0 & 0 & 0 & 0 & 0 & 1-p_1 & p_1
\end{bmatrix}
$$

Discarding phase: Columns 8, 9, 11, 13 are zero columns. So these indices are recorded as the initial discarding states list: $\{7, 8, 10, 12\}$ (since states begin from state 0). Then set the non-zero entries in rows 8, 9, 11, 13 to zero. Then one more zero column, column 10, is found. The discarded states list becomes $\{7, 8, 10, 12, 9,\}$. After set row 10 to a zero row, no more zero column can be found. Rows 8, 9, 10, 11, 13 and columns 8, 9, 10, 11, 13 are removed, and the transition matrix shrinks to the following:

$$
\begin{bmatrix}
1-p_1 & p_1 & 0 & 0 & 0 & 0 & 0 & 0 & 0 & 0 & 0 \\
0 & 0 & 1-p_1 & p_1 & 0 & 0 & 0 & 0 & 0 & 0 & 0 \\
0 & 0 & 0 & 0 & 1-p_1 & p_1 & 0 & 0 & 0 & 0 & 0 \\
0 & 0 & 0 & 0 & 0 & 0 & 1-p_1 & 0 & 0 & 0 & p_1 \\
1-p_1 & p_1 & 0 & 0 & 0 & 0 & 0 & 0 & 0 & 0 & 0 \\
0 & 0 & 1-p_1 & 0 & 0 & 0 & 0 & 0 & 0 & 0 & p_1 \\
0 & 0 & 0 & 0 & 1-p_1 & 0 & 0 & 0 & 0 & 0 & p_1 \\
0 & 0 & 0 & 0 & 0 & 0 & 0 & 0 & 0 & 1-p_1 & p_1 \\
1-p_1 & 0 & 0 & 0 & 0 & 0 & 0 & p_1 & 0 & 0 & 0 \\
1-p_1 & 0 & 0 & 0 & 0 & 0 & 0 & 0 & p_1 & 0 & 0 \\
0 & 0 & 0 & 0 & 0 & 0 & 0 & 0 & 0 & 1-p_1 & p_1
\end{bmatrix}
$$

Lumping phase: After the discarding phase, only 11 states are left. Among them the first 7 states, states $\{0, 1, 2, 3, 4, 5, 6\}$, are no-alarm states, and states $\{7, 8, 9, 10\}$ are alarm states. For the no-alarm states group, the $1-p_1$ successor states set is $\{0, 2, 4, 6\}$, and the p_1 successor states set is $\{1, 3,$

5, 10}. The $1-p_1$ successor states set is a subset of the no-alarm group. However, one element in p_1 successor states set belongs to the alarm group while others belong to the no-alarm group. So the no-alarm group should be partitioned according to its elements' p_1 successor states. As a result, the states are partitioned into three groups: states {3, 5, 6}; states {0, 1, 2, 4}; states {7, 8, 9, 10}. Repeat this procedure until no more partition is needed. Finally, states {0, 4} are in one group; states {7, 10} are in one group. All the other groups have single state. To lump states {0, 4}, pick up a representative state for this group, say state 0; add column 5 to column 1, and then remove column 5 and row 5. To lump states {7, 10}, pick up state 10 as the representative state; add column 7 to column 10, and then remove column 7 and row 7. Eventually, the reduced size transition matrix is obtained as follows:

$$\begin{bmatrix} 1-p_1 & p_1 & 0 & 0 & 0 & 0 & 0 & 0 & 0 \\ 0 & 0 & 1-p_1 & p_1 & 0 & 0 & 0 & 0 & 0 \\ 1-p_1 & 0 & 0 & 0 & p_1 & 0 & 0 & 0 & 0 \\ 0 & 0 & 0 & 0 & 0 & 1-p_1 & 0 & 0 & p_1 \\ 0 & 0 & 1-p_1 & 0 & 0 & 0 & 0 & 0 & p_1 \\ 1-p_1 & 0 & 0 & 0 & 0 & 0 & 0 & 0 & p_1 \\ 1-p_1 & 0 & 0 & 0 & 0 & 0 & 0 & 0 & p_1 \\ 1-p_1 & 0 & 0 & 0 & 0 & 0 & p_1 & 0 & 0 \\ 0 & 0 & 0 & 0 & 0 & 0 & 0 & 1-p_1 & p_1 \end{bmatrix}$$

5.5 Comparative Analysis

For a discussion of advantages and disadvantages of the proposed generalized delay-timers and the conventional delay-timers, their performance is compared in this section in terms of three criteria, namely, accuracy (ROC curve with false and missed alarm rates), latency (detection delay with respect to change in settings) and sensitivity (change in performance with any change in design settings).

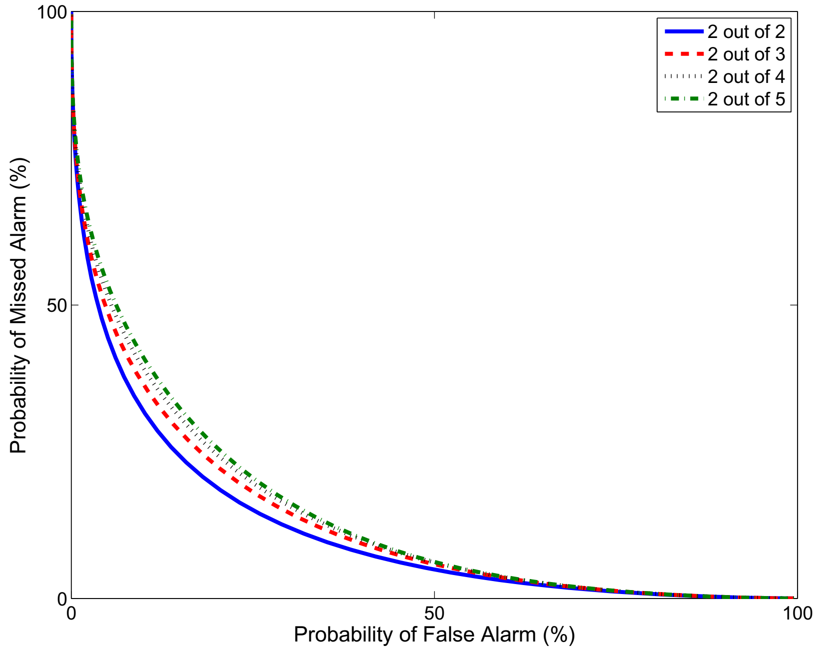

(a)

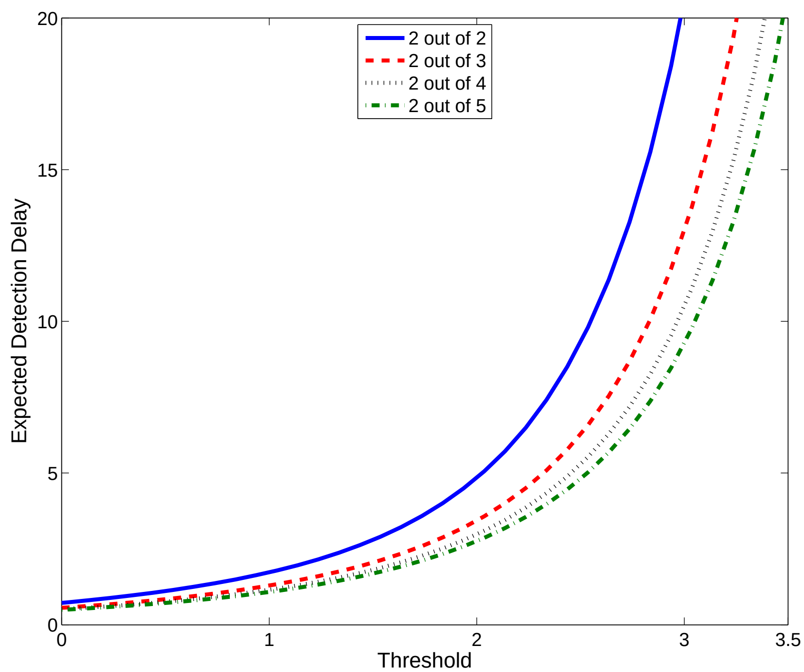

(b)

Figure 5.8: (a) Changes in ROC curves for corresponding changes in the threshold for $n = 2$ to 5, $n_1 = 2$; (b) corresponding changes in EDD curves

5.5.1 Accuracy and Latency

The receiver operating characteristic (ROC) curve is the plot of two alternatives when the decision variable is changed [57]. In our context, the ROC curve is the plot of FAR vs MAR when the threshold changes. It is widely used in signal detection theory for graphical sensitivity analysis. For simplicity of analysis only on-delay timers are considered in this section.

Generally different costs are associated with false and missed alarm rates. Selection of the appropriate point on the ROC curve depends on these costs. Usually a weighted combination of false and missed alarm rates are used to include these associated costs in the design. For simplicity, if $(\text{FAR})^2+(\text{MAR})^2$ is used as the performance index, then the optimum point on the ROC curve will be the point closest to the origin; and the corresponding threshold of the optimum point in the ROC curve will be the optimum operating threshold. In this case, if the threshold is set higher than the optimum point, false alarms will decrease at the cost of increased missed alarms. On the other hand, setting the threshold lower than the optimum point will result in smaller number of missed alarms but more false alarms.

A process variable is considered with Gaussian distribution where fault-free data has mean 0, variance 2 and faulty data has mean 2, variance 2. The data length is 1000 for both fault-free and faulty section; 1 sec uniform sampling is used. The threshold is varied from minimum of the process data to the maximum with 0.05 increment. In Fig. 5.8(a), the corresponding ROC curves are obtained for different delay-timers ($n_1 = 2,\ n = 2 - 5$).

Example 3

It is normally desirable to minimize both FAR and MAR which account for *accuracy* of the alarm design; better accuracy indicates lower false and missed alarm rates. It can be seen from Fig. 5.8(a) that with use of the conventional 2 out of 2 samples delay-timer, the ROC curve is closer to the origin. But when generalized n_1 out of n idea is used, the curves move away from the origin. This indicates that increasing of n with fixed n_1 decreases the accuracy of alarm

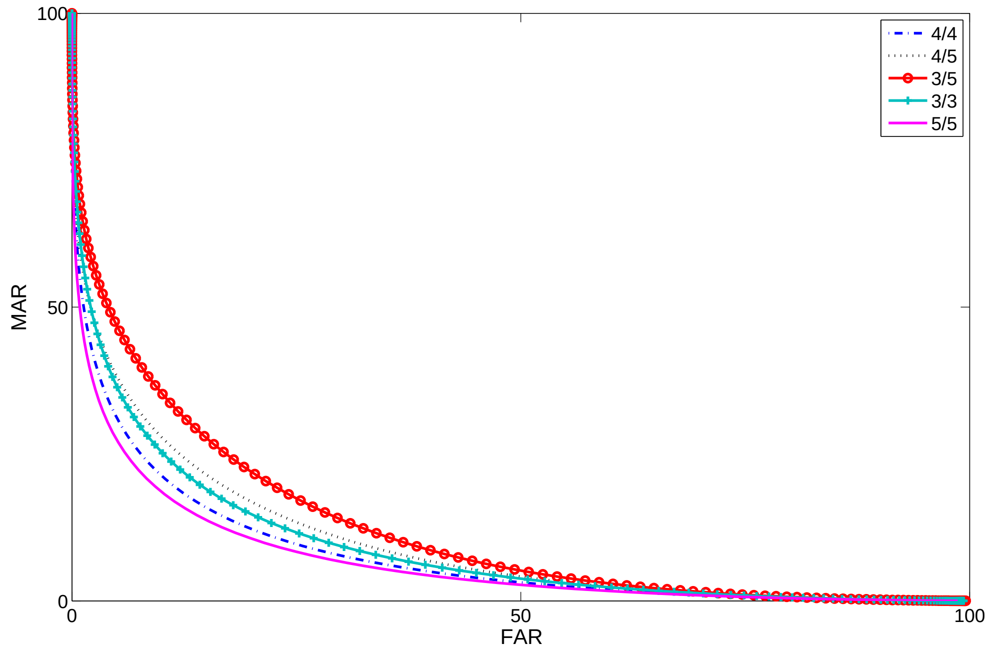

(a)

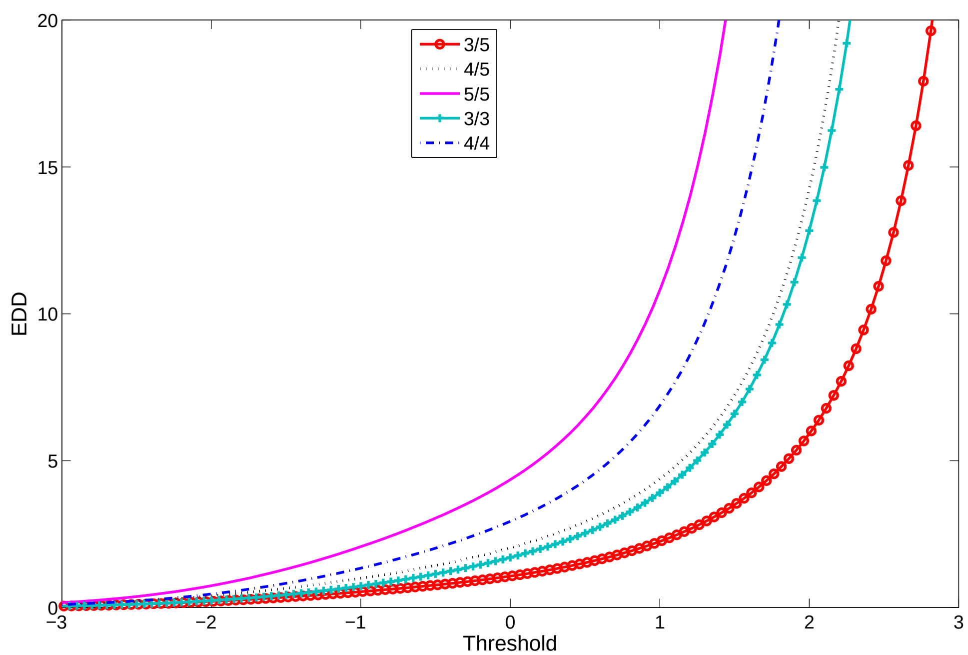

(b)

Figure 5.9: (a) Changes in ROC curves for corresponding changes in the threshold; (b) corresponding changes in EDD curves

systems. On the other hand, in addition to better accuracy a lower detection delay (*latency*) is also a desired feature. Fig. 5.8(b) indicates that increasing of n with fixed n_1 results in lower detection delays. Here conventional delay-timers cause lower FAR and MAR compared to the generalized cases, which is expected; however, they also cause higher detection delays.

Example 4

In the previous example, only n was varied while keeping n_1 fixed. Now a few cases of different n and n_1 in close range would be considered for comparison. Here generalized 3 out of 5, 4 out of 5 and conventional 5 samples on-delay cases are considered. Then the corresponding ROC and EDD curves in these three cases are compared with conventional 3 and 4 samples on-delay timers.

Like the previous example, from Fig. 5.9(a) it can also be seen that a conventional delay-timer has higher accuracy compared to a generalized one. A 5 out of 5 on-delay is more accurate than 4 out of 4 case. Even a 4 out 4 on-delay yields more accurate design than a 4 out of 5 on-delay. The downside is the higher delay in detection. In this case a conventional 5 samples on-delay has the highest and a generalized 3 out of 5 on-delay has the lowest detection delay.

5.5.2 Sensitivity

During practical process operations, it is very likely to adjust alarm design parameters for many reasons. Therefore, it is necessary to investigate the degree to which changes in alarm design parameters affect performance indices. Here, the parameter that changes most frequently is the alarm limit or threshold for a fixed delay-timer. We define sensitivity as the ratio of the infinitesimal change in the function (FAR, MAR or EDD) to the infinitesimal change in the alarm limit (y_{tp}) for a fixed delay-timer:

$$S_{F:t} = \lim_{\Delta y_{tp} \to 0} \frac{\text{Fractional change in the function, F}}{\text{Fractional change in the threshold, } y_{tp}} \tag{5.18}$$

$$= \lim_{\Delta y_{tp} \to 0} \frac{\frac{\Delta F}{F}}{\frac{\Delta y_{tp}}{y_{tp}}} \tag{5.19}$$

$$= \frac{y_{tp}}{F} \frac{\partial F}{\partial y_{tp}}$$

Here F can be any of the FAR, MAR, and EDD quantities derived in earlier sections. As a specific example, equation (5.8) for the false alarm rate of 2 out of n on-delay is considered. Replacing $p_2 = 1 - p_1$ and denoting $p_1 = p$, it can be shown that the sensitivity is

$$S = y_{tp} \frac{(1-p)^n(np^2 - p^2 - np - 2p + 3) - (1-p)^{2n} - 2(1-p)^2}{p(1-p)^n - (1-p)p^2 - 3p - (1-p)^n + 2} f(y_{tp})$$

here $f(y_{tp})$ represents the value of likelihood function in Fig. 2.2.

Consider the sensitivity curves in Fig. 5.10(a) which are obtained for the same set of data in Example 3 with the threshold changing from 0 to 2. It can be seen that for the 2 out of n samples on-delay, a lesser value of n is more sensitive to the threshold change comparative to a lower one. This indicates the conventional delay-timer is more sensitive to changes in threshold than the generalized one.

The following observation also shows that a generalized n_1 out of n on-delay timer gives a less sensitive design compared to the conventional delay-timer. For Example 4, sensitivity curves are shown in Fig. 5.10(b). Here the 3 out of 5 case is the least sensitive and 5 out 5 is most sensitive to any change in the threshold. 4 samples and 4 out of 5 samples on-delays have very similar profiles; similarly for 3 samples and 3 out of 5 samples on-delays. This indicates that for sensitivity, n_1 is more important than n in these cases.

Sensitivity analysis is very important as small changes in the distributions of normal and abnormal data, which may be regarded equivalently as small changes in the threshold, can cause significant deviations in FAR and MAR; such sensitivity is not desirable in practice.

5.6 Conclusion and Future Work

Generalized delay-timers provide more flexibility in alarm design. In this chapter, three performance specifications of alarm delay-timers, namely, the FAR, MAR and EDD, are calculated for generalized delay-timers. Some preliminary sensitivity analysis and comparison of performance of the generalized and conventional frameworks are also discussed. As a future extension, further study on the sensitivity advantage of generalized delay-timers is required by a systematic approach.

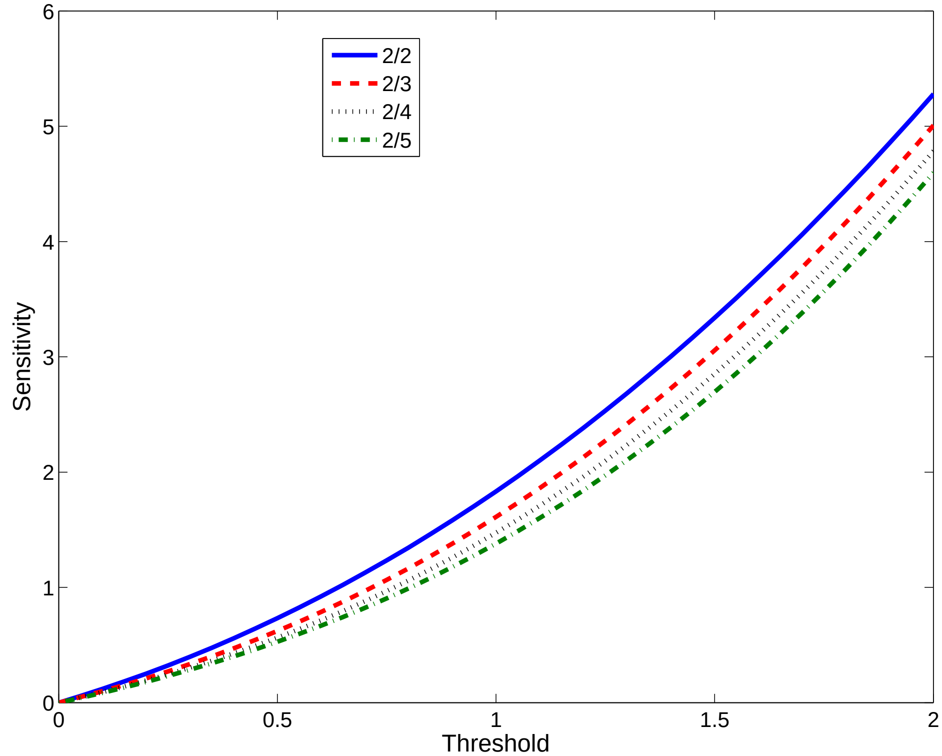

(a)

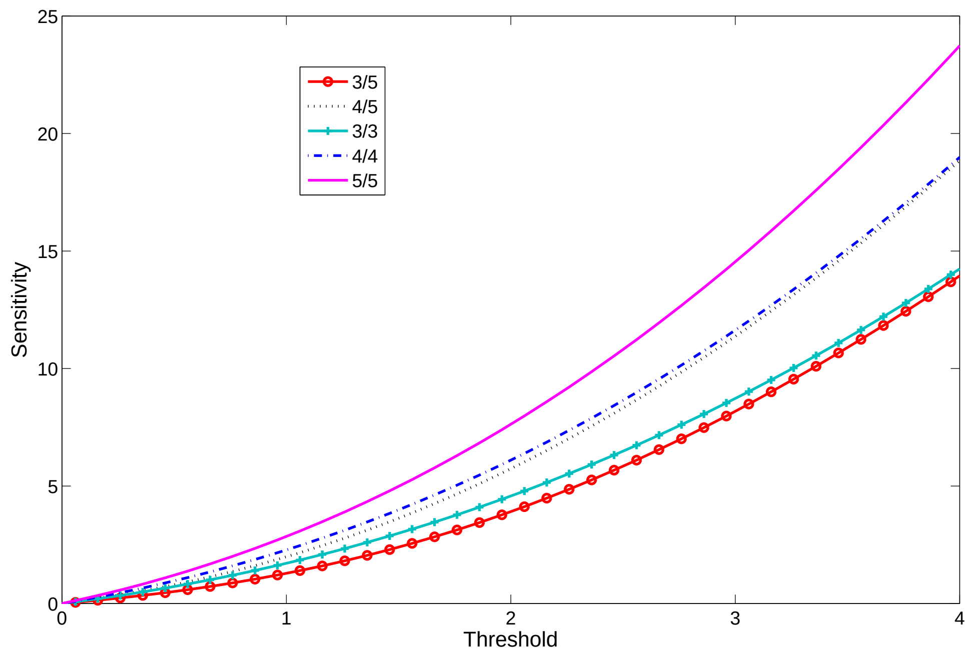

(b)

Figure 5.10: (a) Sensitivity curves for Example 3; (b) sensitivity curves for Example 4

Chapter 6

Industrial Application: Systematic Design and Accuracy vs Latency Analysis

Alarm design and rationalization is a systematic work process of evaluating all alarm settings to check for legitimacy, accuracy and rationale. An efficiently rationalized alarm system is expected to have properly tuned alarm settings with reduced alarm load on the operator. The overall work for alarm rationalization can be divided into several classes - selecting alarm to rationalize, justification and prioritization, operator decision support, classification, setting alarm limits, alarm tuning and advanced alarming, and safety analysis. In practice, the rationalization team requires knowledge from control engineering team, operations, maintenance and other disciplines. However, this chapter focuses on possible applications of developed methods in earlier chapters; some of the rationalization aspects are out of scope because of practical limitations.

The rest of the chapter is organized as follows: in Section 6.1, a systematic alarm design process is discussed based on the methods described in Chapter 3. In Section 6.2, sensitivity vs accuracy is addressed for the generalized delay-timer. Section 6.3 discusses the perturbation of Markov chain. Finally, limitations and future works are discussed in Section 6.4.

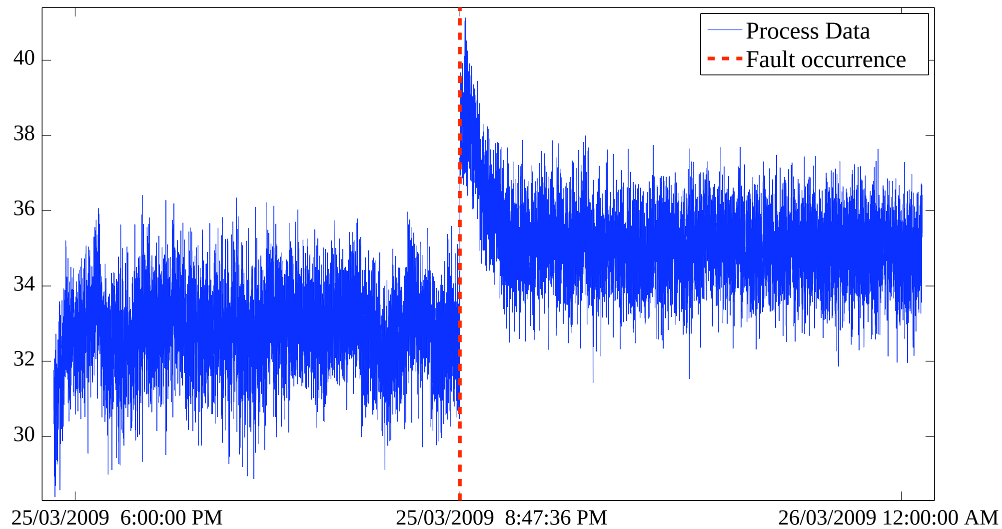

Figure 6.1: Flow variable from an oil-sand industry

Table 6.1: Design parameters selection chart for the case study 1

Delay-timer (n)	Threshold (t)	FAR = MAR (%)	EDD
2	33.97	3.19	1.28
3	33.97	0.64	2.75
4	33.97	0.11	4.44
5	33.97	0.02	6.37

6.1 Systematic Alarm Design

A well designed univariate alarm configuration is expected to fulfill FAR, MAR and EDD requirements. In this section, two case studies are discussed to design an alarm system with optimal balance of these indices.

Case study 1

An actual flow variable from an oil-sand processing facility is considered for case study here for high alarm. The sampling time is 1 *sec* and fault is assumed to occur on March 25, 2009 at time 8:47:36 PM (Fig. 6.1). Histograms of the corresponding fault-free and faulty data can be seen on Fig. 6.2. We want to design an alarm limit such that, FAR $\leq$ 2%, MAR $\leq$ 2% and EDD $\leq$ 8 seconds. Since the sampling time here is 1 *sec*, EDD $\leq$ 8 samples.

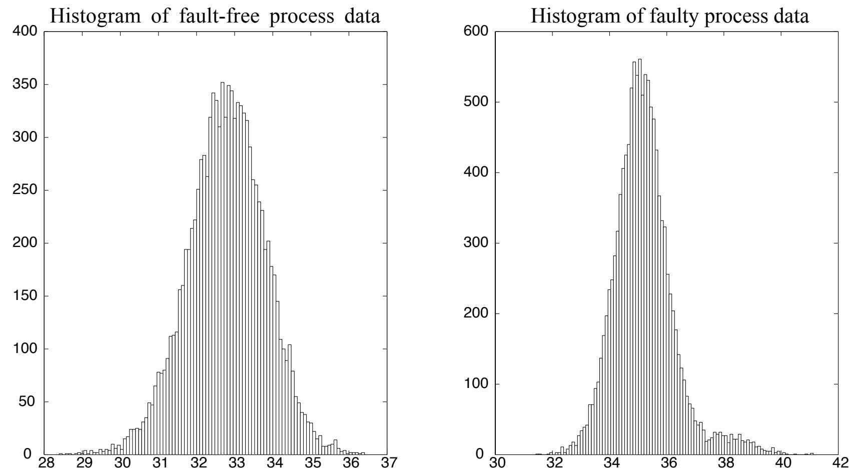

Figure 6.2: Histograms of the corresponding fault-free and faulty data

To design the delay timer, the same four-step process can be followed. Here probabilities required for alarm design are estimated empirically. In step 1, thresholds that satisfy the requirements of FAR = MAR = 2% are estimated from Fig. 6.3. Estimated thresholds are represented by dots here as well and highlighted in Table 6.1. In the next step, the smallest delay-timer n_1 that satisfies FAR = MAR $\leq$ 2% is selected from Fig. 6.3; here $n_1 = 3$. In step 3, the largest delay-timer n_2 for $EDD \leq 8$ samples is estimated from Fig. 6.4; here $n_2 = 5$. Since $n_2 \geq n_1$, according to previous discussions, any n satisfying

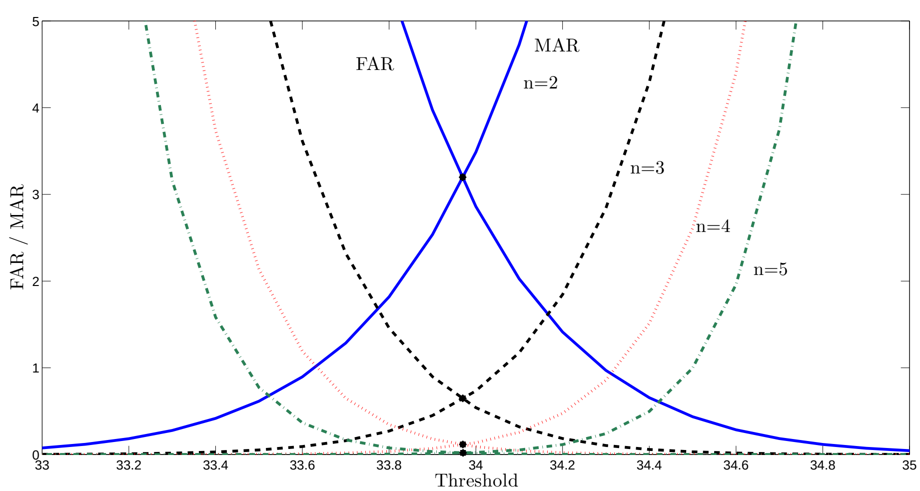

Figure 6.3: Estimation of threshold when FAR = MAR

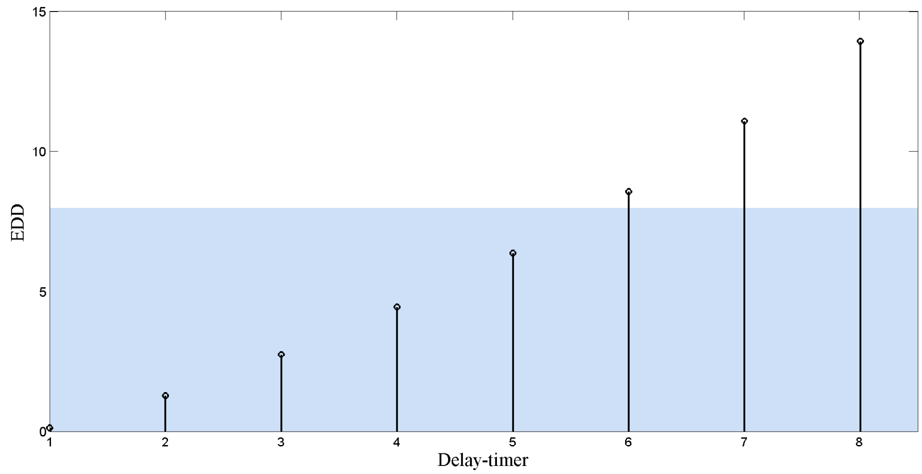

Figure 6.4: Effect on EDD for different delay-timers

$n_1 \leq n \leq n_2$ can be used for the design purpose. In step 4, it can be concluded that, any delay-timer of length in the range $n = 3$ to $n = 5$ can be used for the process data. Optimal threshold limit is approximately 34 and associated detection delays are 2.75 *samples* to 6.37 *samples* respectively.

The obtained results can be compared with a 3-sigma control limit on the Shewhart chart. Here the fault free data has a mean 32.8 and variance 1.04. If a 3-sigma control limit is followed, the threshold will be at 35.84 and a delay-timer of 4 samples result in $\approx 0\%$ FAR but MAR is more than 90%. Whereas, following the proposed method, a better performance can be achieved in terms of both FAR and MAR.

Case study 2

Table 6.2: Design parameter selection chart for the case study 2; $W1$, $W2$ and $W3$ represent three windows of faulty data

(n)	Threshold (t)			FAR = MAR (%)			EDD		
	$W1$	$W2$	$W3$	$W1$	$W2$	$W3$	$W1$	$W2$	$W3$
2	≈10.5	11.19	10.8	3.51	0.001	0.19	1.59	1	1.13
3	≈10.5	11-11.3	10.8	0.77	0	0.01	3.35	2.02	2.25
4	≈10.5	10.8-11.9	10.8-10.9	0.18	0	0	5.35	3.05	3.41
5	≈10.5	10.7-12	10.7-11	0.35	0	0	7.64	4.04	4.6

In the case of different faults resulting in different distributions, it will

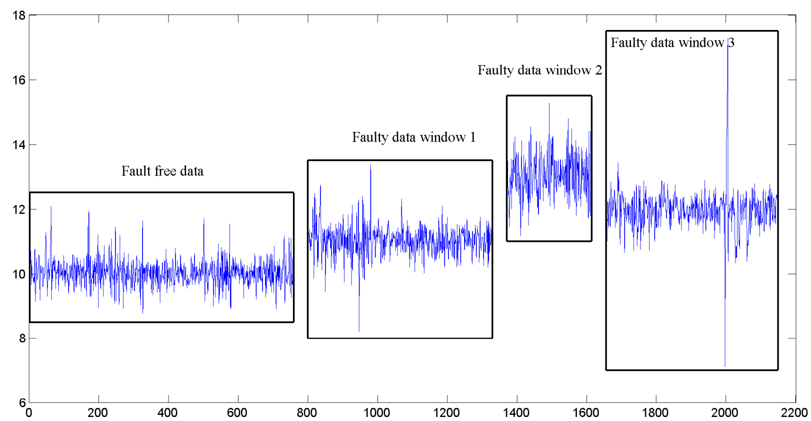

Figure 6.5: Sludge header pressure process data for the second case study

require some experience to select a portion of faulty data suitable for the design. This portion will most likely result in a conservative recommendation of alarm settings, which ensures satisfactory performance for other faults. To show this a second case study with multiple faults is considered. Another actual variable (sludge header pressure) from the same oil-sand processing facility is considered for the second case study for high alarm design. The variable is slow sampled at a sampling period of 1 min. From 1 week duration process data, three different steady-state faulty data windows (Fig. 6.5) are considered for analysis using expert process knowledge. The same steady-state fault-free data is used in three cases, as the distribution of fault-free data is expected to remain constant in normal system operation. With the help of three different faulty data sets, it will be easy to demonstrate how selection of data window affects the design parameters.

Following the same 4-step design process, Table 6.2 is constructed. Analysis is presented in the table for delay-timers, $n = 2$ to 5. For the selected variable, to design a system with FAR = MAR $\leq 5\%$ and EDD ≤ 5 samples, according to Table 6.2, $n = 2$ or 3 can be used if faulty window 1 is considered for design; whereas if window 2 or 3 is considered for analysis, any n ranging from 2 to 5 can be selected. If faulty data window 1 is selected, the optimal threshold of operation will be 10.5, delay-timers are $n = 2$ or 3 and the associated EDD are 1.59 or 3.35 samples respectively. Other delay-timers

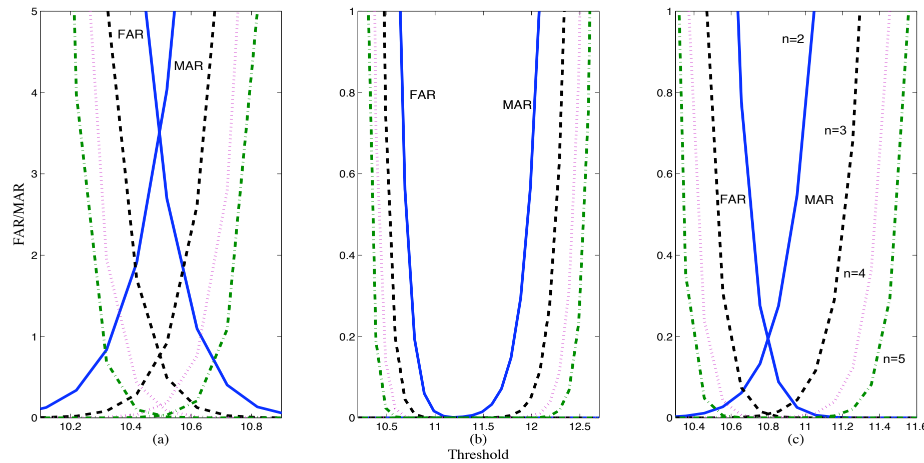

Figure 6.6: Estimation of threshold where FAR = MAR for case study 2

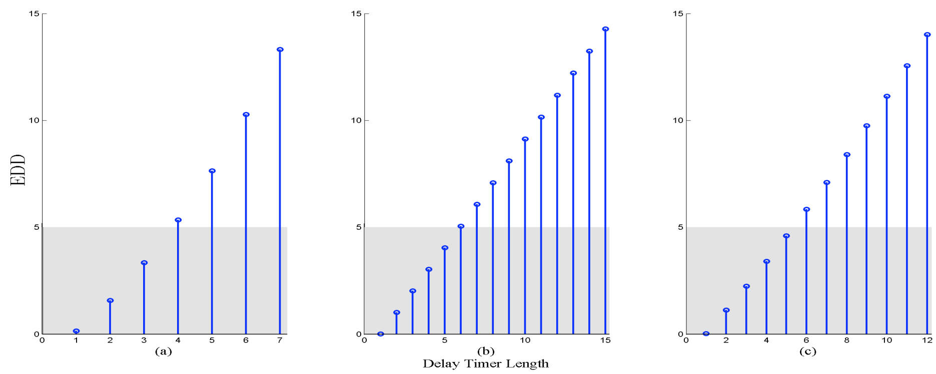

Figure 6.7: Estimation of EDD for case study 2

do not meet the design requirements. Faulty data windows 2 and 3 provide more flexibility in parameter selection which is well expected from the signals as shown in Fig. 6.5. Associated FAR and MAR are also very small in later cases. But if the design is implemented based on the window 2 or 3, it will not be optimal for faults similar to window 1 with a lower mean value that require more conservative design. For example, according to Table 6.2, for faulty data window 2, $n = 3$ and threshold 11.3 are an acceptable design. This design will result in detection delay of 17 samples for faults in window 1. Therefore, selection of fault types is very important and before any change is made, careful safety analysis should be performed.

6.2 Accuracy vs Latency of Design

The ROC curve is a popular way of displaying discriminatory accuracy of a test between two classifiers. There are several ways to use ROC curves in accuracy estimation. For example, if equal weight is given on both the false and missed alarm rates, then accuracy increases as the curve moves closer to the origin. Area under the curve (AUC) is another method widely used as a measure of accuracy [66, 67]. In literature many methods are available to estimate and compare the area under the curve [66, 68]. However, in this work, we take the approach of closeness of the curve to the origin as described in [13].

Case study 3

From an oil-sand processing facility, the same flow measurement as in case study 1 is considered here (Fig. 6.1). Three different combinations of delay-timers are applied on the measured variable to compare their results of FAR, MAR and EDD. Performance of a conventional 5 samples on-delay is compared with 3 out of 5 and 4 out of 5 samples generalized setup. A comparison of FAR, MAR and EDD can be seen from Table 6.3. Here the mean of fault-free

Table 6.3: Comparison of FAR, MAR and EDD changing thresholds for case study 3

On-delay timer	Thresholds	FAR	MAR	EDD
3 out of 5	32.8	30	1.65	3
	33.82	4.65	15.6	4
	34.84	0.1	57.01	5
	35.85	0	90.34	5
4 out of 5	32.8	23.42	2.13	1
	33.82	2.52	19.13	5
	34.84	0.04	64.60	6
	35.85	0	92.71	6
5 out of 5	32.8	15.44	2.73	5
	33.82	1.23	24.08	6
	34.84	0.01	73.81	7
	35.85	0	94.13	7

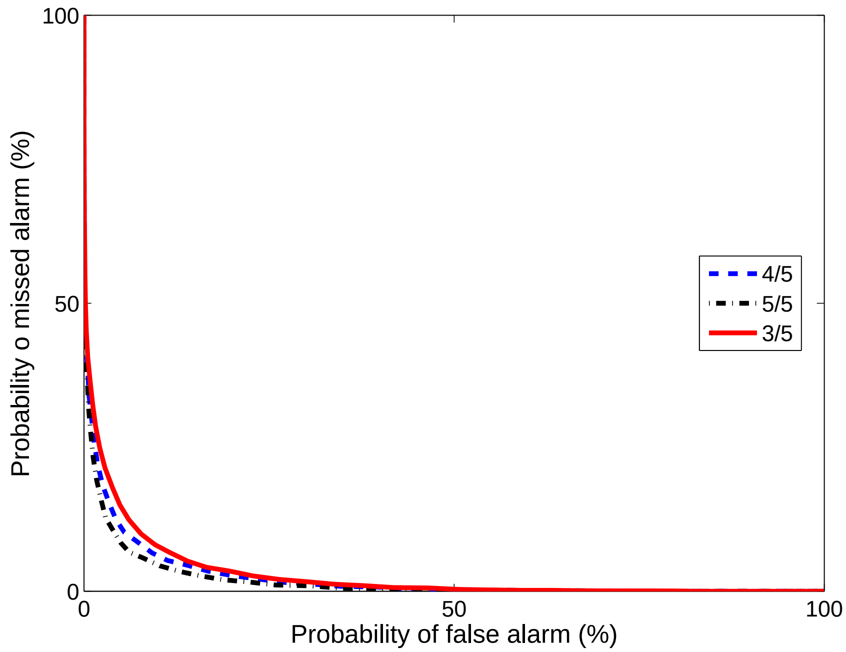

(a)

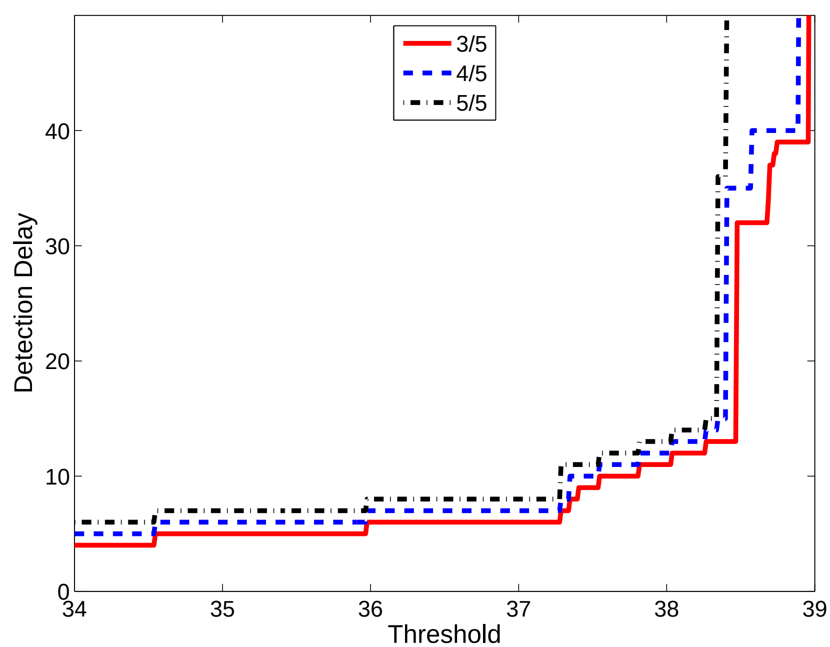

(b)

Figure 6.8: (a) ROC curves for case study 3; (b) EDD curves for case study 3 changing thresholds

data is 32.8 and variance is 1.04. The chart is obtained following a 3-sigma limit of Shewhart chart and setting thresholds at one sigma distance.

From Fig. 6.8(a) and 6.8(b), it can be seen that conventional setup is more accurate if equal weight is given on false and missed alarms as the curve is closest to the origin. However, the generalized configuration causes lower detection delay, as was also observed in previous simulation examples in Chapter 5. This kind of chart can be followed to determine operating settings of the delay-timer. Depending on design requirements of FAR, MAR and EDD, operating thresholds and on-delay configuration can be fixed. For example, if the requirement is $\leq 5\%$ MAR and ≤ 10 samples EDD irrespective of FAR, then either of generalized 3 or 4 out of 5 samples and conventional 5 samples on-delay timers can be used in setting the threshold at 32.8. But if the requirement is changed to $\leq 5\%$ FAR and < 5 samples EDD, then the conventional setup cannot satisfy the conditions. A 3 out of 5 samples generalized setup is required in setting the threshold at 33.82. In practice, any change in alarm configuration setting requires significant process knowledge, and detailed safety analysis is a must before any change is made.

6.3 Perturbation in Markov Processes

The alarm design method case studies discussed here are primarily dependent on historical process data and expert process knowledge. With advent of modern DCS, a large quantity of data is normally stored nowadays in the data historian. The historical process data and expert process knowledge can be used in combination for effective alarm design. Once alarm settings are configured, the next important question is how well the design performs under changed circumstances. The process may change from time to time bringing the question of effectiveness of design under varying process conditions. To be precise, the question can further be narrowed down to the sensitivity of ergodic Markov processes, which is the basis of developed methods discussed in earlier chapters. Perturbation of Markov processes is a large area of research and is beyond the scope in this thesis. However, some relevant work in the literature is highlighted in this section.

Suppose that an irreducible Markov process with transition matrix $\mathbf{P}$ is perturbed by a matrix $\mathbf{E}$ such that $\tilde{\mathbf{P}} = \mathbf{P} - \mathbf{E}$ is also irreducible. If $\pi \in R^{1\times n}$ denotes the stationary distribution of $\mathbf{P}$, then $\pi\mathbf{P} = \pi$ and $\pi u = 1$ with $u = (1, \cdots, 1)^T \in R^{n\times 1}$ and $\tilde{\pi}$ is the stationary distribution vector of perturbed transition probability matrix $\tilde{\mathbf{P}}$. Perturbation does not alter stochastic nature of the matrix. For $\mathbf{E} = \mathbf{P} - \tilde{\mathbf{P}}$, the relationship with invariant vector is given by [58]

$$\|\pi - \tilde{\pi}\| \leq \kappa \|\mathbf{E}\|_\infty$$

where, κ is the condition number.

Impact of changes in transition probabilities on stationary distribution and fundamental matrix is discussed in [59]. Later, some other condition numbers in terms of fundamental matrix of Markov chains are developed [60, 61, 62, 63]. However, the condition number in terms of mean first passage time is more relevant for the transition probability matrices considered here as discussed in [64]. If m_{ij} denote the mean first passage time from state i to state j in the unperturbed chain, the absolute change in the jth stationary probability is given by [64]

$$\|\pi_j - \tilde{\pi_j}\|_\infty \leq \frac{1}{2}\text{max}_j \left[\frac{\text{max}_{i\neq j} m_{ij}}{m_{jj}}\right] \|\mathbf{E}\|_\infty$$

If the condition number is relatively small, it can be inferred that the stationary probability is not unduly sensitive to perturbation in $\mathbf{P}$.

6.4 Conclusion and Future Work

The alarm design and rationalization process is heavily dependent on historical process data. Since from time to time process nature changes because of many reasons, the design needs to be reviewed and updated regularly as required. Furthermore, selection of data window is a real challenge because of varying process conditions. Operators working in the control room also behave subjectively and often differ in procedures followed. These limitations can be addressed in the future with virtual object modeling and work flow data mining.

Chapter 7

Concluding Remarks

Process safety is a critical concern nowadays in industries. Although it may be far from reality to achieve inherent safety, an effective monitoring system is an important step in designing protection layers. Because of the advantages offered by modern DCS systems, it is nowadays possible to monitor virtually every aspect of a process plant. However, the challenging part is to present the information to the operator efficiently and assist in taking preventative steps before any incident happens. Many of the major accidents in the past happened only because of misleading and overwhelming information in the control panel where operators failed to identify and acknowledge the problem in a timely manner. Therefore, alarm management and design have paramount importance for safe process operations.

This thesis explores quantitative relationship between the commonly used univariate alarm design methods and associated performance measures. In the literature model-based fault detection is covered extensively. Although the signal-based method is most widely used and easy to implement compared to model-based methods, it did not receive much attention in academia. The ISA 18.2 and EEMUA 191 standards are recently published as a guideline for alarm management and design; but industries are still far from what is recommended by these standards. In order to comply with ISA 18.2 and EEMUA 191, there is no alternate other than following a systematic alarm system design and rationalization method.

Delay-timers and deadbands are two very common alarm design techniques used in the industry. These methods can be implemented easily in most modern DCS systems and are effective in reducing false and nuisance alarms. However, there is a common misconception that 10-second or any other configuration of delay-timer delays the alarm activation by ten seconds or so, which is hardly the case in reality. In Chapter 3, the detection delay is calculated for simple limit checking, deadbands and delay-timers. The alarm systems with deadbands and delay-timers are modeled using Markov processes; and historical process data is used to estimate the invariant probability vector. Also an optimal alarm design method is discussed that allows compromise between the false alarm rate, the missed alarm rate and the detection delay.

Filtering is another widely applied method in industry for noise suppression. Noisy signal often cause nuisance and chattering alarms and filtering can effectively reduce this problem. However, the downside is filtering delays alarm activation similar to that of delay-timers and deadbands. Two most commonly used filters in the industry are the moving average filter and exponentially weighted moving average filter. The main problem in computation of the detection delay caused by filtering is correlation among the samples of filtered data. In Chapter 4, the detection delay is calculated for moving average filters considering the correlation among contiguous samples.

The idea of conventional delay-timer technique is extended to generalized delay-timer in Chapter 5. The purpose of the delay-timer is to avoid unnecessary alarms when a signal temporarily overshoots or undershoots the limit. In the conventional method, the process signal is required to stay in the alarm state for a specified period of time before activating an alarm. The specified period of time requirement for delay-timer settings is often rigid and sensitive to process condition changes. For example, a 60-second on-delay high alarm setting on a level variable requires the variable to remain constantly above the limit at least for 60 seconds. If the measured variable falls below the limit in that 60 second window even for 1 second, the alarm is not activated. It is not impractical to imagine a case where in the considered 60-second window few samples randomly fails to meet the requirement in an abnormal situation.

Therefore in the proposed generalized delay-timer method the condition is relaxed to n_1 out of n consecutive samples requirement. When $n_1 = n$, the generalized and conventional methods are same. For the proposed generalized method, the false alarm rate, the missed alarm rate and the detection delay are calculated. Advantages and disadvantage of the proposed method are discussed in terms of sensitivity and accuracy of design.

Chapter 6 considered the application of developed methods to industrial problems. Three case studies are discussed including alarm limit and delay-timer settings, incorporating expert knowledge in alarm design, and accuracy vs sensitivity comparison for the proposed generalized delay-timer setup. The calculation of false alarm rates, missed alarm rates and detection delays for various methods depends on historical process data to estimate probabilities. Therefore, the question of effectiveness of design under changed process conditions is an important one. Case studies 1 and 2 address this issue and in case study 3 it is shown that the proposed generalized delay-timer is less sensitive compared to conventional case. However, in terms of accuracy, the conventional setup is more accurate.

7.1 Major Thesis Contributions

This thesis focuses on developing quantitative relationship among commonly used alarm design methods and performance measures; and the major contributions of this thesis are summarized below:

- Chapter 3 presented the hitting time concept to compute detection delay for the simple alarm limit design, the delay-timer and the deadband techniques. An alarm design method is also discussed that balances among the false alarm rate, the missed alarm rate and the detection delay.

- Chapter 4 discussed the detection delay caused by the moving average filter considering correlation among contiguous samples. A method to design filter order is also given.

- Chapter 5 extended the conventional delay-timer method to a generalized setup. Advantages and disadvantages of the proposed method are compared with conventional delay-timers in terms of sensitivity and accuracy.

- Chapter 6 presented application of the developed method to industrial problems. With several case studies, possible application and rationale are demonstrated.

7.2 Directions for Future Work

Alarm systems design, management and rationalization are comparatively new area of research in academia. Recently published two standards, the ISA 18.2 and the EEMUA 191, have given an opportunity to the industry to compare their performance index against recommended values. There are lot of opportunities to advance this study and the following are some suggested areas that could be pursued in future research.

- **Human Factors in Alarm Design**

  In the process plant, the action of operators sitting in the control panel is very important. When abnormality occurs, alarms raised in the control panel require appropriate corrective actions from operators to avoid any damage. However, the critical issue here is subjective nature of operators sitting in front of the console. The purpose of the alarm system is to alert, inform and guide an operator. But, human limitations cannot be ignored and time required to respond to an alarm as well as possible differences in interpretation of root cause may vary from one operator to another. Therefore, it is quite natural that an effective alarm system cannot be designed without taking human factors into consideration. Some preliminary work is discussed on behavior simulation using a virtual object model [69, 70]. There are scopes for extending the work to evaluate effectiveness of alarm systems in terms of operators' action and work flow mining to establish best practice.

- **Alarm Flood and Causality Analysis**

  Alarm flood or alarm shower is a major problem in process industries and is a main contributing factor of many catastrophic incidents in the past. During alarm floods, operators are overwhelmed with information and often fail to recognize the root cause of problems. The problem of alarm flood is addressed based on similarity analysis and pattern matching in [21, 43]. Apart from similarity analysis or pattern matching, another method to identify root cause of abnormality is causality detection [71, 72]. Computation of dependent industrial alarms based on causality detection is discussed in [44]. However, in the future this work can be extended to prediction based alarm systems design to detect forthcoming alarm floods and identify root causes of problems at an early stage.

- **Sensitivity of Design**

  The computation of the false alarm rate, the missed alarm rate and the detection delay discussed in Chapter 3 and 5 uses invariant probability vectors of Markov processes obtained from the historical process data. In a process plant, the operating conditions may change from time to time. In this thesis, sensitivity of FAR, MAR and EDD is discussed in terms of changes in alarm limit. However, another important topic to be addressed is sensitivity due to perturbation of Markov processes, which is the basis of calculation for the invariant probability vector or stationary distributions. In [58], a comparative study of perturbation bounds for the stationary distribution of a Markov chain is discussed. The work can be further extended to the domain of alarm systems design and analysis.

  The historical process data is a great resource for effective alarm design.

In this thesis, the distribution is assumed to be known a priori and data is assumed to be independent and identically distributed (IID). The IID assumption on data distribution, although restrictive to some extent, is not impractical [71]. Therefore, application of the proposed method has some limitations. However, in the future the problem of non IID distribution can be addressed.

Appendix A

Proof of Expected Detection Delay for Delay-Timers

The proof of expected detection delay in Section 3.3 is presented here for the general case. Assume n-samples on-delay and m-samples off-delay; the expected detection delay is given by

$$E(DD) = \sum_{z=0}^{\infty} z\ P(DD = z) = \pi_n P_f Q(I-Q)^{-2} \left[0 \cdots 0\ 1 \cdots 1\right]^T$$

$$= \frac{p_2^{m-1}\left(p_1^n q_1 \sum_{i=0}^{n-1} q_2^i + p_2 \left(\sum_{j=0}^{n-1} p_1^j \sum_{k=0}^{n-j-1} q_2^k - q_2^n \sum_{i=0}^{n-1} p_1^i\right)\right)}{q_2^n \left(p_2^m \sum_{i=0}^{n-1} p_1^i + p_1^n \sum_{i=0}^{m-1} p_2^i\right)}$$

First, we invert $I - Q$. It can be verified that

$(I-Q)^{-1} =$

$$\begin{bmatrix}
\frac{1}{q_2^n} & \frac{1}{q_2^{n-1}} & \frac{1}{q_2^{n-2}} & \frac{1}{q_2^{n-3}} & \cdots & \frac{1}{q_2^2} & \frac{1}{q_2} & 1 & 0 & \cdots & 0 \\
\frac{1-q_2^{n-1}}{q_2^n} & \frac{1}{q_2^{n-1}} & \frac{1}{q_2^{n-2}} & \frac{1}{q_2^{n-3}} & \cdots & \frac{1}{q_2^2} & \frac{1}{q_2} & 1 & 0 & \cdots & 0 \\
\frac{1-q_2^{n-2}}{q_2^n} & \frac{1-q_2^{n-2}}{q_2^{n-1}} & \frac{1}{q_2^{n-2}} & \frac{1}{q_2^{n-3}} & \cdots & \frac{1}{q_2^2} & \frac{1}{q_2} & 1 & 0 & \cdots & 0 \\
\vdots & \vdots & \vdots & \vdots & \vdots & \vdots & \vdots & \vdots & \vdots & \vdots & \vdots \\
\frac{1-q_2}{q_2^n} & \frac{1-q_2}{q_2^{n-1}} & \frac{1-q_2}{q_2^{n-2}} & \frac{1-q_2}{q_2^{n-3}} & \cdots & \frac{1-q_2}{q_2^2} & \frac{1}{q_2} & 1 & 0 & \cdots & 0 \\
0 & 0 & 0 & 0 & \cdots & 0 & 0 & 1 & 0 & \cdots & 0 \\
0 & 0 & 0 & 0 & \cdots & 0 & 0 & 0 & 1 & \cdots & 0 \\
\vdots & \vdots & \vdots & \vdots & \vdots & \vdots & \vdots & \vdots & \vdots & \ddots & \vdots \\
0 & 0 & 0 & 0 & \cdots & 0 & 0 & 0 & 0 & \cdots & 1
\end{bmatrix}$$

Now,

$$(I-Q)^{-1} \times \left[\begin{array}{cccccc} 0 & \cdots & 0 & 1 & \cdots & 1 \end{array}\right]^T = \left[\begin{array}{ccc} 1 & \cdots\cdots & 1 \end{array}\right]^T$$

$$(I-Q)^{-2} \times \begin{bmatrix} 0 \\ \vdots \\ 0 \\ 1 \\ \vdots \\ 1 \end{bmatrix} = (I-Q)^{-1} \times (I-Q)^{-1} \times \begin{bmatrix} 0 \\ \vdots \\ 0 \\ 1 \\ \vdots \\ 1 \end{bmatrix} = (I-Q)^{-1} \times \begin{bmatrix} 1 \\ \vdots \\ \vdots \\ \vdots \\ 1 \end{bmatrix}$$

For the rest of the proof, calculation for the $n-$th row of the matrix $(I-Q)^{-1}$ is shown only; calculation for rows 1 and $(n+1)$ to $(n+m)$ are quite straight-forward. For rows 2 to $n-1$, the same procedure of calculation for the $n-$th row can be followed. For row n of the matrix $(I-Q)^{-1}$

$$\left[\begin{array}{cccccccc} \frac{1-q_2}{q_2^n} & \frac{1-q_2}{q_2^{n-1}} & \cdots & \frac{1-q_2}{q_2} & \frac{1}{q_2} & 1 & 0 & \cdots & 0 \end{array}\right] \times \begin{bmatrix} 1 \\ \vdots \\ \vdots \\ \vdots \\ 1 \end{bmatrix}$$

$$= \frac{1+q_2^n}{q_2^n}$$

Let

$$S_1 = (I-Q)^{-2} \times \left[\begin{array}{cccccc} 0 & \cdots & 0 & 1 & \cdots & 1 \end{array}\right]^T$$

$$= \left[\underbrace{\begin{array}{cccc} \frac{\sum_{i=0}^{n-1} q_2^i + q_2^n}{q_2^n} & \frac{\sum_{i=0}^{n-2} q_2^i + q_2^n}{q_2^n} & \cdots & \frac{1+q_2^n}{q_2^n} \end{array}}_{n} \underbrace{\begin{array}{ccc} 1 & \cdots & 1 \end{array}}_{m} \right]^T$$

and

$$S_2 = Q(I-Q)^{-2} \left[\begin{array}{cccccc} 0 & \cdots & 0 & 1 & \cdots & 1 \end{array}\right]^T = Q \times S_1$$

For row n of matrix Q

$$\left[\underbrace{1-q_2 \quad 0 \quad \cdots \quad 0}_{n} \; \underbrace{q_2 \quad 0 \quad \cdots \quad 0}_{m} \right] \times S_1 = \frac{1}{q_2^n}$$

Following a similar process for other rows

$$S_2 = Q(I-Q)^{-2} \times \begin{bmatrix} 0 & \cdots & 0 & 1 & \cdots & 1 \end{bmatrix}^T$$

$$= \left[\underbrace{\frac{\sum_{i=0}^{n-1} q_2^i}{q_2^n} \quad \frac{\sum_{i=0}^{n-2} q_2^i}{q_2^n} \quad \cdots \quad \frac{\sum_{i=0}^{n-(n+1)} q_2^i}{q_2^n} \quad \frac{1}{q_2^n}}_{n} \; \underbrace{0 \quad \cdots \quad 0}_{m} \right]^T$$

Let

$$S_3 = P_f Q(I-Q)^{-2} \begin{bmatrix} 0 & \cdots & 0 & 1 & \cdots & 1 \end{bmatrix}^T = P_f \times S_2$$

For row n of matrix P_f

$$\left[\underbrace{1-q_2 \quad 0 \quad \cdots \quad 0}_{n} \; \underbrace{q_2 \quad 0 \quad \cdots \quad 0}_{m} \right] \times S_2 = \frac{1-q_2^n}{q_2^n}$$

Following a similar process for other rows

$$S_3 = P_f Q(I-Q)^{-2} \begin{bmatrix} 0 & \cdots & 0 & 1 & \cdots & 1 \end{bmatrix}^T = P_f \times S_2$$

$$= \left[\underbrace{\frac{\sum_{i=0}^{n-1} q_2^i - q_2^n}{q_2^n} \quad \frac{\sum_{i=0}^{n-2} q_2^i - q_2^n}{q_2^n} \quad \cdots \quad \frac{1-q_2^n}{q_2^n}}_{n} \right.$$

$$\left. \underbrace{0 \quad \cdots \quad 0 \quad \frac{q_1 \sum_{i=0}^{n-1} q_2^i}{q_2^n}}_{m} \right]^T$$

Finally,

$$\pi_n P_f Q(I-Q)^{-2} \begin{bmatrix} 0 \\ \vdots \\ 0 \\ 1 \\ \vdots \\ 1 \end{bmatrix} = \pi_n \times S_3$$

$$= \left[\underbrace{p_2^m \quad p_1 p_2^m \quad \cdots \quad p_1^{n-1} p_2^m}_{n} \underbrace{p_1^n \quad p_2 p_1^n \quad \cdots \quad p_2^{m-1} p_1^n}_{m} \right]$$

$$\times S_3$$

$$= \frac{p_2^{m-1} \left(p_1^n q_1 \sum_{i=0}^{n-1} q_2^i + p_2 \left(\sum_{j=0}^{n-1} p_1^j \sum_{k=0}^{n-j-1} q_2^k - q_2^n \sum_{i=0}^{n-1} p_1^i \right) \right)}{q_2^n \left(p_2^m \sum_{i=0}^{n-1} p_1^i + p_1^n \sum_{i=0}^{m-1} p_2^i \right)}.$$

Bibliography

[1] D. H. Rothenberg, *Alarm management for process control : a best-practice guide for design, implementation, and use of industrial alarm systems*, Momentum Press, New York, NY, 2009.

[2] I. Izadi, S.L. Shah, D. S. Shook, and T. Chen, *An introduction to alarm analysis and design*, In proceedings of the 7th IFAC Symposium on Fault Detection, Supervision and Safety of Technical Processes, pp. 645-650, June 30 - July 3, 2009, Barcelona, Spain.

[3] P. Dittrick, *BP reports $32 billion charge related to oil spill in gulf*, Oil & Gas Journal; vol. 108, no. 28, pp. 34, Aug 2010.

[4] National Commission on the BP Deepwater Horizon Oil Spill and Offshore Drilling, *Deep Water: The Gulf Oil Disaster and the Future of Offshore Drilling*, Report to the President, 2011.

[5] Buncefield Major Incident Investigation Board, *The Buncefield Incident 11 December 2005: The final report of the Major Incident Investigation Board*, Crown copyright, 2008.

[6] US Chemical Safety and Hazard Investigation Board, *Investigation report: refinery explosion and fire*, no. 2005-04-I-TX, March 2007.

[7] Health and Safety Executive, *The explosion and fires at the Texaco refinery, Milford Haven, 24 July 1994*, HSE Books, 1997.

[8] Occupational Safety and Health Administration, *Phillips 66 company Houston chemical complex explosion and fire*, Report to the President, 1990.

[9] C. Perrow, *Normal Accidents: Living with High-Risk Technologies*, Princeton University Press, New Jersey, 1999.

[10] AIChE/CCPS, *Guidelines for engineering design for process safety*, American Institute of Chemical Engineers, Center for Chemical Process Safety, New York, 2012.

[11] J. Nishiguchi and T. Takai, *IPL2 and 3 performance improvement method for process safety using event correlation analysis*, Computers & Chemical Engineering, vol. 34, no. 12, pp. 2007-2013, 2010.

[12] J. Ahnlund, T. Bergquist, and L. Spaanenburg, *Rule-based reduction of alarm signals in industrial control*, Journal of Intelligent and Fuzzy Systems, IOS press, vol. 14, no. 2, pp. 73-84, 2003.

[13] I. Izadi, S. L. Shah, D. S. Shook, S. R. Kondaveeti, and T. Chen, *Optimal alarm design*, In proceedings of the 7th IFAC Symposium on Fault Detection, Supervision and Safety of Technical Processes, pp. 651-656, June 30 - July 3, 2009, Barcelona, Spain.

[14] J. Chen and R. Patton, *Robust Model-Based Fault Diagnosis for Dynamic Systems*, Kluwer Academic Publishers, Boston, 1999.

[15] J. J. Gertler, *Fault Detection and Diagnosis in Engineering Systems*, Marcel Dekker, New York, 1998.

[16] S. X. Ding, *Model-Based Fault Diagnosis Techniques: Design Schemes, Algorithms, and Tools*, Springer-Verlag, Berlin, Heidelberg, 2008.

[17] R. Isermann, *Fault-Diagnosis Systems: An Introduction from Fault Detection to Fault Tolerance*, Springer-Verlag, Berlin, Heidelberg, 2006.

[18] International Society of Automation, *Management of Alarm Systems for the Process Industries*, ANSI/ISA18.2 2009.

[19] Engineering Equipment and Materials Users Association (EEMUA), *Alarm Systems-A Guide to Design, Management and Procurement*, EEMUA Publication 191, 2007.

[20] F. Yang, S.L. Shah, and D. Xiao, *Correlation analysis of alarm data and alarm limit design for industrial processes*, In proceedings of the 2010 American Control Conference (ACC), pp. 5850 - 5855, 30 June - 2 July, 2010, Baltimore, USA.

[21] K. Ahmed, I. Izadi, T. Chen, D. Joe, and Tim Burton, *Similarity analysis of industrial alarm flood data*, IEEE Transaction on Automation Science and Engineering, vol. 10, no. 2, pp. 452-457, April 2013.

[22] S. R. Kondaveeti, *Advanced analysis and redesign of industrial alarm systems*, PhD thesis, University of Alberta, 2013.

[23] N. A. Adnan, I. Izadi, and T. Chen, *Computing Detection Delays in Industrial Alarm Systems*, In proceedings of the American Control Conference (ACC 2011), pp. 786-791, June 29 - July 1, 2011, San Francisco, CA, USA.

[24] N. A. Adnan, I. Izadi, and T. Chen, *On expected detection delays for alarm systems with deadbands and delay-timers*, Journal of Process Control, vol. 21, no. 9, pp. 1318-1331, 2011.

[25] F. Higuchi, I. Yamamoto, T. Takai, M. Noda, and H. Nishitani, *Use of event correlation analysis to reduce number of alarms*, In proceedings of the 10th International Symposium on Process Systems Engineering, pp. 1521-1526, August 16-20, 2009, Salvador.

[26] Y. Luo, X. Liu, M. Noda, and H. Nishitani, *Systematic design approach for plant alarm systems*, Journal of Chemical Engineering of Japan, vol. 40, no. 9, pp. 765-772, September 2007.

[27] B. G. Liptak, *Instrument Engineers' Handbook: Process Control and Optimization (4 ed.)*, vol. 2, pp. 59-63, CRC Press, Boca Raton, Florida, 2006.

[28] M. Mariton, *Detection delays, false alarm rates and the reconfiguration of control systems*, International Journal of Control, Taylor & Francis, vol. 49, no. 3, pp. 981-992, March 1989.

[29] M. Basseville and I.V. Nikiforov, *Detection of Abrupt Changes: Theory and Application*, PTR Prentice-Hall Inc. 1993.

[30] Q. Zhao and M. Kinnaert, *Statistical properties of CUSUM based fault detection schemes for fault tolerant control*, In proceedings of the 48th IEEE Conference on Decision and Control, pp. 7831-7836, December 15-18, 2009, Shanghai, China.

[31] S. Yang and Q. Zhao, *Probability distribution characterisation of fault detection delays and false alarms*, IET Control Theory and Applications, vol. 6, no. 7, pp. 953-962, 2012.

[32] A. Wald, *Sequential Analysis*, Dover Publications, 1973.

[33] N. A. Adnan, Y. Cheng, I. Izadi, and T. Chen, *Study of generalized delay-timers in alarm configuration*, Journal of Process Control, vol. 23, no. 3, pp. 382395, 2013.

[34] N. A. Adnan, Y. Cheng, I. Izadi, and T. Chen, *A generalized delay-timer for alarm triggering*, In proceedings of the American Control Conference (ACC 2012), pp. 6679-6684, June 27-29, 2012, Montreal, QC.

[35] F. Higuchi, I. Yamamoto, T. Takai, M. Noda, and H. Nishitani, *Use of event correlation analysis to rationalize plant alarm system*, In proceedings of the 5th International Symposium on Design, Operation and Control of Chemical Processes, pp. 1-7, July 25-28, 2010, Singapore.

[36] X. Liu, M. Noda and H. Nishitani, *Evaluation of plant alarm systems by behavior simulation using virtual subject*, Computers & Chemical Engineering, vol. 34, no. 3, pp. 374-386, December 2010.

[37] A. Hugo, *Estimation of alarm deadbands*, In proceedings of the 7th IFAC Symposium on Fault Detection, Supervision and Safety of Technical Processes, pp. 663-667, June 30 - July 3, 2009, Barcelona, Spain.

[38] E. Naghoosi, I. Izadi, and T. Chen, *Estimation of alarm chattering*, Journal of Process Control, vol. 21, no. 9, pp. 1243-1249, 2011.

[39] B. Hollifield and E. Habibi, *The Alarm Management Handbook*, PAS, 2006.

[40] E. Naghoosi, I. Izadi, and T. Chen, *A study on the relation between alarm deadbands and optimal alarm limits*, In proceedings of the American Control Conference (ACC 2011), pp. 3627-3632, June 29 - July 1, 2011, San Francisco, CA.

[41] J. Xu and J. Wang, *Averaged alarm delay and systematic design for alarm systems*, In proceedings of the 49th IEEE Conference on Decision and Control, pp. 6821-6826, December 15-17, 2010, Atlanta, GA, USA.

[42] N. A. Adnan and I. Izadi *On detection delays of filtering in industrial alarm systems*, In proceedings of the 21st Mediterranean Conference on Control and Automation, pp. 113-118, June 25-28, 2013, Crete, Greece.

[43] Y. Cheng, I. Izadi, and T. Chen, *Pattern matching of alarm flood sequences by a modified SmithWaterman algorithm*, Chemical Engineering Research and Design, vol. 91, no. 6, pp. 1085-1094, June 2013.

[44] J. Folmer and B. Vogel-Heuser, *Computing dependent industrial alarms for alarm flood reduction*, In proceedings of the 9th International Multi-Conference on Systems, Signals and Device, pp. 1-6, March 20-23, 2012, Chemnitz, Germany.

[45] S. R. Kondaveeti, I. Izadi, S. L. Shaha, T. Black and T. Chen, *Graphical tools for routine assessment of industrial alarm systems*, Computers and Chemical Engineering, vol. 46, pp. 39-47, November 2012.

[46] I. Izadi, S.L. Shah, and T. Chen, *Effective resource utilization for alarm management*, In proceedings of the 49th IEEE Conference on Decision and Control, pp. 6803-6808, December 15-17, 2010, Atlanta, GA.

[47] A. Papoulis, and S.U. Pillai, *Probability, Random Variables and Stochastic Processes*, 4th Ed., Tata Mcgraw-Hill Publishing Company Ltd., New Delhi, 2002.

[48] G. F. Lawler, *Introduction to Stochastic Processes*, 2nd Ed., Chapman & Hall/CRC, 2006.

[49] J. A. Swets, *Measuring the accuracy of diagnostic systems*, Science, vol. 240, no. 4857, pp. 1285-1293, 1988.

[50] W. R. Gilks, S. Richardson, and D. J. Spiegelhalter, *Markov Chain Monte Carlo in Practice*, Boca Raton, FL. Chapman & Hall, 1996.

[51] Y. Cheng, I. Izadi, and T. Chen, *On Optimal Alarm Filter Design*, International Symposium on Advanced Control of Industrial Processes, pp.139-145, May 23-26, 2011, Hangzhou, China.

[52] S. Theodoridis and K. Koutroumbas, *Pattern Recognition*, 4th ed., Academic Press, San Diego, CA, 1999.

[53] A. Genz and F. Bretz, *Computation of Multivariate Normal and t Probabilities*, Springer, Berlin, Heidelberg, 2009.

[54] M. Evans and T. Swartz *Approximating Integrals via Monte Carlo and Deterministic Methods*, Oxford University Press Inc., New York, NY, 2000.

[55] *Statistical Quality Control handbook*, 1st Ed., Western Electric Company, Indianapolis, Indiana, 1956.

[56] J. E. Hopcroft, *An n log n algorithm for minimizing states in a finite automaton*, Theory of Machines and Computations, pp. 189-196, 1971.

[57] B. C. Levy, *Principles of Signal Detection and Parameter Estimation*, Springer, 2008.

[58] G. E. Cho, C. D. Meyer, *Comparison of perturbation bounds for the stationary distribution of a Markov chain*, Linear Algebra and its Applications vol. 335 pp. 137-150, 2001.

[59] P. J. Schweitzer, *Perturbation theory and finite Markov chains*, Journal of Applied Probabilities, vol. 5, pp. 401-413, 1968.

[60] C. D. Meyer, *The condition of a finite markov chain and perturbation bound for the limiting probabilities*, SIAM Journal of Algebraic Discrete Methods vol. 1, pp. 273-283, 1980.

[61] R. Funderlic, C. D. Meyer, *Sensitivity of the stationary distribution vector for an ergodic Markov chain*, Linear Algebra and its Applications, vol. 76, pp. 117, 1986.

[62] E. Seneta, *Perturbation of the stationary distribution measured by ergodicity coefficients*, Advances in Applied Probability, vol. 20, pp. 228-230, 1988.

[63] I. Ipsen, C. Meyer, *Uniform stability of Markov chains*, SIAM Journal on Matrix Analysis and Applications, vol. 15, pp. 1061-1074, 1994.

[64] G. E. Cho, C. D. Meyer, *Markov chain sensitivity measured by mean first passage times*, Linear Algebra Applications, vol. 316, pp. 21-28, 2000.

[65] A. E. Bradley, *The use of the area under the ROC curve in the evaluation of machine learning algorithms*, Pattern Recognition, vol. 30, no. 7, pp. 1145-1159, 1997.

[66] E. R. DeLong, D. M. DeLong and D. L. Clarke-Pearson, *Comparing the areas under two or more correlated receiver operating characteristic*

curves: a nonparametric approach, Biometrics, vol. 44, no. 3, pp. 837-845, 1988.

[67] J. A. Swets and R. M. Pickett, *Evaluation of Diagnostic Systems: Methods from Signal Detection Theory*, Academic Press, New York, 1982.

[68] K. Lange and E. Brunner, *Sensitivity, specificity and ROC-curves in multiple reader diagnostic trialsA unified, nonparametric approach*, Statistical Methodology, vol. 9, pp. 490-500, 2012.

[69] Y. Jin, Y. Yamashita, and H. Nishitani, *Human modeling and simulation for plant operations*, Computers and Chemical Engineering vol. 28, pp. 1967-1980, 2004.

[70] X. Liu, M. Noda, and H. Nishitani, *Evaluation of plant alarm systems by behavior simulation using a virtual subject*, Computers and Chemical Engineering, vol. 34 pp. 374-386, 2010.

[71] M. Bauer, J. W. Cox, M. H. Caveness, J. J. Downs, and N. F. Thornhill, *Finding the direction of disturbance propagation in a chemical process using transfer entropy*, IEEE Transactions on Control Systems Technology, vol. 15, no. 1, pp. 12-21, 2007.

[72] P. Duan, F. Yang, T. Chen, and S. L. Shah, *Direct causality detection via the transfer entropy approach*, accepted for publications in the IEEE Transactions on Control Systems Technology.